Near-field sea-level variability in northwest Europe and ice sheet stability during the Last Interglacial

Long, A.J.[1*], Barlow, N.L.M. [1], Busschers, F.S. [2], Cohen, K.M. [3], Gehrels, W.R.[4] & Wake, L.M.[5]

[1]Long, A.J. Department of Geography, Durham University, Lower Mountjoy, Durham DH1 3LE UK, a.j.long@durham.ac.uk

[1]Barlow, N.L.M., Department of Geography, Durham University, Lower Mountjoy, Durham DH1 3LE UK, n.l.m.barlow@durham.ac.uk

[2]Busschers, F.S. TNO, Geological Survey of the Netherlands, Princetonlaan 6, P.O. Box 80015, 3508 TA Utrecht, The Netherlands, freek.busschers@tno.nl

[3]Cohen, K.M. Department of Physical Geography, Faculty of Geosciences, Utrecht University, POBOX 800.115, 3508 TC Utrecht, The Netherlands, K.M.Cohen@uu.nl

[4]Gehrels, W.R. Environment Department, University of York, Heslington, York YO10 5DD, UK, roland.gehrels@york.ac.uk

[5]Wake, L.M. Department of Geography, University of Northumbria, Ellison Place, Newcastle upon Tyne, NE1 8ST UK, leanne.wake@northumbria.ac.uk

*Corresponding author (email: a.j.long@durham.ac.uk, tel: 0044 191 334 1913, fax: 0044 191 334 1801

ABSTRACT

Global sea level during the Last Interglacial (LIG, Marine Isotope Sub-stage 5e) peaked between c. 5.5 and 9 m above present, implying significant melt from Greenland and Antarctica. Relative sea level (RSL) observations from several far- and intermediate-field sites suggest abrupt fluctuations or jumps in RSL during the LIG highstand that require one or more episodes of ice-sheet collapse and regrowth. Such events should be manifest as unique sea-level fingerprints, recorded in far-, intermediate- and near-field sites depending on the source(s) of ice-mass change involved. To date, though, no coherent evidence of such fluctuations has been reported from near-field RSL

studies in northwest Europe. This is an important problem because RSL fluctuations during the LIG are portrayed as warning signs for how polar ice sheets may behave in a future, warmer than present, world. Here we review the evidence for RSL change during the LIG using stratigraphic data from the best resolved highstand records that exist in the near-field of northwest Europe, from a range of settings that include lagoonal, shallow marine, tidal flat, salt marsh and brackish-water fluviatile environments. Consideration of previously published stratigraphic records from two sites in the Eemian coastal-marine embayment that existed in the central Netherlands, yields no clear indications for abrupt RSL change during the attainment of the near-field highstand. Nor do we find any such indications in other records from countries bordering the North Sea, the Baltic Sea and the White Sea. Two modelling experiments that explore the global signal of hypothetical sea-level oscillations caused by partial collapse and regrowth of either the Greenland or Antarctic LIG ice-sheet, show that the North Sea region is relatively insensitive to mass changes sourced from Greenland but should clearly register events with an Antarctic origin, especially those that occur late in the LIG. The lack of evidence for abrupt sea-level fluctuations at this time in northwest Europe concurs with a lack of clear near-field evidence for ice sheet collapse.

Keywords: sea level; interglacial; ice sheet collapse; Eemian; MIS 5e; glacio-isostatic adjustment

1. Introduction

Several studies, mainly from low latitude sites suggest that polar ice-sheet collapse late in the Last Interglacial caused an already high sea level to jump abruptly by a further 2 to 6 m (e.g. Chappell, 1974; Bloom et al., 1974; Stein et al., 1993; Stirling et al., 1998; Thompson and Goldstein, 2005; Hearty et al., 2007; Rohling et al., 2008; Blanchon et al., 2009; O'Leary et al., 2013; Dabrio et al., 2013). Although not all studies document such variability (e.g. Muhs et al., 2002; Muhs et al., 2011), reports of multi-meter scale sea-level jumps raise concern regarding the potential instability of polar ice sheets in what remains of the current interglacial. Such a collapse would have generated a distinctive geometry, or fingerprint, of global sea-level rise that palaeo sea-level studies can aim to detect (e.g. Mitrovica et al., 2001; Hay et al., 2014). However, no conclusive evidence for such a jump has been reported in relative sea-level (RSL) or ice-sheet records from higher latitude settings (e.g. Zagwijn, 1983; Funder et al., 2002; Lambeck et al., 2006) and, as a result, the global fingerprint of this event is not known. This has led to uncertainty as to whether the jump is indeed global in nature – i.e. triggered by polar ice-sheet collapse - or simply the product of regional (e.g. climate) or local (e.g. tectonic) processes.

The aim of this paper is to review the European near-field evidence for abrupt relative sea-level (RSL) change during the LIG highstand (as defined and dated in the far-field) by scrutinising previously published records from northwest Europe, where the LIG is known as the 'Eemian'. We start by reviewing RSL evidence from sites located distant to the MIS 6 ice sheets, to identify key features that characterise many of these studies. Next, we consider how such abrupt oscillations might be preserved in the near-field stratigraphic record, drawing in part on sedimentary principles that have been established from working on equivalent Holocene sequences (e.g. Vis et al., 2015). We focus on evidence from the coastal deposits preserved in the Amsterdam and Amersfoort glacial basins (central Netherlands), which have a superbly preserved depositional record of the LIG transgression and RSL highstand. The region is the bio- and chronostratigraphical type region of the 'Eemian' (Harting, 1874; 1875, Zagwijn, 1961; Turner, 2002) and data from here, as well as from other sites in the Netherlands, are critical for constraining the LIG RSL highstand in northwest Europe (e.g. Zagwijn, 1983; 1996; Streif, 1990).

We find no compelling signs of abrupt RSL oscillations during the near-field highstand in the coastal deposits of the Netherlands, or from elsewhere in northwest Europe. We note, however, that due to solid earth deformation and equatorial syphoning the attainment of this highstand may be several thousand years later to that observed in far- and intermediate-field sites, meaning that if fluctuations occurred early in the interglacial, these could have happened before the near-field highstand was attained. The lack of evidence for abrupt sea-level fluctuations during the latter part

of the LIG in northwest Europe concurs with a lack of clear near-field evidence for ice sheet collapse at this time.

2. Sea-level changes during the Last Interglacial

Evidence for higher-than-present sea level during the LIG is recorded in emergent landforms and sediments that include coral reef tracts, bioerosional notches as well as nearshore deposits (e.g. Szabo et al., 1994; Stirling et al., 1998; Muhs et al., 2002; Bruggermann et al., 2004; Hearty et al., 2007; Rohling et al., 2008; Thompson et al., 2011; O'Leary et al., 2013; Dutton et al., 2015). Consideration of four RSL records selected from different parts of the world exemplify elements of LIG sea-level behaviour that are common to many far- and intermediate-field RSL records that record sea-level oscillations within the LIG highstand (Figure 1).

From the Seychelles, Dutton et al. (2015) report evidence from raised coral deposits of an early "rapid collapse" of a polar ice sheet, likely part of Antarctica, by 128.6 ± 0.8 k yr ago that pushed sea level to at least +5.9 ± 1.7 m above present (Figure 1A). This was followed by a slower rise of a further c. 2 m, at a rate of c. 0.22 ± 0.04 m/k yr that is attributed to partial melt of the Greenland Ice Sheet, thermal expansion and the loss of mountain glaciers. Peak eustatic sea level of c. 7.6 ± 1.7 m was reached at c. 125 k yr ago, after which sea level fell and the Seychelles RSL record ends.

Our second example is based on the calibration to sea level of a stable oxygen isotope record of sea surface temperatures obtained from planktonic foraminifera extracted from core KL11, located in the central part of the Red Sea (Rohling et al., 2008) (Figure 1B). The record contains two main and one subsidiary sea-level fluctuation of 4 to 10 m. Sedimentological observations from adjacent Red Sea coastlines are cited by Rohling et al. (2008) as supporting evidence of a fluctuating RSL during the LIG highstand (e.g. Orszag-Sperber et al., 2001; Bruggermann et al., 2004).

The next two examples document sea-level changes from the middle and towards the end of the LIG. From the Yucatán Peninsula (Mexico), an intermediate field location relative to the former Laurentide Ice Sheet, Blanchon et al. (2009) identify a 2 to 3 m RSL jump that they attribute to a short-lived (c. 1500 yr) interval of ice sheet instability that is 'tentatively' dated to c. 121 k yr ago (Figure 1C). The evidence for this sea-level jump is the sudden demise of an outer lower reef (developed to a sea-level at +3 m) that coincided with backstepping and accretion of an inner patch-reef (to a c. 3 meter elevation; see also Blanchon, 2010). Finally, in far-field western Australia, O'Leary et al. (2013; see also O'Leary et al., 2008) use stratigraphic and geomorphic mapping with U-series dating of fossil coral reefs to identify two architecturally distinct LIG highstand units that are separated by an unconformity contact and a palaeosol. These coral reef units are interpreted as

indicating two phases to the LIG highstand; the former forming over the period 127 to 119 k yr ago under slow 3 m RSL fall from an initial highstand and the second unit deposited late in the interglacial, dated to 118.1 ± 1.4 k yr ago. The two units are observed at c. 2.5 m and c. 5-6 m above present MSL. O'Leary et al. (2013) include a glacial isostatic adjustment (GIA) modelling analysis as part of their study and propose a broadly stable "eustatic" sea level (i.e. ice-volume equivalent) of c. +3 to 4 m between 127 and 119 k yr ago and one at +9 m for c. 118 k yr ago, implying a c. 5 m sea-level jump late in MIS 5e (Figure 1E). Although the tectonic stability of the region has been challenged (Whitney and Hengesh, 2015), the sea-level jump component has not.

From these studies we identify the following as important elements of sea-level change during the LIG highstand:

1. LIG sea-level oscillations are recorded at the start, during the middle and towards the end of the LIG highstand, and are often interpreted as evidence for polar ice-sheet collapse. The North American and European ice masses are typically assumed to have only contributed to RSL rise early in MIS 5e (up to 127 k yr ago: Rohling et al., 2008; O'Leary et al., 2013). Chronological differences reflect, in part, the duration of the different records and the interval of time when sea level was higher than present, which is when sedimentary records are preserved. Several far-field sites record unconformities and palaeosols within double-reef architectures, from which meter-scale RSL oscillations are reconstructed. In the intermediate field, younger reef elements bury older elements and a marked sea-level jump is inferred against a broadly stable background RSL trend.

2. It is claimed by some studies that there was at least one interval during the main LIG highstand when RSL fell and then rose, possibly abruptly, to re-attain a LIG highstand, several meters higher than before. In the coral reef examples discussed above, the RSL fluctuation during the MIS 5e highstand was c. 3 to 5 m in amplitude. The fluctuation seems best characterised as a multi-millennia period of relatively stable sea level that terminated with a short-lived period of relatively rapid rise, the midpoint of which is dated to between c. 121 and 118 k yr ago.

3. Rates of sea-level change calculated from one of the Red Sea isotope records (core KL11), suggest RSL fluctuations with magnitudes of up to 10 m in 1-2 k yr or less, with peak rates of rise of 2.1 cm yr and fall of -1.8 cm yr during the LIG highstand (Rohling et al., 2008). The size of the Red Sea RSL fluctuations are approximately twice as large as those inferred from most reef records.

154 These different elements of the LIG sea level records form a basis for considering how near-
155 field, low energy depositional environments might have responded to such changes.
156
157 **3. Relative sea-level change and coastal evolution on near-field coasts in northwest Europe**
158 The LIG near-field coasts of northwest Europe differ to their far- and intermediate-field
159 counterparts in several ways. Because of their proximity to the Saalian (MIS 6) ice sheets, RSL
160 records from this region were strongly impacted by GIA. In some peripheral locations, such as the
161 Netherlands, forebulge collapse meant that the background (millennial) rate of RSL rise was
162 relatively stable late into the LIG (Lambeck et al., 2006). This contrasts with the situation in far- and
163 some intermediate-field sites where RSL was already falling by this time (Figure 2).
164
165 A second difference is that the LIG highstand coastal deposits can be well preserved in
166 sedimentary depocenters, some of which have recorded post depositional subsidence, and are
167 relatively complete based on known biostratigraphical changes established from northwest
168 European terrestrial pollen zones (Müller, 1974). Most paleo-coastal records occur as infills of deep
169 Saalian depressions that provided accommodation space for deposition as well as a good chance of
170 preservation during RSL fall at the end of the LIG. Many depressions also experienced post
171 depositional subsidence which further aided preservation.
172
173 A third difference is the abundance of fine-grained minerogenic and organic sediments that
174 have accumulated in North Sea estuaries, tidal inlets, and coastal lagoons. These environments
175 provide excellent archives from which to develop RSL records and reconstruct system-wide
176 responses to abrupt or gradual sea-level forcing. Where these sequences have remained
177 waterlogged since their deposition and include fossiliferous successions from intertidal to supratidal
178 and terrestrial facies, the strong vertical zonation of coastal plant and animal communities with
179 respect to tidal inundation can yield well-constrained sea-level data.
180
181 For many of the above reasons, near-field coastal systems are intensively studied for
182 Holocene sea level; in northwest Europe they have been used to identify short-term (centennial)
183 early-Holocene sea-level jumps of 1 to 3 m (e.g. Hijma and Cohen, 2010), instantaneous events such
184 as tsunami and storms (e.g. Dawson et al., 1988), as well as gradual multi-century to millennial-scale
185 RSL fluctuations (e.g. Denys and Bateman, 1995; Beets and Van der Spek, 2000; Kiden et al., 2002;
186 Waller and Long, 2003). There are differences between Holocene and LIG coastal environments (e.g.
187 Cohen et al., 2014), largely due to variations in substrate topography and composition, due to the

configuration of the main rivers (Busschers et al., 2007; 2008; Peeters et al. 2015) and, potentially, due to differences between the Holocene and LIG deglaciation, GIA and RSL histories. Nevertheless the methods and understanding developed from Holocene RSL studies are instructive when considering potential LIG RSL changes.

4. A conceptual model of Last Interglacial-type sea-level oscillations recorded in the near-field coastal architecture of northwest Europe

An abrupt RSL rise would cause the landward and upwards migration of an estuary and associated environments; indeed entirely new estuaries might develop in previously freshwater valley settings with freshwater swamps rapidly replaced by fluvial-tidal open-water environments. Hijma and Cohen (2010; 2011) record such a change at the time of an early Holocene sea-level jump that preceded the 8.2 ka BP cold event, when RSL in the Netherlands rose by c. 4 m in a few centuries due in part to the sudden drainage of Lakes Agassiz and Ojibway on the margins of the Laurentide Ice Sheet. In the Rhine-Meuse palaeovalley the coastline moved landward by c. 30 km and fluvial-deltaic wetland forests and open reed and sedge wetlands were transformed into tidal flats (Hijma and Cohen, 2011; Bos et al., 2012).

Within transgressed valleys, wind and wave energy would increase as surface area and water depth also increase (e.g. as happened in the mid to late Holocene within the Delaware Estuary, USA; Fletcher et al., 1990). Extensive flood tidal deltas would develop during the initial establishment of tidal inlets and barrier systems, and would migrate landwards (depending on sediment availability; Beets and Van der Spek, 2000), potentially over tidal flat and lagoonal environments. Alternatively, if sediment supply were deficient or sea-level rise very rapid, coastal barriers might be unable to migrate landwards and become drowned, with new barriers forming inland (e.g. Hijma et al., 2010). Eventually, the position of the barrier system would stabilize. In the lagoonal settings that result from that stage, an event of abrupt sea-level rise would potentially erode and rework marginal unconsolidated basin deposits.

From a lithostratigraphic perspective, an abrupt rise in RSL would see the development of extensive transgressive overlaps that mark the facies change from predominately fresh/brackish-water to marine deposits. In lagoons, any fall in salinity stratification might see the accumulation of more massive clastic deposits and a reduction in anoxic-tolerant biota, whilst reworking of marginal basin deposits might disrupt trends in litho- and biostratigraphy associated with more gradual sedimentation.

From a highstand, a rapid RSL fall (such as that associated with one of the Red Sea RSL oscillations; Rohling et al., 2008) would reverse many of the above processes. Mid-estuary tidal flood basins would be replaced by fluvial channel environments and migrate downstream, replacing former salt marsh and tidal flats. A raised estuarine terrace might develop, creating a depositional environment for freshwater floodplain sediments. Gravel and sand barriers would consolidate as increased sediment is made available due to shallower near-shore waters. In shallow coastal lagoons, the frequency of tidal inundation would fall sharply, and a freshening of the lagoon be accompanied by enhanced salinity stratification. Tidal inlets would likely constrict when sea level in the lagoon behind it falls and their tidal prism is reduced.

From a stratigraphic perspective a fall in sea level would be manifest in a variety of ways; there may be a hiatus or abrupt lithological change that marks a cessation or abrupt change in sediment accretion, or the widespread development of (partly erosive) regressive overlaps or soil horizons that mark the lithostratigraphical change between predominately brackish-water and fresh-water deposits (e.g. Peeters et al., 2015). Regressive overlaps would extend seawards and fall in elevation. An increase in salinity stratification within deeper lagoons might coincide with the accumulation of finer-grained, potentially laminated, organic-rich sediments and a fall in the occurrence of open coast biota.

Multiple meter-scale oscillations in sea-level in a few millennia (or less), would be more disruptive. In deep depositional centres they could create stacked sequences of estuarine and freshwater deposits characterised by multiple changes in sedimentary type, and along fringes leave complex erosional contacts and sedimentary hiatuses. Also the architectural properties of the record (i.e. the spatial continuity and uniformity of stratigraphic bounding surfaces), would be affected by the propensity for erosion to destroy older sequences deposited during earlier episodes of sea-level change.

5. Evidence for near-field Last Interglacial relative sea-level changes in northwest Europe

The higher than present sea levels of the LIG had a profound impact on the geometry of northwest European coasts. In the Southern North Sea, LIG shorelines were established inland of the present coastline, with shallow inner shelf seas developing in the Netherlands, Belgium and Germany (e.g. Jelgersma et al., 1979; Zagwijn, 1983; 1989; Paepe and Baeteman, 1979; Behre et al., 1979; De Gans et al., 2000; Streif, 2004; Peeters et al., 2015) (Figure 3). In England, coastal LIG

deposits (Ipswichian stage) are preserved in parts of Lincolnshire and Cambridgeshire (e.g. Gaunt et al., 1974; Gao and Boreham, 2011), within the Thames Estuary (e.g. Gibbard, 1985; Preece, 1999; Bridgland, 1994), and at several sites along the English Channel coast (e.g. Bates et al., 1997; 2010; West and Sparks, 1960; Preece et al., 1990). Based on their pollen assemblages, most of these coastal sequences preserve sediments that span only a relatively short interval of the LIG RSL record.

Thicker, more complete LIG sequences are recorded in the Baltic and White Sea, and also on the North Sea coast of Germany and the Netherlands. LIG sequences occur in the White Sea region (reviewed by Grøsfjeld et al., 2006), the eastern Baltic at Peski (Karelian Isthmus, Russia; e.g. Miettinen et al., 2002; Miettinen et al., 2014) as well as in the western Baltic in the Lower Vistula region (Poland; e.g. Marks et al., 2014) and at Mommark (Denmark; e.g. Erikkson et al., 2006). On the North Sea coast of Germany, thick (c. 20 m) LIG records are described from Dagebüll (e.g. Temler et al., 1995; Win et al., 2000). Notwithstanding these long records, the most complete near-field sedimentary record for LIG RSL changes in northwest Europe is preserved in the Saalian glacial basins of the Netherlands.

Lobes of the Saalian Scandinavian ice sheet reached their maximum southward expansion at c. 160 k yr ago (within MIS 6) (Busschers et al., 2008) and in the central Netherlands excavated a series of deep glacial basins up to -100 m NAP (Dutch Ordnance Datum = approximately mean sea level). These became depositional traps during the deglaciation stages (Drenthe and Warthe Substages of the Saalian), the Eemian (before and after the marine transgression), and the last glacial (Weichselian) (de Gans et al., 1987; Busschers et al. 2007; 2008; Peeters et al. 2015) (Figure 4). The main Amsterdam and (adjacent) Amersfoort Basins have a sill in the base of the in situ Eemian sediments with a present height of c. -40 m that separated them from the Eemian Rhine Valley towards the north (Cleveringa et al., 2000; Gunnink et al., 2012; Peeters et al., 2015). This sill controlled the timing of initial marine inundation and influenced tidal mixing in each lagoon (Van Leeuwen et al., 2000), at least until sediment accumulation exceeded their heights.

Many hundreds of boreholes exist from the Amsterdam Basin (Figure 5). A key site is the Amsterdam Terminal borehole (Figure 4) (Bosch et al., 2000; van Leeuwen et al., 2000; de Gans et al., 2000; Beets and Beets, 2003; Beets et al., 2003; Busschers et al., 2007; Peeters et al., 2015). The Eemian fill comprises a c. 30 m thick sequence of clay-rich sediments that are overlain by a wedge of shell-rich sand that is up to 20 m thick in the north of the basin and which disappears to the south. The deposits are mainly shallow marine in origin and span six distinct pollen zones (NW European

pollen zones E1 to E6) (Zagwijn, 1983; de Gans et al., 2000) that include a brief initial temperate terrestrial stage (E1, E2), the main RSL transgression (in E3-E4a), the highstand (during E4b, E5) and the start of the subsequent regression and RSL fall at the end of the LIG (E6). A broadly similar sedimentary fill is found in the Amersfoort Basin. Here, the key cored sites (including the stratotype site Amersfoort-1) (Zagwijn, 1961; Cleveringa et al., 2000), are from a more marginal, shallower setting (Figure 6). Importantly, the upper part of the Amersfoort-1 LIG record preserves a fining-upwards sequence that formed as tidal flats were replaced by salt marsh and then freshwater peat (Zagwijn, 1961; Cleveringa et al., 2000).

Zagwijn's (1983; 1996) RSL graph of Dutch Eemian RSL changes (Figure 1F) uses index points that have ages inferred from pollen biostratigraphy and altitudes established with respect to high tide level. The graph shows RSL rise from c. -25 m NAP to a highstand of c. -8 m NAP during E5, before falling during E6. A preceding part of the curve, that spans the initial rise from -45 to -25 m, is based on the inundation of the Amsterdam basin and on offshore (North Sea) cores. The highstand sea-level index points used by Zagwijn (1983) and Streif (1990) are collected from several sites scattered along the fringe of the Eemian embayment in the central Netherlands. They have been influenced differentially by the effects of long-term sediment compaction, tectonics and isostatic motions, the latter including GIA. Kooi et al. (1998) estimate that the long-term net effect of these processes varies between c. 12 and 18 cm/k yr. Recent re-analysis of the Zagwijn (1983) data, updated by Streif (1990), corrects for each of these effects (Figure 1F; Lambeck et al., 2006; Kopp et al., 2009).

The approximate duration of the European regional pollen zones is known from annually varved lake deposits in northwest Germany (Müller, 1974). The key pollen zones for the purposes of this study, those that span the culmination of the LIG RSL transgression and highstand in the Netherlands, are E4b (duration c. 1-1.2 k yrs) and E5 (duration c. 4 k yrs). Although the duration of the transgression and highstand is reasonably well-known, there is debate regarding its numerical age. Zagwijn (1983) originally dated the highstand peak to late in the LIG (c. 120 k yr ago), based on correlation with the deep sea oxygen isotope record of MIS 5e (Shackleton and Opdyke, 1973). A late LIG highstand (c. 123 k yr ago) is also proposed by more recent correlation of the NW European Eemian to tied terrestrial pollen and marine $\delta^{18}O$ records and implies a lag between the start of MIS 5e and the far-field LIG highstand of c. 4-5 k yr (Sanchez-Goñi et al., 1999 ; Shackleton et al., 2002; 2003). A relatively late LIG sea-level highstand compared to that seen in the far-field is compatible with what is seen during the Holocene.

In contrast, Funder et al. (2002) correlated the highstand with that recorded by far-field coral reefs to 128 ± 1 k yr ago (McCulloch and Esat, 2000; Shackleton, 2000). Beets et al. (2006) also prefer this timing, correlating the Eemian transgression to the main rise in benthic $\delta^{18}O$ at the start of MIS 5e. Kopp et al. (2009) establish a numerical age for the Zagwijn (1983) sea-level curve by tuning this against the global oxygen isotope stack of Lisiecki and Raymo (2005). From this they propose a broad, flat peak to the highstand that lasted between c. 127-121 k yr ago.

More recently, it has been proposed that the start of the terrestrial Eemian in northwest Europe is even younger than that proposed by Sanchez-Goñi et al. (1999) and Shackleton et al. (2002; 2003) (c. 123 k yr ago). A key line of supporting evidence comes from palaeomagnetic investigations of the Blake Event, a prominent dipole moment low (Singer et al., 2014). In Neumark Nord 2, Germany, it is identified in the earliest part of the LIG pollen sequence (Sier et al., 2011). A second study of the Blake Event (supported by luminescence dating) by Sier et al. (2015) from a core drilled at Rutten – in the area of the Zagwijn (1983) sea-level data - places the start of the Eemian (zone E1) to c. 121 k yr ago, and by implication the sea-level highstand (zone E4b) was attained at c. 119 k yr ago (Figure 7). In this model, the end of the nearfield highstand (end of zone E5) correlates with the end of MIS 5e, whilst the following early stage of RSL fall (zone E6) correlates with the start of MIS 5d (at c. 114 k yr ago).

6. Evidence for last interglacial ('Eemian') sea-level oscillations or jumps in the Netherlands

We now focus our attention on the evidence for RSL changes during the sea-level highstand of the Dutch Eemian sequences, starting with the lower-energy sequence recorded in Amersfoort-1. By the start of E5, sedimentation had already infilled the original basin to above its sill elevation and, as a result, the basin was operating as a tidal lagoon. Any large RSL oscillation during the LIG highstand should be manifest in the core between c. -23 m NAP and -10.5 m NAP (the latter representing the level at which freshwater peat accumulation begins). This interval spans pollen zones E4b to E6 (Figure 7).

Following the initial tidal inundation in E2, several proxies indicate that water depths and accommodation space increased due to RSL rise (Cleveringa et al., 2000). The lithology records an up-core transition from shallow-water, brackish clay-rich sands and shells to a sand with shells that coarsens upwards. The transition between these facies is dated to the end of E4b and the start of E5 (c. -22.50 m NAP). Molluscs and foraminifera above this level point to a deepening and an increase

in salinity, with some of the latter taxa washed in from the North Sea inner shelf. Maximum water depths of c. 10 m are inferred between core depths of -18.8 m to -16.8 m NAP. Accommodation space decreased above this level as sedimentation outstripped the slowing rate of RSL rise. The coarsening-upwards trend in the sands seen in the second half of E5 indicates an increase in wave action and related hydrodynamic processes. Heavy mineral data and the setting of the site indicate the sands were likely derived from the local reworking of ice-pushed ridges close to the basin margins. Changes in the molluscan and ostracod assemblages point to local reworking within these sands, most likely owing to wave or current processes.

Towards the end of E5 (c. -14.50 m NAP) the shelly sands described above are abruptly overlain by c. 4 m of clays and sandy clays. Cleveringa et al. (2000) suggest a discontinuity in sedimentation (they use the term 'hiatus') between the shelly sands and overlying clays, also noting an abrupt change in molluscan and foraminiferal assemblages that indicate a change from a lagoon to an 'estuary-like water body surrounded by mudflats' (Figure 6). The uppermost fine-grained deposits were deposited under tidal mudflat and then salt marsh conditions. They record the final infilling of the basin during the broad RSL highstand that culminated in freshwater peat formation as RSL started to fall. The stratigraphic cross-section of the Amersfoort area compiled by Zagwijn (1983) (Figure 5) shows only a single regressive contact to the overlying freshwater peat that can be traced across the basin to its margins; there are no intercalations of organic or minerogenic sediments at the basin margins.

In the Amsterdam Terminal borehole, a thick sequence of clays and silts formed during the latter part of E4 and throughout E5 (van Leeuwen et al., 2000). Crumbly and then homogenous silty clays grade upwards into a laminated silty clay at c. -46 m NAP. Foraminifera and dinoflagellates indicate a steady deepening of the lagoon, and a strengthening of the exchange of water with the open sea that created a well-ventilated water column (van Leeuwen et al., 2000). An increase in tidal influence is also suggested by an increase in salt marsh pollen frequencies. This phase of unobstructed exchange of water with the open coast ended shortly after the start of E5 when the deposition of laminated finer-grained clays indicates the establishment of more restricted, lagoonal conditions. Drawing analogies with the Holocene development of coastal beach barriers - which in this region stabilised c. 6.5 k yr ago (e.g. Beets & Van de Spek, 2000), some 1.5-2 k yrs after Holocene RSL had begun to slow (Hijma & Cohen, 2010) - van Leeuwen et al. (2000) and de Gans et al. (2000) interpret these changes as recording a phase of sand barrier development in the sill area which restricted tidal inflow and lead to lagoonal stratification.

The final phase of the LIG highstand in the Amsterdam Terminal borehole above -38 m NAP comprises an upward coarsening trend with massive silty clays that contain increasingly thicker laminations of sand during the latter part of E5 (van Leeuwen et al., 2000). Foraminifera and molluscs suggest deposition in a large, tidally-affected lagoon that was shallowing, and which once had an unobstructed exchange of water with the open marine areas to the north. This may record the breakdown of a former barrier or spit (Van Leeuwen et al., 2000; de Gans et al., 2000). Van Leeuwen et al. (2000) propose reworking of these coarse sands by tidal channels as accommodation space fell further, as shown by a shell-rich lag deposit containing clay pebbles reworked from mudflats, encountered at c. -32 m NAP. However, Busschers et al. (2007) and Peeters et al. (2015) indicated that this lag is the base of a much younger (MIS 4) fluvial channel belt of the Rhine system.

In summary, the Amersfoort-1 and Amsterdam Terminal cores contain no evidence for abrupt oscillations in RSL during the LIG highstand (E4-E5). The discontinuities that do exist can all be explained by analogy to mid-Holocene coastal dynamics, without invoking vertical changes in RSL (other than RSL rise at the onset of the highstand and fall towards the end, Figure 4). The hiatuses seen in the Amersfoort-1 core are not seen within the finer-grained sediments that accumulated in the deeper-water setting of the Amsterdam Terminal core, away from the basin margins. Nor does the latter contain evidence for large-scale input of sand, organic material and/or pollen that might suggest sudden RSL rise and associated erosion of basin valley flanks by wave or tidal processes.

7. A critical evaluation of the near-field relative sea-level record from northwest Europe

7.1 Issues of dating and vertical precision in near-field relative sea-level records

It could be argued that the relatively poor vertical precision of the near-field LIG sea-level index points may hinder our ability to identify RSL oscillations/jumps; indeed we note that the highstand sediments in the Amsterdam Terminal core (but not the Amersfoort-1 core) are silty clays and coarse shelly sands that are not ideal for developing detailed RSL records. The chronology of these records is a floating one based on pollen zones and their registration in annually laminated lacustrine sediments elsewhere in NW Europe. The absolute age-models for the sequence vary between studies (see above) and this makes direct correlation with other, better-dated sequences from far- and intermediate-field settings difficult. The near-field highstand record is also considerably shorter than the far-field highstand, such that the former does not overlap all of the latter (i.e. the near-field Eemian sea-level record cannot overlap *both* the Seychelles *and* the Yucatán records of MIS 5e). We also note that during the main Eemian transgression, when sea level rose rapidly from c. -45 m NAP (the lowest sea-level indicator) to c. -15 m NAP (the start of the local

426 Dutch highstand), we cannot currently rule out the possibility of a sea-level jump within the earliest
427 part of the Eemian (during E1-E3). However, when considering the sedimentary architectures from
428 which these index-points are derived (by analogy to the reef studies reviewed in section 2) the
429 resolution is similar and we identify no evidence for sea-level jumps in the time interval considered.
430
431 *7.2 Local and regional signals in the last interglacial sea level records of northwest Europe*
432 Looking beyond the Netherlands, we see no evidence for abrupt RSL changes in the adjacent
433 Eemian sequences described by Temler (1995) and Winn et al. (2000) from North Germany. LIG
434 marine deposits from south and east England typically only span brief time intervals and also record
435 no evidence for synchronous abrupt RSL changes (e.g. West and Sparks, 1960; West et al., 1970;
436 Holyoak and Preece, 1985). In Trafalgar Square (London), LIG deposition occurred at the landward
437 limit of tidal influence. This setting should have been sensitive to abrupt RSL changes in the LIG
438 highstand, yet only gradual changes are observed (Gibbard, 1985; Preece, 1999).
439
440 Elsewhere in northwest Europe, two extensive reviews from the Baltic/White Sea regions
441 also find no evidence for such events during the RSL highstand (Funder et al., 2002; Lambeck et al.,
442 2006). Indeed, of the examples of gradual changes in LIG RSL inferred from detailed litho- and
443 biostratigraphy we highlight the study of Grøsfjeld et al. (2006) from the White Sea region of
444 northwest Russia and the multiproxy examination of displaced marine sediments in the Mommarck
445 area of southern Denmark (e.g. Haila et al., 2006; Kristensen and Knudsen, 2006) as two further
446 records which document gradual RSL rise and then fall over the LIG highstand.
447
448 It would be misleading, though, to suggest that the possibility of RSL fluctuations in the LIG
449 have not been made from northwest European sites. For example, Hollin (1977) interpreted
450 evidence from the Thames Estuary as evidence for a two-phase RSL record in the LIG, including a
451 jump from c. 0 m to +16 m at the end of the interglacial that they attribute to an Antarctic 'surge'.
452 More recently, two studies suggest salinity variations during the LIG RSL highstand from the White
453 Sea. Diatoms from Peski, on the Karelian Isthmus, suggest a brief mid-Eemian lowering in salinity
454 that Miettinan et al. (2014) speculate could be related to a mid-LIG (c. 126 k yr ago in their age
455 model) sea-level fall. At Cierpieta, in the Lower Vistula region of Poland, Marks et al. (2014) report a
456 short-lived 'transgressive pulse' that happened about 6.2-6.6 k yrs into the interglacial (during the
457 end of E5 or start of E6) and was associated with an increase in tidal and littoral diatoms. However,
458 each of these studies is equivocal in one or more ways; the study of Hollin (1977) is now recognised
459 as flawed because all of the high level sites they thought were from the LIG are now attributed to

MIS 7 or older (e.g. Bridgland, 1994; Penkman et al., 2011), whilst the Baltic sites are sensitive to climate-driven changes in freshwater discharge and changes in tidal dynamics that accompanied the evolution of the LIG White Sea (Miettinen et al., 2014; Marks et al., 2014).

In summary, the resolution of the near-field RSL reconstructions from the LIG is not as detailed as those from the Holocene. Nevertheless the size of the sea-level signal that we are testing for is much larger than any RSL variation during the Holocene highstand. Moreover, we would expect a large oscillation/jump in RSL to be a regional signal, with evidence preserved in many of the near-field coastal sequences described above. We see no evidence for regionally synchronous changes of this nature (other than the initial rapid transgression) and observe that synchronous regional sea-level fall is first recorded at the onset of zone E6, in the last millennia of the Eemian.

Section 8.1

8.1 Sea-level signals of Last Interglacial ice sheet instability

The size of the LIG sea-level oscillations/jumps reconstructed in several far- and intermediate-field RSL studies implicates either Greenland and/or Antarctica as potential sources, although other ice masses may have contributed too (see below). Sea-level fingerprinting provides a means to assess such a possibility, as previous studies predict spatially variable sea-level changes consequential to ice sheet collapse events. Hay et al. (2014) show that the ability to identify rapid collapse events in sea-level records should be more robust than with current gradual melting because the sea-level fingerprint of a sudden event is less sensitive to uncertainties in the geometry of the melt region and will dominate over the signal from steric effects.

One hypothesis for the lack of obvious sea-level oscillation/jump in the Netherlands (and elsewhere in northwest Europe) is that this reflects the geographical proximity of these sites to the LIG Greenland Ice Sheet. To test this hypothesis, we present a pair of experiments in which we modified global ice sheet deglaciation histories (ICE-5G; Peltier, (2004) and HUY-2; Simpson et al. (2009)) to simulate hypothetical episodes of ice sheet collapse/regrowth in Greenland or Antarctica. The combined ICE-5G-HUY-2 deglaciation history detailed in Simpson et al. (2009) focuses on sea-level change since the Last Glacial Maximum with the sea level calculation initiated at 122 k yr ago. In this model, sea level reached +8 m above present at 122 k yr ago until an abrupt fall at 116 k yr ago.

493 We modify the ICE-5G-HUY-2 deglaciation history by adding several synthetic eustatic sea-
494 level fluctuations between 127 and 116 k yr ago. We limit the mass fluxes from Greenland
495 (experiment G1) to the equivalent of ± 2-3 m eustatic sea level, and the mass fluxes from Antarctica
496 (experiment A1) equal to ± 5 m (Figure 8, Table S1). Note that the timing and number of fluctuations
497 differ in each experiment and that our interest is in the relative size of the sea-level signal between
498 sites and not their absolute values. Moreover, although these models are purely illustrative, we
499 present a 'realistic' ice sheet history by allowing the geometry of the Greenland Ice Sheet to oscillate
500 between states representative of 122 k yr ago and 110 k yr ago during the period of interest. For
501 Antarctica, we construct oscillations in mass balance by applying scaling factors for ice thickness
502 uniformly across the ice sheet, which we consider adequate for the purposes of this experiment (see
503 Mitrovica et al. (2009) for details of the influence of more complex melt patterns). The scaling
504 factors and details of ice sheet deglaciation for the period 127-117 k yr ago used in both scenarios
505 are detailed in Supplementary Information (Table S1). Global ice extent outside of the target areas
506 of each experiment (Greenland and Antarctica) is fixed at its 122 k yr ago extent during the LIG
507 maximum.
508
509 We input the resulting loading histories into the sea-level model presented in Mitrovica and
510 Milne (2003) and Kendall et al. (2005), and use this to predict RSL changes at the Netherlands,
511 Seychelles, Red Sea, the Yucatán Peninsula, Bahamas and Western Australia (Figure 8). In the sea-
512 level model, we do not include calculation of the Earth response to pre-LIG changes in global ice and
513 ocean loads since the aim of this experiment is only to test sensitivity for recording jump-events and
514 not to accurately reproduce any specific global or regional sea-level history. The sea-level change
515 associated with pre-LIG glaciation-deglaciation cycles will not alter the magnitude of the applied LIG
516 oscillations in each experiment but rather superimpose them on a long-term secular trend. We
517 present the results for experiments A1 and G1 in which Antarctica and Greenland, respectively, are
518 subjected to growth-collapse periods during the LIG.
519
520 Model results for an Antarctica-only source for the sea-level fluctuations show that all sites
521 track the modified eustatic curve reasonably closely, especially late in the LIG (after 123 ky ago),
522 when the Northern Hemisphere has almost completely deglaciated (Figure 8). This overall pattern is
523 in agreement with other sea-level fingerprint experiments (Mitrovica et al., 2001; Hay et al., 2014)
524 and shows that all of these sites should be sensitive to sea-level oscillations sourced from
525 Antarctica. An Antarctic-sourced sea level oscillation seen in the Yucatán Peninsula, for example,
526 should be manifest at the same time, and with a broadly similar amplitude, in each of the other

sites. Of course, whether the signal is actually preserved in coastal stratigraphic data would depend on the particular local RSL history (including background rates of tectonic- and GIA- and hydroisostasy-induced subsidence, e.g. in Yucatán, in the Netherlands). It is conceivable that in near-field sites, such as the Netherlands, RSL was potentially below present at the time of both an early and a late interglacial sea-level jump recorded in far- and intermediate-field settings, i.e. after c. 128 k yr (Seychelles) and before c. 119 k yr ago (Yucatán Peninsula).

Model results for a Greenland-only source show more considerable differences between the study sites (Figure 8). Because of the proximity of the Netherlands to Greenland and a deglaciating Eurasian Ice Sheet, the predicted sea-level record for this site is effectively 'blind' to the oscillations (±2 m) recorded in each of the far-field sites (see also Mitrovica et al. (2001)). This experiment raises the possibility that the lack of obvious sea-level oscillations/jumps in the Netherlands is because abrupt RSL changes observed in far-field sites were sourced from Greenland.

8.2 Near-field records of ice-sheet instability

The experiments above show that the Netherlands is potentially sensitive to abrupt sea-level changes sourced from Antarctica, an advantage over other far-field RSL sites that are potentially unable to discriminate between Antarctic and Greenland contributions. Marine diatoms and cosmogenic isotopes from beneath the West Antarctic Ice Sheet (WAIS) indicate exposure to marine conditions at an unspecified interglacial (Scherer et al., 1993; Scherer et al., 1998), but they cannot be ascribed with any confidence to the LIG. Bryozoan diversity data suggest an open seaway between the Weddell and Ross Sea at some time in the late Quaternary (Barnes and Hillenbrand, 2010; Vaughen et al., 2011). Rapid collapse of WAIS should result in massive discharges of icebergs, meltwater and significant IRD (Hillenbrand et al., 2009), yet no such evidence is recorded in sea bed cores from sites close to Antarctica (e.g. O'Cofaigh et al., 2001; Hillenbrand et al., 2002). A review of 17 marine records from the wider Southern Ocean by Capron et al. (2014) reveals no evidence of synchronous abrupt warming or cooling events during the main part of the LIG that might trigger, or record, abrupt Antarctic instability.

Ice-core records from Antarctica provide an important source for identifying abrupt changes in climate and associated changes in ice sheet surface elevation that could be related to sea-level changes, although as Bradley et al. (2012) show, the location of many ice cores, mainly in East Antarctica, is not ideal for testing models of WAIS collapse. Common to most Antarctic ice cores is an early (c. 128 k yr ago, using the AICC2012 timescale; Bazin et al., 2013) maximum in LIG air

561 temperatures, 1-4 °C warmer than present and lasting c. 3 k yrs, that was followed by a multi-
562 millennial scale plateau (126-122 k yr ago; Masson-Delmotte et al., 2011) of stable temperatures
563 (Jouzel et al., 2007). This was followed by a cooling into the glacial inception at c. 110 k yr ago
564 (Capron et al., 2012).
565
566 Steig et al. (2015) note that the $\delta^{18}O$ data from Mt. Moulton (West Antarctica) show a
567 statistically significant smaller difference between LIG and Holocene values than is seen in East
568 Antarctic ice cores. This is consistent with the differences predicted by a climate model that includes
569 WAIS collapse that was well underway by ~130 k yr ago. Steig et al. (2015) note several caveats to
570 this study; it assumes a fixed linear correlation between temperature and the ice core isotope data,
571 whilst the Mt Moulton record implies relatively low and high $\delta^{18}O$ values in MIS 5e and the coldest
572 part of the glacial period (~20-40 k yr ago) compared to other ice core records. Moreover, there is
573 no strong evidence that WAIS was significantly thicker during this period. Model experiments by
574 Holden et al. (2010) of the impact of meltwater on the Antarctic Meridional Overturning Circulation
575 and associated air temperatures over Antarctica also require WAIS melting so as to satisfactorily
576 predict the observed peak temperatures in the early part of the LIG.
577
578 These data-model studies suggest, contrary to the geological evidence, that the early LIG
579 warmth may have been associated with ice-sheet retreat that contributed to the higher than present
580 sea levels observed during the LIG. But the relationship between atmospheric warmth and mass
581 change in Antarctica is complex; indeed a period of warmth in the mid Holocene in Antarctica
582 between c. 4.5 and 2 k yr ago (Bentley et al., 2009; Sterkin et al., 2012) coincided with a 30%
583 increase in ice accumulation over West Antarctica (Siegert and Payne, 2004), whilst Frieler et al.
584 (2015) use a combination of ice core data and modelling to derive a continental-scale increase in
585 accumulation of approximately 5 ± 1 % K^{-1}, that would have competed with surface melting and
586 dynamical loss at the ice sheet margin by other processes. So, although it is overly-simplistic to
587 assume warmer air temperatures equate directly to ice-sheet mass loss, the main observation we
588 draw from the Antarctic ice cores is that there is only one interval of significant warmth, and that
589 this happened early in the LIG.
590
591 Turning to Greenland, evidence for LIG ice sheet behaviour is provided by sea-bed cores that
592 contain proxies for Greenland vegetation cover, run-off and IRD. Pollen and spores from a sea-bed
593 core located off southeast Greenland (core HU-90-014-013) indicate single peaks in relative
594 abundances that implicate only a single interval of reduced ice cover in southern Greenland (de

595 Vernal and Hillaire-Marcel, 2008). Sr-Nd-Pb isotope ratios of silt-sized sediment in a core offshore of
596 the southern tip of Greenland also indicate that the southern part of the ice sheet underwent
597 continued retreat throughout much of the last interglacial (Coleville et al., 2011), although there is
598 no evidence for multiple phases of ice-sheet collapse followed by regrowth. Records of Ti and Fe
599 present in core MD99-2227, from the same region, suggest high but steady run-off throughout the
600 main part of the LIG (Carlson et al., 2008; Carlson and Windsor, 2012).
601
602 Several records from the North Atlantic and Baffin Bay have evidence for one or more
603 cooling episodes during the broad oxygen isotope plateau of the LIG that may record ice-sheet
604 instability, although not necessarily all are attributed to Greenland (e.g. Maslin et al., 1998; Bauch,
605 2011; Schwab et al., 2014). Sea surface temperature reconstructions and foraminiferal assemblages
606 from core MD03-2664 (southwest Greenland) (Irvani et al., 2012), indicate a warm early start to MIS
607 5e that was interrupted at c. 126 k yr ago by a 1.6 k yrs cooling event. This was accompanied by a
608 significant freshening that is attributed to enhanced Greenland run-off. Galassen et al. (2014)
609 identify multiple such transient cooling events that they relate to variations in North Atlantic Deep
610 Water (NADW) production. Some of these are reminiscent of the 8.2 k yr cold event (see also Bauch,
611 2011); indeed one is described in detail by Nicholl et al. (2012) who trace a red carbonate layer along
612 the Labrador and Greenland margins of the Labrador Sea that they source to a large outburst flood
613 from a LIG glacial Lake Agassiz, dated to c. 124.5 k yr ago. Variations in NADW during the latter part
614 of the LIG are also identified by Galassen et al. (2014) at c. 119.5 and 116.8 k yr ago that are
615 attributed to (unspecificed) non-Greenland forcing.
616
617 The North Greenland Eemian Ice Drilling core (NEEM) records a maximum in air
618 temperatures of +8 ± 4 °C (compared to the average of the last millennium) during the early Eemian
619 (c. 126 k yr ago) (NEEM Members, 2013). Regular summer melt events occur between 127 and
620 118.3 k yr ago, and the NEEM Members (2013) conclude that the GIS contributed no more than c. 2
621 m to the LIG highstand. The NEEM core records a cooling after c. 121 k yr ago that broadly tracks
622 the decline in northern hemisphere insolation. In NGRIP there is an abrupt cooling assigned to c.
623 119 k yr, followed by relatively stable depleted $\delta^{18}O$ phase (Greenland stadial 26) until c. 115 k yr
624 ago (NGRIP Community Members, 2004). If the NEEM CH_4 tuned age-model (NEEM Members, 2013)
625 is applied to the lower part of the NGRIP core (from Greenland stadial 24 towards the LIG), these
626 ages become 1.5-2 k yrs younger (Sier et al. 2015).
627

628 Other potential near-field sources capable of driving abrupt sea-level changes include the
629 Laurentide and Fennoscandinavian ice sheets. These are normally excluded from discussions on LIG
630 sea-level (and GIA modelling) since it is assumed that by the peak of MIS 5e they had melted, or
631 were too small to drive meter-scale changes in global sea level. However, the MIS 6
632 Fennoscandinavian Ice Sheet was significantly larger than its LGM counterpart, accounting for up to
633 50% of the total northern hemisphere ice volume (Svendsen et al., 2004; Lambeck et al., 2006). It is
634 conceivable that this ice sheet may have continued to melt late into the LIG, and the GIA response
635 and RSL signal in its near-field delayed in comparison to Termination I. In the eastern and northern
636 Nordic Seas, Van Nieuwenhove et al. (2013) note that peak ocean temperatures occurred relatively
637 late in the LIG, and implicate meltwater run-off from a residual Norwegian ice mass until as late as c.
638 122-120 k yr ago (see also Bauch and Erlenkeuser (2008)). The absence of significant Laurentide-
639 sourced IRD-events during MIS 6 beyond the Labrador Sea could be because the configuration of the
640 Laurentide Ice Sheet was different to that of other glacials (i.e. smaller), or that no ice stream existed
641 in Hudson Strait in MIS 6 (Naafs et al., 2013), in which case the ice sheet may have been more stable.
642 Indeed, as noted above, Nichol et al. (2012) identify an abrupt drainage event that they attribute to
643 former glacial Lake Agassiz in the Hudson Bay region at c. 124.5 k yr ago. A smaller and more stable
644 Laurentide Ice Sheet might, therefore, have still been retreating during much of the interval covered
645 by the Seychelles LIG sea level record, which is interpreted to reflect only Antarctic and Greenland
646 contributions (Dutton et al., 2015).
647
648 The above discussion highlights that ice sheets other than Greenland and Antarctica may
649 have played a role in causing sea level to vary during the LIG highstand and that their configurations
650 and retreat dynamics during Termination II and MIS 5e were probably different to those during
651 Termination I and the Holocene. However, as yet there is no compelling evidence for significant ice-
652 sheet collapse in Antarctica or for polar ice sheet *regrowth* during the LIG that is required to explain
653 abrupt oscillations in sea level, other than at the end of the highstand.
654
655 **9. Reflections on Last Interglacial sea-level studies**
656 Our first reflection is that few far- and intermediate-field RSL studies attribute sea-level
657 jumps to known periods of ice-sheet instability. There is a large body of literature that has
658 reconstructed abrupt oscillations in RSL during the LIG from far- and intermediate-field settings. Our
659 intention in this study is not to criticise these reconstructions, although we note that in several
660 studies that assert there is more than one LIG highstand the deposits are poorly dated or undated.
661 Rather we aim to highlight the lack of evidence for equivalent changes in the near-field in northwest

662 Europe, and the lack of any coherent evidence for significant collapse and regrowth events from
663 Greenland or Antarctica during the peak LIG capable of driving abrupt, meter-scale RSL fluctuations.
664
665 A second reflection is on the importance of using uninterrupted stratigraphic sequences to
666 test for sea-level oscillations/jumps. In the Netherlands, it is the elevation of the basin sills that
667 connected them to the Rhine Valley and the North Sea which provides the primary elevation control
668 during the initial LIG transgression, whilst during the highstand the vertical RSL constraint is obtained
669 from intertidal and salt marsh deposits and overlying terrestrial peat. It is the stratigraphic
670 successions preserved in these sequences that are the key to testing for large amplitude sea-level
671 fluctuations/jumps. The value of stratigraphically constrained data applies equally in the far- and
672 intermediate-field settings.
673
674 A third observation is that there are periods during the LIG when different RSL records have
675 been used to invoke episodes of abrupt sea-level change when at other sites RSL is stable or
676 changing little. Mindful of the fingerprint discussion above, rapid jumps in sea level at one site
677 should be recorded at the same time at others (as supposed to gradual sea-level change resulting in
678 a spatially and temporally variable highstand). Between-site variability therefore indicates that one
679 or more of the records in conflict must reflect site- (or region-) specific processes. One example
680 illustrates this point; Thompson et al. (2011) report that RSL on the Bahamas fell from c. +4 m at 123
681 k yr ago to 0 m and then rose again to + 6 m by 119.2 k yr ago. But in this same 4 k yr interval, RSL
682 on the Yucatán Peninsula was stable until a sudden 3 m jump tentatively dated at c. 121 k yr ago
683 (Blanchon et al., 2009). Meanwhile in the Red Sea, using the Grant et al. (2012) chronology, there is
684 a rather modest (c. 2 m) oscillation in this interval (Figure 1). It is difficult, if not impossible, to
685 reconcile these records with each other.
686
687 The above example underscores our fourth reflection, namely the need for precise age
688 constraints from LIG sea-level reconstructions so as to enable robust chronological comparisons
689 between sites and with the ice-sheet records and models. In practice, dating LIG sea-level records is
690 a major challenge. In the Netherlands, the duration of the RSL record is determined with respect to
691 'floating' varve chronologies and associated pollen zones (e.g. Caspers et al., 2002; Funder et al.,
692 2002; Sirocko et al., 2005). Indeed, in some instances chronologies for the near-field RSL records are
693 developed by aligning records with a single interglacial sea-level highstand identified in the far-field,
694 regardless of potential differential GIA between these regions (e.g. Funder et al., 2002). In the
695 intermediate- and far-fields, U-Th dating provide the potential for precise and accurate dating

696 control, but age determinations require careful screening to ensure that only the most trustworthy
697 dates are used in any analysis. In a recent LIG database exercise, Dutton and Lambeck (2012) discard
698 about two thirds of available U-Th dates by following a robust screening procedure (see also
699 Medina-Elizalde (2013)). The importance of different age models is also evident in the way that the
700 Red Sea sea-level record has shifted c. 6 k yr (from the early to the middle part of the LIG, Figure 1B)
701 since its original publication (Rohling et al., 2008), whilst we note also that single-site chronologies
702 can also be uncertain; the timing of the Yucatán sea-level jump at c. 121 k yr ago is only 'tentatively'
703 dated (Blanchon et al., 2008).
704
705 In Europe, debate regarding the absolute age of the Eemian deposits means that correlation
706 with other intermediate- and far-field records is unclear. The oldest suggested age for the Eemian
707 highstand is c. 129 k yr ago (Funder et al., 2002) and, if correct, would mean that the initial sea-level
708 jump recorded in the Seychelles by Dutton et al. (2015) could be recorded in the main Dutch
709 transgression. The more conventional age-model, based on palynological correlation to the Iberian
710 Peninsula and its offshore marine record (Sanchez-Goni et al., 1999; Shackleton et al., 2003) has the
711 highstand (within E4 and E5) spanning from 124 to 119 k yr ago. If correct, it would mean that
712 Seychelles sea-level jump happened when much of the Netherlands was dry land and the coastline
713 well offshore in the southern North Sea. Conversely, the late LIG sea-level jumps recorded on the
714 Yucatán Peninsula/Bahamas and Western Australia (c. 121 to 118 k yr ago) would have happened
715 (but are not recorded) during the final phase the Dutch highstand. The youngest proposed
716 chronology has the highstand spanning from 119 to 114 k yr ago (Sier et al., 2015). This model would
717 mean that the proposed Yucatán and/or western Australia oscillations happened during the main
718 transgression phase (E3). Close interval sampling of multiple cores taken across these key time
719 intervals from the flooding surface in the Amersfoort Basin would potentially help test the latter two
720 hypotheses.
721
722 A final observation is that well-constrained ice-margin histories mean that it is now possible
723 to infer upper bounds to individual Holocene sea-level jumps, but this is not yet the case in the LIG.
724 Indeed, the challenge in reconstructing the 8.2 k yr sea-level jump (Hijma and Cohen, 2010), which
725 required excellent dating control and detailed sedimentological investigations, highlights the
726 potential of this approach to LIG deposits but also the scale of the challenge ahead. We therefore
727 encourage caution against seeking to link RSL data from single sites or regions to ice-sheet behaviour
728 until such time that abrupt sea-level changes are replicated in near-, intermediate- and far-field

729 sites, or robust ice-sheet histories demonstrating unequivocal evidence for collapse and regrowth
730 events are established.
731
732 **10. Conclusions and future research priorities**
733 Abrupt jumps or oscillations in RSL caused by the partial or full collapse and regrowth of an
734 ice sheet should be recorded globally as distinct, spatially-variable, RSL signatures. For decades,
735 investigations in far- and intermediate-field sites have identified evidence that sea level during the
736 LIG was several meters higher than present. Additionally, there is also a large body of literature that
737 argues for significant, meter-scale fluctuations in RSL during the LIG highstand, which have been
738 attributed to largely unidentified ice-sheet collapse and regrowth events.
739
740 Near-field stratigraphic sequences from the Amsterdam and Amersfoort Basins (the
741 Netherlands) provide data that imply stable or only gradually changing ice volumes during the LIG
742 highstand of this part of northwest Europe. Reviews of other LIG marine records from northwest
743 Europe yield no compelling evidence for widespread abrupt changes in RSL during the LIG highstand,
744 changes that, based on our understanding of how coastal systems in this region typically respond to
745 Holocene forcings, should be clearly identifiable.
746
747 The fact that the near-field LIG records lack clear evidence for abrupt RSL change requires
748 explanation if we are to be confident in making predictions for how the polar ice sheets may behave
749 in a future, warmer-than-present world. A lack of direct field evidence from Greenland and
750 Antarctica for collapse/regrowth events within the LIG RSL highstand is a significant challenge to
751 ongoing and future glaciological and palaoceanographic research. Although sea-level modelling
752 experiments predict that the Netherlands is relatively insensitive to Greenland ice-mass change, the
753 latter had already lost significant mass at the time of the LIG sea-level highstand and cannot have
754 been the sole source of large fluctuations/jumps in sea level during the LIG. Present approaches to
755 reconstructing LIG ice mass sources are hamstrung by poor chronologies for the deglacial history of
756 Antarctica, Greenland, as well as other northern hemisphere ice sheets, parts of which may have
757 persisted late into the LIG.
758
759 The differences noted in this study provide directions for future research in near-,
760 intermediate- and far-field RSL studies, in the LIG and other older interglacials, that may be used as
761 analogues for future sea-level change. For sites in the near-field, a priority must be replication of
762 further, more detailed investigation of fine-grained tidal flat and salt marsh deposits formed during

763 the LIG highstand, including with closer sampling intervals across key stratigraphic changes that span
764 periods of hypothesised ice sheet collapse. One such period – spanning the hypothesised sea-level
765 jump observed c. 121 k yr ago – can be tested for by detailed study of the period of rapid
766 transgression that marks the early part of the Eemian in the Dutch RSL record.
767
768 **Acknowledgments**
769 Funding for this work was provided by UK Natural Environment Research Council grant
770 "Using interglacials to assess future sea-level scenarios (iGlass)" (NE/I008675/1). This paper has
771 benefited from discussions with members of PALSEA2 (an INQUA International Focus Group and a
772 PAGES working group) and is a contribution to that program and the INQUA Commission on Coastal
773 and Marine Processes. Our understanding of the Dutch Eemian sediments improved considerably
774 from examination of the Amsterdam Terminal and Amersfoort borehole sediments at TNO, the
775 Geological Survey of the Netherlands, and we thank Jeroen Schokker for his help in facilitating this.
776 We are grateful to David Bridgland, Mike Bentley and Glenn Milne for comments on an early version
777 of this paper, and to Dan Muhs for his detailed comments during the review process. Thanks also to
778 Chris Orton for help with the drafting of several figures
779
780 **References**
781 Barlow, N.L.M., Shennan, I., Long, A.J., Gehrels, W.R., Saher, M.H., Woodroffe, S.A., Hillier, C., 2013.
782 Salt marshes as late Holocene tide gauges. Glob. Plan. Change 106, 90-110.
783 Barnes, D. K. A., Hillenbrand,C.-D., 2010. Faunal evidence for a late Quaternary trans-Antarctic
784 seaway. Global Change Biol., doi:10.1111/j.1365-2486.2010.02198.x.
785 Bates, M.R., Parfitt, S.A., Roberts, M.B., 1997. The chronology, palaeogeography and archaeological
786 significance of the marine Quaternary record of the West Sussex Coastal Plain, Southern England,
787 U.K. Quat. Sci. Rev. 16, 1227–1252
788 Bates, M.R., Briant, R.M., Rhodes, R.J., Schwenninger, J-L., Whittaker, J.E., 2010. A new chronological
789 framework for Middle and Upper Pleistocene landscape evolution in the Sussex/Hampshire Coastal
790 Corridor, UK. Proc. Geol. Ass. 121, 369–392.
791 Bauch, H.A., 2013. Interglacial climates and the Atlantic meridional overturning circulation: is there
792 an Arctic controversy? Quat. Sci. Rev. 63, 1-22.
793 Bauch, H.A., Erlenkeuser, H., 2008. A "critical" climatic evaluation of last interglacial (MIS 5e) records
794 from the Norwegian Sea. Polar Res 27, 135–151.
795 Bazin, L., Landais, A., Lemieux-Dudon, B., Toyé Mahamadou Kele, H., Veres, D., Parrenin, F.,
796 Martinerie, P., Ritz, C., Capron, E., Lipenkov, V., Loutre, M.-F., Raynaud, D., Vinther, B., Svensson, A.,

Rasmussen, S. O., Severi, M., Blunier, T., Leuenberger, M., Fischer, H., Masson-Delmotte, V., Chappellaz, J., Wolf, E., 2013. An optimized multi-proxy, multi-site Antarctic ice and gas orbital chronology (AICC2012). 120–800 ka. Clim. Past 9, 1715-1731.

Beets, C.J., Beets, D.J., 2003. A high resolution stable isotope record of the penultimate deglaciation in lake sediments below the city of Amsterdam, the Netherlands. Quat. Sci. Rev. 22, 195-207.

Beets, D.J., van der Spek, A.J., 2000. The Holocene evolution of the barrier and back-barrier basins of Belgium and the Netherlands as a function of late Weichselian morphology, relative sea-level rise and sediment supply. Geol. en Mijnb. 79, 3-16.

Beets, D.J., Beets, C.J., Cleveringa, P., 2006. Age and climate of the late Saalian early Eemian in the type-area, Amsterdam basin, The Netherlands. Quat. Sci. Rev. 25, 876-885.

Behre, K.-E., Menke, B., Streif, H., 1979. The Quaternary geological development of the German part of the North Sea. In: Oele E., Schüttenheim, R.T.E., Wiggers, A.J. (Eds.): The Quaternary History of the North Sea. Acta Universitatis Upsaliuensis, pp. 85-113.

Bentley, M.J., Hodgson, D.A., Smith, J.A., Ó Cofaigh, C., Domack, E.W., Larter, R.D., Roberts, S.J., Brachfeld, S., Leventer, A., Hjort, C., Hillenbrand, C.-D., Evans, J., 2009. Mechanisms of Holocene palaeoenvironmental change in the Antarctic Peninsula region. Holocene 19, 51-69.

Blanchon, P., 2010. Reef demise and back-stepping during the last interglacial, northeast Yucatán. Coral Reefs 29, 481–498.

Blanchon, P., Eisenhauer, A., Fietzke, J., Liebetrau, V., 2009. Rapid sea-level rise and reef back-stepping at the close of the last interglacial highstand. Nature, 458, 881-884.

Bloom, A. J., Broecker, W.S., Chappell, J., Matthews, R.K., Mesolella, K.J., 1974. Quaternary sea level fluctuations on a tectonic coast: New 230Th/234U dates from the Huon Peninsula, New Guinea, Quat. Res., 4, 185–205.

Bos, I.J., Busschers, F.S., Hoek, W.Z., 2012. Organic-facies determination: a key for understanding facies distribution in the basal peat layer of the Holocene Rhine-Meuse delta, The Netherlands. Sedimentol. 59, 676-703.

Bosch, J.H.A., Cleveringa, P., Meijer, T., 2000. The Eemian stage in the Netherlands: history, character and new research. Geol. en Mijnb. 79, 135–145.

Bradley, S.L., Siddall, M., Milne, G.A., Masson-Delmotte, V., Wolff, E., 2012. Where might we find evidence of a Last Interglacial West Antarctic Ice Sheet collapse in Antarctic ice core records? Glob. Plan. Change 88-89, 64-75.

Bridgland, D.R., 1994. Quaternary of the Thames. Chapman Hall, London.

Bruggemann, J.H., Buffler, R.T., Guillaume,M.M., Walter, R.C., von Cosel, R., Ghebretensae, B.N., Berhe, S.M., 2004. Stratigraphy, palaeoenvironments and model for the deposition of the Abdur

831 Reef Limestone: context for an important archaeological site from the last interglacial on the Red
832 Sea Coast of Eritrea. Palaeogeogr. Palaeoclimatol. Palaeoecol. 20, 179–206.
833 Busschers, F.S., Kasse, C., van Balen, R.T., Vandenberghe, J., Cohen, K.M., Weerts, H.J.T., Wallinga, J.,
834 Johns, C., Cleveringa, P., Bunnik, F.P.M., 2007. Late Pleistocene evolution of the Rhine-Meuse system
835 in the southern North Sea basin: imprints of climate change, sea-level oscillation and glacio-isostacy.
836 Quat. Sci. Rev. 26, 3216–3248.
837 Busschers, F.S., Van Balen, R.T., Cohen, K.M., Kasse, C., Weerts, H.J.T., Wallinga, J., Bunnik, F.P.M.,
838 2008. Response of the Rhinee Meuse fluvial system to Saalian ice-sheet dynamics. Boreas 37, 377-
839 398.
840 Carlson, A.E., Windsor, K., 2012. Northern Hemisphere ice-sheet responses to past climate warming.
841 Nat. Geosci. 5, 607-613.
842 Carlson, A.E., Stoner, J.S., Donnelly, J.P., Hillaire-Marcel, C., 2008. Response of the southern
843 Greenland Ice Sheet during the last two deglaciations. Geology 36, 359-362
844 Capron, E., Landais, A., Chappellaz, J., Buiron, D., Fischer, H., Johnsen, S.J., Jouzel, J., Leuenberger,
845 M., Masson-Delmotte,V., Stocker, T.F., 2012. A global picture of the first abrupt climatic event
846 occurring during the last glacial inception. Geophys. Res. Lett. L15703, doi:10.1029/2012GL052656.
847 Capron, E., Govin, A., Stone, E. J., Masson-Delmotte, V., Mulitza, S., Otto-Bliesner, B., Sime, L.,
848 Waelbroeck, C., Wolff, E., 2014. Temporal and spatial structure of multi-millennial temperature
849 changes at high latitudes during the Last Interglacial. Quat. Sci. Rev. 103, 116-133.
850 Caspers, G., Merkt, J., Müller, H., Freund, H., 2002. The Eemian interglaciation in northwestern
851 Germany. Quat. Res. 58, 49–52.
852 Chappell, J., 1974. Geology of coral terraces, Huon Peninsula. New Guinea: A study of Quaternary
853 tectonic movements and sea-level changes. Geol. Sot. Am. Bull. 85, 553-570.
854 Cleveringa, P., Meijer, T., Van Leeuwen, R.J.W., De Wolf, H., Pouwer, R. Lissenberg, T., Burger, A.W.,
855 2000. The Eemian type locality at Amersfoort in the central Netherlands: redeployment of old and
856 new data. Geol. en Mijnb. 79, 197-216.
857 Cohen, K.M., MacDonald, K., Joordens, J.C.A., Roebroeks, W., Gibbard, P.L., 2012. The earliest
858 occupation of north-west Europe: a coastal perspective. Quat. Int. 271, 70-83.
859 Colville, E. J., Carlson, A. E., Beard, B. L., Hatfield, R. G., Stoner, J. S., Reyes, A. V., Ullman, D. J., 2011.
860 Sr-Nd-Pb isotope evidence for ice-sheet presence on southern Greenland during the Last Interglacial.
861 Science, 333, 620–623.
862 De Gans, W., De Groot, T., Zwaan, H., 1987. The Amsterdam basin, a case study of a glacial basin in
863 The Netherlands. In: Van der Meer, J.J.M. (Ed.), Tills and Glaciotectonics. Balkema, Rotterdam, pp.
864 205-216.

De Gans, W., Beets, D.J., Centineo, M.C., 2000. Late Saalian and Eemian deposits in the Amsterdam glacial basin. Geol. En Mijnb. 79, 147-160.

Dabrio, C.J., Zazo, C., Cabero, A., Goy, J.L., Bardají, T., Hillaire-Marcel, C., González-Delgado, J.A., Lario, J., Silva, P.G.,Borja F., García-Blázquez, A.M., 2013. Millennial/submillennial-scale sea-level fluctuations in western Mediterranean during the second highstand of MIS 5e. Quat. Sci. Rev. 30, 335-346.

Dawson, A.G., Long, D., Smith, D.E., 1988. The Storegga Slide: evidence from eastern Scotland for a possible tsunami. Mar. Geol. 82, 271–276.

Denys, L., Baeteman, C., 1995. Holocene evolution of relative sea-level and local mean tide in Belgium. Mar. Geol. 124, 1-19.

Deschamps, P., Durand, N., Bard, E., Hamelin, B., Camoin, G., Thomas, A.L., Henderson, G.M., Okuno, J., Yokoyama, Y., 2012. Ice sheet collapse and sea-level rise at the Bølling warming, 14,600 yr ago. Nature 483, 559–564.

Dutton, A., Lambeck, K., 2012. Ice volume and sea level during the last interglacial. Science 337, 216–219.

Dutton, A., Webster, J.M., Zwartz, D., Lambeck, K., Wohlfarth, B., 2015. Tropical tales of polar ice: evidence of Last Interglacial polar ice sheet retreat recorded by fossil reefs of the granitic Seychelles islands. Quat. Sci. Rev., 107, 182-196.

Eiríksson, J., Kristensen, P. H., Lykke-Andersen, H., Brooks, K., Murray, A., Knudsen, K. L., Glaister, C., 2006. A sedimentary record from a deep Quaternary valley in the southern Lillebælt area, Denmark: Eemian and Early Weichselian lithology and chronology at Mommark. Boreas 35, 320-331.

Fletcher, C.A., Knebel, H.J., Kraft, J.C., 1990. Holocene evolution of an estuarine coast and tidal wetlands. Geol. Soc. Amer. Bull. 102, 283−297.

Frieler, K., Clark, P.U.., He, F., Buizert, C., Reese, R., Ligtenberg, S.R.M., van den Broeke, M.R., Winkelmann, R., Levermann, A., 2015. Consistent evidence of increasing Antarctic accumulation with warming. Nature Clim. Change, DOI: 10.1038/NCLIMATE2574.

Fruergaard, M., Andersen, T.J., Nielsen, L.H., Madsen, A.T., Johannessen, P.N., Murray, A.S., Kirkegaard, L., Pejrup, M., 2011. Punctuated sediment record resulting from channel migration in a shallow sand-dominated micro-tidal lagoon, Northern Wadden Sea, Denmark. Mar.Geol. 280, 91-104.

Funder, S., Demidov, I., Yelovicheva, Y., 2002. Hydrography and mollusc faunas of the Baltic and the White Sea-North Sea seaway in the Eemian. Palaeogeog., Palaeoclim., Palaeoecol. 184, 275-304.

Galaasen, E.V., Ninnemann, U.S., Irvali, N., Kleiven, H.F., Rosenthal, Y., Kissel, C., Hodell, D.A., 2014. Rapid reductions in North Atlantic Deep Water during the peak of the last interglacial period. Science 343, 1129-1132.

Gaunt, G.D., Bartley, D.D., Harland, R., 1974. Two interglacial deposits proved in boreholes in the southern part of the Vale of York and their bearing on contemporaneous sea levels. Bull. Geol. Surv. Gt. Brit. 48, 1-23.

Gao, C., Boreham, S., 2011. Ipswichian (Eemian) floodplain deposits and terrace stratigraphy in the lower Great Ouse and Cam valleys, southern England, UK. Boreas 40, 303-319.

Gibbard, P.L., 1985. The Pleistocene history of the Middle Thames Valley. Cambridge University Press: Cambridge.

Grant, K.M., Rohling, E.J., Bar-Matthews, M., Ayalon, A., Medina-Elizalde, M., Bronk Ramsey, C., Satow, C., Roberts, A.P., 2012. Rapid coupling between ice volume and polar temperature over the past 150 kyr. Nature 491, 744–747.

Grøsfjeld, K., Funder, S., Seidenkrantz, M.-S., Glaister, C., 2006. Last interglacial marine environments in the White Sea region, northwestern Russia. Boreas 35, 493-520.

Gunnink, J.L., Bosch, J.H.A., Siemon, B., Roth, B., Auken, E., 2012. Combining ground-based and airborne EM through artificial neural networks for modelling hydrogeological units under saline groundwater conditions. Hydrol. Earth Sys. Sci. 16, 3061–3074.

Haila, H., Miettinen, A., Eronen, M., 2006. Diatom succession of a dislocated Eemian sediment sequence at Mommark, South Denmark. Boreas 35, 378-384.

Harting, P., 1874. De bodem van het Eemdal. In: Verslagen en verhandelingen van de Koninklijke Akademie van Wetenschappen, serie II: deel VIII, pp. 282-290.

Harting, P., 1875. Le système Eemien. Archives Néerlandaises des Sciences Exactes et Naturelles de la Societé Hollandaise des Sciences à Haarlem, pp. 443-454.

Hay, C., Mitrovica, J.X., Gomez, N., Creveling, J.R., Austermann, J., Kopp, R.E., 2014. The sea-level fingerprints of ice-sheet collapse during interglacial periods. Quat. Sci. Rev. 87, 60-69.

Hearty, P.J., Hollin, J.T., Neumann, A.C., O'Leary, M.J., McCulloch, M., 2007. Global sea level fluctuations during the Last Interglaciation (MIS 5e). Quat. Sci. Rev. 26, 2090-2112.

Hijma, M.P., Cohen, K.M., 2010. Timing and magnitude of the sea-level jump preluding the 8200 yr event. Geology 38, 275-278.

Hijma, M.P., Cohen, K.M., 2011. Holocene transgression of the Rhine river mouth area, The Netherlands/Southern North Sea: palaeogeography and sequence stratigraphy. Sedimentology 58, 1453-1485.

930 Hijma, M.P., Van der Spek, A.J.F., Van Heteren, S., 2010. Development of a mid-Holocene estuarine
931 basin, Rhine-Meuse mouth area, offshore the Netherlands. Mar. Geol. 271, 198-211.

932 Hillenbrand, C.-D., Kuhn, G., Frederichs, T., 2009. Record of a Mid-Pleistocene depositional anomaly
933 in West Antarctic continental margin sediments: an indicator for ice-sheet collapse? Quat. Sci. Rev.
934 28, 1147-1159.

935 Hillenbrand, C.-D., Fütterer, D.K., Grobe, H., Frederichs, T., 2002. No evidence for a Pleistocene
936 collapse of the West Antarctic Ice Sheet from continental margin sediments recovered in the
937 Amundsen Sea. Geo-Marine Lett. 22, 51-59.

938 Holden, P.B., Edwards, N.R., Wolff, E.W., Lang, N.J., Singarayer, J.S., Valdes, P.J., Stocker, T.F., 2010.
939 Interhemispheric coupling, the West Antarctic Ice Sheet and warm Antarctic interglacials. Clim. Past
940 6, 431-443.
941 Hollin, J.T., 1977. Thames interglacial sites, Ipswichian sea levels and Antarctic ice surges. Boreas 1,
942 33–52.
943 Holyoak, D.T., Preece, R.C., 1985. Late Pleistocene interglacial deposits at Tattershall, Lincolnshire.
944 Phil. Trans. R. Soc. Lond. B311, 193-236.
945 Irval, N., Ninnemann, U.S., Galaasen, E.V., Rosenthal, Y., Kroon, D., Oppo, D.W., Kleiven, H.F., Darling,
946 K., Kissel, C., 2012. Rapid switches in subpolar North Atlantic hydrography and climate during the
947 Last Interglacial (MIS 5e). Paleoceanography 27, PA2207.
948 Jelgersma, S., Oele, E., Wiggers, A.J., 1979. Depositional history and coastal development in the
949 Netherlands and the adjacent north sea since the Eemian. In: Oele, E., Schüttenhelm, R.T.E.,
950 Wiggers, A.J. (Eds.), The Quaternary History of the North Sea, Acta Universitatis Upsaliensis,
951 Symposium Universitatis Upsaliensis Annum Quingentesimum Celebrantis: 2, Uppsala, Sweden, pp.
952 115-142.
953 Jouzel, J., Masson-Delmotte, V., Cattani, O., Dreyfus, G., Falourd, S., Hoffmann, G., Minster, B.,
954 Nouet, J., Barnola, J. M., Chappellaz, J., Fischer, H., Gallet, J. C., Johnsen, S., Leuenberger, M.,
955 Loulergue, L., Luethi, D., Oerter, H., Parrenin, F., Raisbeck, G., Raynaud, D., Schilt, A., Schwander, J.,
956 Selmo, E., Souchez, R., Spahni, R., Stauffer, B., Steffensen, J. P., Stenni, B., Stocker, T. F., Tison, J. L.,
957 Werner, M., and Wolff, E. W., 2008. Orbital and millennial Antarctic climate variability over the past
958 800 000 years. Science 317, 793–796.
959 Kendall, R.A., Mitrovica, J.X., Milne, G.A., 2005. On post-glacial sea level. Part II. Numerical
960 formulation and comparative results on spherically symmetric models. Geophys. J. Int. 161, 679–
961 706.

962 Kiden, P., Denys, L., Johnston, P., 2002. Late Quaternary sea-level change and isostatic and tectonic
963 land movements along the Belgian–Dutch North Sea coast: geological data and model results. J.
964 Quat. Sci. 17, 535-546.
965 Kooi, H., Johnston, P., Lambeck, K., Smither, C., Molendijk, R., 1998. Geological causes of recent (100
966 yr) vertical land movement in the Netherlands. Tectonophysics 299, 537-558.
967 Kopp, R.E., Simons, F.J., Mitrovica, J.X., Maloof, A.C., Oppenheimer, M., 2009. Probabilistic
968 assessment of sea level during the last interglacial stage. Nature 462, 863-868.
969 Kopp, R.E., Simons, F.J., Mitrovica, J.X., Maloof, A.C., Oppenheimer, O., 2013. A probabilistic
970 assessment of sea level variations within the Last Interglacial stage. Geophys. J. Int. 193, 711-716.
971 Kristensen, P.H., Knudsen, K.L., 2006: Palaeoenvironments of a complete Eemian sequence at
972 Mommark, south Denmark: foraminifera, ostracods and stable isotopes. Boreas 35, 349-366.
973 Lambeck, K., Purcell, A., Funder, S., Kjær, K.H., Larsen, E., Möller, P., 2006. Constraints on the Late
974 Saalian to early Middle Weichselian ice sheet of Eurasia from field data and rebound modelling.
975 Boreas 35, 539-575.
976 Lisiecki, L.E., Raymo, M.E., 2005. A Pliocene-Pleistocene stack of 57 globally distributed benthic $\delta^{18}O$
977 records. Palaeoceanography 20, PA1003, doi:10.1029/2004PA001071.
978 Lourens, L.J., 2004. Revised tuning of Ocean Drilling Program Site 964 and KC01B (Mediterranean)
979 and implications for the D18O, tephra, calcareous nannofossil and geomagnetic reversal
980 chronologies of the past 1,1 Mys. Paleoceanog. 19, PA3010–PA.
981 McCulloch, M.T., Esat, T., 2000. The coral record of Last Interglacial sea levels and sea surface
982 temperatures. Chem. Geol. 169, 107–129.
983 Marks, D.G., Gałązka, G., Krzymińska, J., Nita, M., Stachowicz-Rybka, R., Witkowski, A., Woronko, B.,
984 Dobosz, S., 2014. Marine transgressions during Eemian in northern Poland: a high resolution record
985 from the type section at Cierpięta Leszek. Quat. Int. 328-329, 45-59.
986 Masson-Delmotte, V., Buiron, D., Ekaykin, A., Frezzotti, M., Gallée, H., Jouzel, J., Krinner, G., Landais,
987 A., Motoyama, H., Oerter, H., Pol, K., Pollard, D., Ritz, C., Schlosser, E., Sime, L. C., Sodemann, H.,
988 Stenni, B., Uemura, R., Vimeux, F., 2011. A comparison of the present and last interglacial periods in
989 six Antarctic ice cores. Clim. Past 7, 397–423.
990 Medina-Elizalde, M., 2013. A global compilation of coral sea-level benchmarks: implications and
991 new challenges. Earth Plan. Sci. Let. 362, 310-318.
992 Miettinen, A., Rinne, K., Haila, H., Hyvärinen, H., Eronen, M., Delusina, I., Kadastik, E., Kalm, V.,
993 Gibbard, P.L., 2002. The marine Eemian of the Baltic: new pollen and diatom data from Peski, Russia,
994 and Põhja-Uhtju, Estonia. J. Quat. Sci. 17, 445-458.

995 Miettinen, A., Head, M.J., Knudsen, K.L., 2014. Eemian sea-level highstand in the eastern Baltic Sea
996 linked to long-duration White Sea connection. Quat. Sci. Rev. 86, 158-174.
997 Mitrovica, J.X., Milne, G.A., 2003. On post-glacial sea level: I. General theory. Geophys. J. Int. 154,
998 253–267.
999 Mitrovica, J.X., Gomez, N, Clark, P.U., 2009. The sea-level fingerprint of West Antarctic
1000 collapse. Science 323, 753.
1001 Mitrovica, J.X., Tamisiea, M.E., Davis, J.L., Milne, G.A., 2001. Recent mass balance of polar ice sheets
1002 inferred from patterns of global sea-level change. Nature 409, 1026–1029.
1003 Muhs, D.R., Simmons, K.R., Steinke, B., 2002. Timing and warmth of the last interglacial period: new
1004 U-series evidence from Hawaii and Bermuda and a new fossil compilation for North America. Quat.
1005 Sci. Rev. 21, 1355–1383.
1006 Muhs, D.R., Pandolfi, J.M., Simmons, K.R., Schumann, R.R., 2012. Sea-level history of past interglacial
1007 periods from uranium-series dating of corals, Curaçao, Leeward Antilles islands. Quat. Res. 78, 157–
1008 169.
1009 Muhs, D.R., Meco, J., Simmons, K., 2014. Uranium-series ages of corals, sea level history, and
1010 palaeozoogeography, Canary Islands, Spain: an exploratory study for two Quaternary interglacial
1011 periods. Palaeogeogr. Palaeoclimatol. Palaeoecol. 394, 99–118.
1012 Müller, H., 1974. Pollenanalytische Untersuchungen und Jahresschichtenzählungen an der Eem-
1013 zeitlichen Kieselgur von Bispingen/Luhe. Geologisches Jahrbuch reihe A 21, 149-169.
1014 Naafs, B.D.A., Hefter, J., Stein, R., 2013. Millennial-scale ice rafting events and Hudson Strait
1015 Heinrich(-like) events during the late Pliocene and Pleistocene: a review. Quat. Sci. Rev. 80, 1–28.
1016 NEEM Community Members, 2013. Eemian interglacial reconstructed from Greenland folded NEEM
1017 ice core strata. Nature 493, 489-494.
1018 NGRIP Community Members, 2004. High-resolution record of Northern Hemisphere climate
1019 extending into the last interglacial period. Nature 431, 147-151.
1020 Nicholl, J.A.L., Hodell, D.A., Naafs, B.D.A., Hillaire-Marcel, C., Channell, J.E.T.,Romero, O.E., 2012. A
1021 Laurentide outburst flooding event during the last interglacial period. Nat. Geosci. 5, 901-904.
1022 O'Cofaigh, C.O., Dowedeswell, J.A., 2001. Late Quaternary iceberg rafting along the Antarctic
1023 Peninsula continental rise and in the Weddell and Scotia Seas. Quat. Int. 56, 308–321.
1024 O'Leary, M.J., Hearty, P.J., McCulloch, M.T., 2008. Geomorphic evidence of major sea- level
1025 fluctuations during marine isotope substage-5e, Cape Cuvier, Western Australia. Geomorph. 102,
1026 595-602.

O'Leary, M.J., Hearty, P.J., Thompson, W.G., Raymo, M.E., Mitrovica, J.X., Webster, J.M., 2013. Ice sheet collapse following a prolonged period of stable sea level during the last interglacial. Nat. Geosci. 6, 796-800.

Orszag-Sperber, F., Plaziat, J.-C., Baltzer, F., Purser, B.H., 2001. Gypsum salina and coral reef relationships during the Last Interglacial (Marine Isotopic Stage 5e) on the Egyptian Red Sea coast: a Quaternary analogue for Neogene marginal evaporites? Sed. Geol. 140, 61-85.

Osete, M.-L., Martin-Chivelet, J., Rossi, C., Edwards, R.L., Egli, R., Munoz-Garcia, M.B., Wang, X., Pavon-Carrasco, J., Heller, F., 2012. The Blake geomagnetic excursion recorded in a radiometrically dated speleothem. Earth Plan. Sci. Lett. 353-354, 173-181.

Paepe, R., Baeteman, C., 1979. The Belgian coastal plain during the Quaternary. In E. Oele, Schüttenhelm, R.T.E., Wiggers, A.J. (Eds), The Quaternary History of the North Sea, 143—146. Acta Univ. Ups. Symp. Univ. Ups. Annum Quingentesimum Cele- brantis: 2, Uppsala.

Peeters, J., Busschers, F.S., Stouthamer, E., 2015. Fluvial evolution of the Rhine during the last interglacial-glacial cycle in the southern North Sea basin: a review and look forward. Quat. Int. 357, 176-188

Peltier, W. R,. 2004. Global glacial isostasy and the surface of the ice-age Earth: the ICE-5G (VM2) model and GRACE. Annu. Rev. Earth Plan. Sci. 32, 111-149.

Penkman, K.E.H., Preece, R.C., Bridgland, D.R., Keen, D.H., Meijer, T., Parfitt, S.A., White, T.S., Collins, M.J., 2011. A chronological framework for the British Quaternary based on *Bithynia opercula*. Nature 476, 446-449.

Preece, R.C., 1999. Mollusca from Last Interglacial fluvial deposits of the River Thames at Trafalgar Square, London. J. Quat. Sci. 14, 77-89.

Preece, R.C., Scourse, J.D., Houghton, S.D., Knudsen, K.L., Penney, D.N., 1990. The Pleistocene sea-level and neotectonic history of the eastern Solent, southern England. Phil. Trans. R. Soc. Lond. B328, 425–477.

Rahmstorf, S., 2007. A semi-empirical approach to projecting future sea-level rise. Science 315, 368–370.

Rohling, E.J., Grant, K., Hemleben, C., Siddall, M., Hoogakker, B.A.A., Bolshaw, M., Kucera, M., 2008. High rates of sea-level rise during the last interglacial period. Nat. Geosci. 1, 38-42.

Rohling, E.J., Grant, K., Bolshaw, M., Roberts, A.P., Siddall, M., Hemleben, Ch., Kucera, M., 2009. Antarctic temperature and global sea level closely coupled over the past five glacial cycles. Nat. Geosci. 2, 500–504.

Rohling, E.J., Braun, K., Grant, K., Kucera, M., Roberts, A.P., Siddall, M., Trommer, G., 2010. Comparison between Holocene and Marine Isotope Stage-11 sea-level histories. Earth Plan. Sci. Lett. 291, 97–105.

Sanchez-Goñi, M.F., Eynaud, F., Turon, J.L., Shackleton, N.J., 1999. High resolution palynological record off the Iberian margin: direct land–sea correlation for the last interglacial complex. Earth and Plan. Sci. Lett. 171, 123–137.

Schellmann, G., Radtke, U., 2004. A revised morpho- and chronostratigraphy of the Late and Middle Pleistocene coral reef terraces on southern Barbados (West Indies). Earth Sci. Rev. 64, 157–187.

Scherer, R., 1993. There is direct evidence for Pleistocene collapse of the West Antarctic Ice Sheet. J. Glaciol. 39, 716–722.

Scherer, R. P., Aldahan, A., Tulaczyk, S., Possnert, G., Engelhardt, H., Kamb, B., 1998. Pleistocene collapse of the West Antarctic Ice Sheet. Science 281, 82–85.

Shackleton, N.J., 2000. The 100,000-year ice age cycle identified and found to lag temperature, carbon dioxide, and orbital eccentricity. Science 289, 1897-1902.

Shackleton, N.J., Opdyke, N.D., 1973. Oxygen isotope and palaeomagnetic stratigraphy of equatorial Pacific core V28-238: oxygen isotope temperatures and ice volumes on a 10^5 and 10^6 year scale. Quat. Res. 3, 39– 55.

Shackleton, N.J., Chapman, M., Sanchez-Goñi, M.F., Pailler, D., Lancelot, Y., 2002. The classic marine isotope substage 5e. Quat. Res. 58, 14–16.

Shackleton, N.J., Sanchez-Goñi, M.F., Pailler, D., Lancelot, Y., 2003. Marine Isotope Substage 5e and the Eemian interglacial. Glob. Plan. Change 36, 151-155.

Siegert, M.J., Payne, A.J., 2004. Past rates of accumulation in central West Antarctica. Geophys. Res. Lett. 31, L12403.

Sier, M.F., Roebroeks, W., Bakels, C.C., Dekkers, M.J., Brühl, E., De Loecker, D., Gaudzinski-Windheuser, S., Hesse, N., Jagich, A., Kindler, L., Kuijper, W.J., Laurat, T., Mücher, H.J., Penkman, K.E.H., Richter, D., Van Hinsbergen, D.J.J., 2011. Direct terrestrial-marine correlation demonstrates surprisingly late onset of the Last Interglacial in central Europe. Quat. Res. 75, 213-218.

Sier, M.J., Peeters, J., Dekkers, M.J., Parés, J.M., Chang, L., Busschers, F.S., Cohen, K.M., Wallinga, J., Bunnik, F.P.M., Roebroeks, W., 2015. The Blake Event near the Eemian type locality – A diachronic onset of the Eemian in Europe. Quat. Geochron. 28, 12-28

Simpson, M.J.R., Milne, G.A., Huybrechts, P., Long, A.J., 2009. Calibrating a glaciological model of the Greenland ice sheet from the last glacial maximum to present-day using field observations of relative sea level and ice extent. Quat. Sci. Rev. 28, 1631-1657.

Singer, B.S., Guillou, H., Jicha, B.R., Zanella, E., Camps, P., 2014. Refining the Quaternary geomagnetic instability time scale (GITS): Lava flow recordings of the Blake and Post-Blake excursions. Quat. Geochron. 21, 16-28.

Stein, M., Wasserburg, G.J., Aharon, P., Chen, J.H., Zhu, Z.R., Bloom, A., Chappell, J., 1993. TIMS U-series dating and stable isotopes of the Last Interglacial event in Papua New Guinea. Geochim. Cosmochim. Acta 57, 2541-2554.

Sterken, M., Roberts, S.J., Hodgson, D.A., Vyverman, W., Balbo, A.L., Sabbe, K., Moreton, S.G., Verleyen, E., 2012. Holocene glacial and climate history of Prince Gustav Channel, northeastern Antarctic Peninsula. Quat. Sci. Rev. 31, 93-111.

Stirling, C.H., Esat, T.M., Lambeck, K., McCulloch, M.T., 1998. Timing and duration of the last interglacial; evidence for a restricted interval of widespread coral reef growth. Earth Planet. Sci. Lett. 160, 745–762.

Streif, H., 1990. Quaternary sea-level changes in the North Sea, an analysis of amplitudes and velocities. In: Brosche, P., Sündermann, P.J. (Eds.), Earth's Rotation from Eons to Days, Springer-Verlag Berlin Heidelberg, pp. 201-214.

Streif, H., 2004. Sedimentary record of Pleistocene and Holocene marine inundations along the North Sea coast of Lower Saxony, Germany. Quat. Int. 112, 3-28.

Svendsen, J.I., Alexanderson, H., Astakhov, V.I., Demidov, I., Dowdeswell, J.A.,Funder, S., Gataullin, V., et al., 2004. Late Quaternary ice sheet history of northern Eurasia. Quat. Sci. Rev. 23, 1229-1271.

Szabo, B. J., Ludwig, K. R., Muhs, D. R., Simmons, K. R., 1994. Thorium-230 ages of corals and duration of the last interglacial sea-level high stand on Oahu, Hawaii. Science 266, 93–96.

Temler, H., 1995. Neue Ergebnisse zum Aufbau des Eem-Interglazials in Nordfriesland. Meyniana 47, 83-100.

Thompson, W., Goldstein, S.L., 2005. Open-system coral ages reveal persistent suborbital sea-level cycles. Science 308, 401–404.

Thompson W.G., Curran, H.A., Wilson, M.A., White, B., 2011. Sea-level oscillations during the last interglacial highstand recorded by Bahamas corals. Nat. Geosci. 4, 684-687.

Turner, C., 2002. Formal status and vegetational development of the Eemian interglacial in northwestern and southern Europe. Quat. Res. 58, 41-44.

de Vernal, A., Hillaire-Marcel, C., 2008. Natural variability of Greenland climate, vegetation and ice volume during the last million years. Science 320, 1622-1625.

Van Leeuwen, R.J.W., Beets, D., Bosch, J.H.A., Burger, A.W., Cleveringa, P., Van Harten, D., Herngreen, G.F.W., Kruk, R.W., Langereis, C.G., Meijer, T., Pouwer, R., De Wolf, H., 2000.

Stratigraphy and integrated facies analysis of the Eemian in Amsterdam- Terminal. Geol. en Mijnb. 79, 161-196.

Vaughan, D.G., Barnes, D.K.A., Fretwell,P.T., Bingham, R.G., 2011. Potential seaways across West Antarctica. Geochm. Geophys. Geosys. 12, 1-11.

Vis, G-J.,. Cohen, K.M., Westerhoff, W.E., Ten Veen, J.H., Hijma, M.P., van der Spek, A.J.F., Vos. P.C., 2015. Paleogeography. In: Shennan, I., Long, A.J., Horton, B.P. (eds). Handbook of Sea-Level Research, American Geophysical Union (Wileys), p. 514-535.

Waller, M.J., Long, A.J., 2003. Holocene coastal evolution and sea-level change on the southern coast of England: a review**.** J. Quat. Sci. 18, 351-360.

West, R.G., Sparks, B.W., 1960. Coastal interglacial deposits of the English Channel. Phil. Trans. R. Soc. Lond. B306, 95-133.

Winn, K., Glos, R., Averdieck, F.R., Erlenkeuser, H., 2000. On the age of the marine Eem in northwestern Germany. Geologos 5, 41-56.

Zagwijn,W.H., 1961. Vegetation, climate and radiocarbon datings in the Late Pleistocene of the Netherlands. Part I: Eemian and Early Weichselian. Mededelingen van de Geologische Stichting, Nieuwe Serie 14, 15-45.

Zagwijn, W.H., 1974. The palaeogeographic evolution of The Netherlands during the Quaternary. Geol. en Mijnb. 53, 369-385.

Zagwijn, W.H., 1983. Sea-level changes in The Netherlands during the Eemian. Geol. en Mijnb. 437-450.

Zagwijn, W.H., 1989. The Netherlands during the Tertiary and the Quaternary: a case history of coastal lowland evolution. Geol. en Mijnb. 68, 107-120.

Zagwijn, W.H., 1996. An analysis of Eemian climate in Western and Central Europe. Quat. Sci. Rev., 15, 451-469.

List of Figures

Figure 1: Illustrative relative sea-level records from the last interglacial: A: The Seychelles (Dutton et al., 2015). B: The Red Sea, core KL11 using the age models of Rohling et al. (2008) and Grant et al. (2012); C: Yucatán Peninsula (Mexico) (Blanchon et al., 2009); D: The Bahamas (Thompson and Goldstein, 2005); E: Western Australia (O'Leary et al., 2013), the dashed green line is an inferred sea-level curve based on a minimum coral palaeodepth; and F: The Netherlands. The graph shows the original data of Zagwign (1983) and an enlarged dataset (Streif, 1990) which has been corrected for GIA, compaction and tectonics (Lambeck, 1996).

Figure 2: Schematic relative sea-level histories recorded at near- and far-field sites during the last interglacial (modified from Cohen et al., 2012). Note that the highstand occurs earlier in the far-field compared to the near-field. A fluctuating sea-level history is depicted for illustrative purposes to show how such a record might be recorded in each setting.

Figure 3: Location map of Northwest Europe showing last interglacial site names referred to in the text.

Figure 4: Reconstruction depicting (A) the Netherlands, (B) the Last Interglacial coastal configuration in the Netherlands during the sea-level highstand (modified from Peeters et al. (2015)), (B) the glacial basins in the Netherlands (modified from Cleveringa et al. (2000)).

Figure 5: Simplified lithostratigraphy in the Amersfoort Basin (modified from Zagwijn (1983)). Position of pollen zones are approximate, based upon Zagwijn (1983).

Figure 6: Summary lithology and selected biostratigraphic data from the Amersfoort-1 and Amsterdam Terminal boreholes (modified from Van Leeuwen et al. (2000) and Cleveringa et al. (2000))

Figure 7: The Zagwign (1983) Netherlands sea level curve plotted against the established pollen zone chronology (in black) and Sier et al. (2015) chronology (in grey). The approximate timing of the Seychelles and Western Australia sea level jumps (as shown in Figure 1) are marked.

Figure 8: Sea-level predictions associated with hypothetical collapse/regrowth cycles of the Greenland and Antarctic ice sheets. Experiments G1 and A1 assume that Greenland and Antarctica, respectively, are subjected to growth-collapse cycles with amplitudes that vary between c. ± 2-3 and 5 m. A) Predictions assuming a Greenland-only origin for sea-level oscillations/jumps; B) Predictions assuming an Antarctic-only origin. Two periods of mass loss are shown for Greenland (122-121 k yr, 120-119 k yr) and three for Antarctica (123-122 k yr, 120-119 k yr, 118-117 k yr). Details of experimental set-up associated with each model are provided in Supplementary Information Table S1.

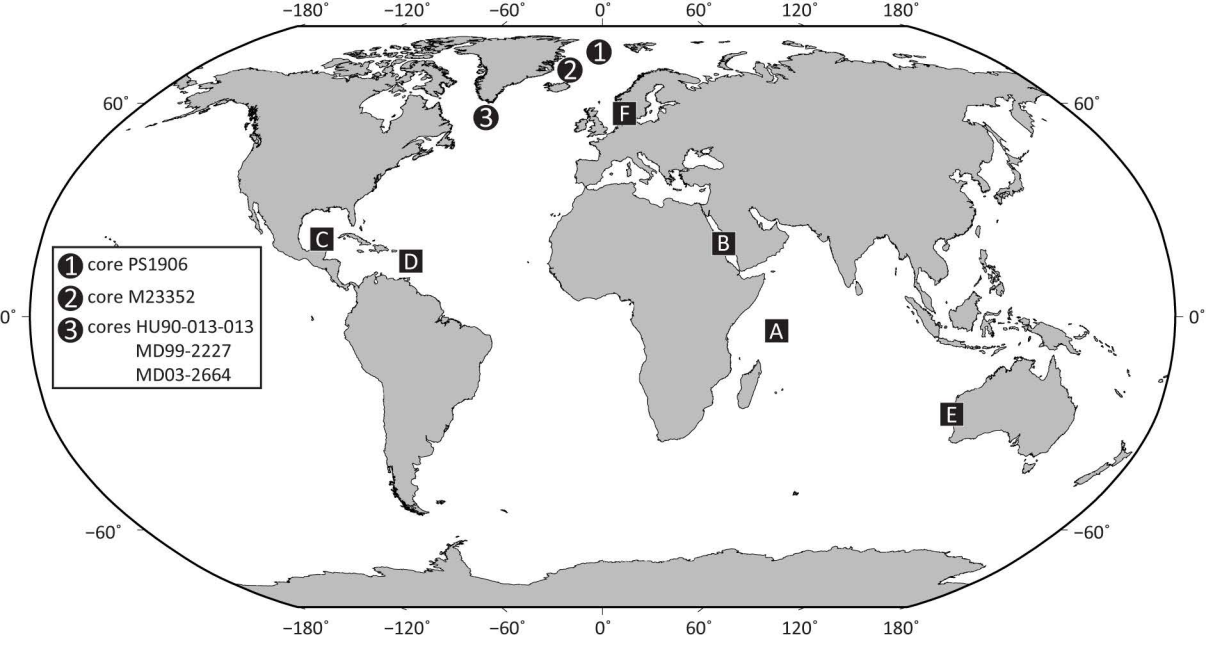
1 core PS1906
2 core M23352
3 cores HU90-013-013
MD99-2227
MD03-2664
A
B
C
D
E
F

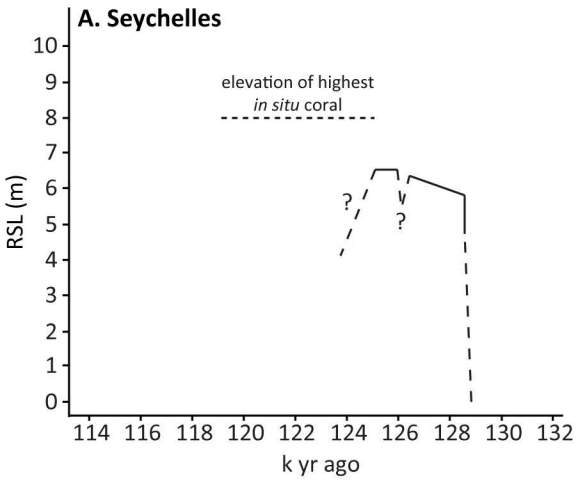
A. Seychelles
elevation of highest
in situ coral
RSL (m)
k yr ago

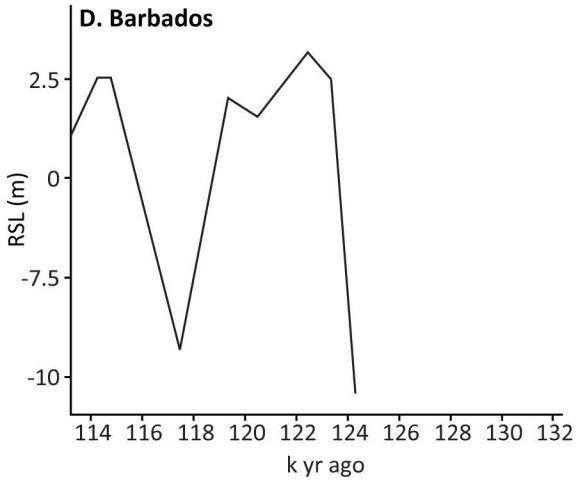
D. Barbados
RSL (m)
k yr ago

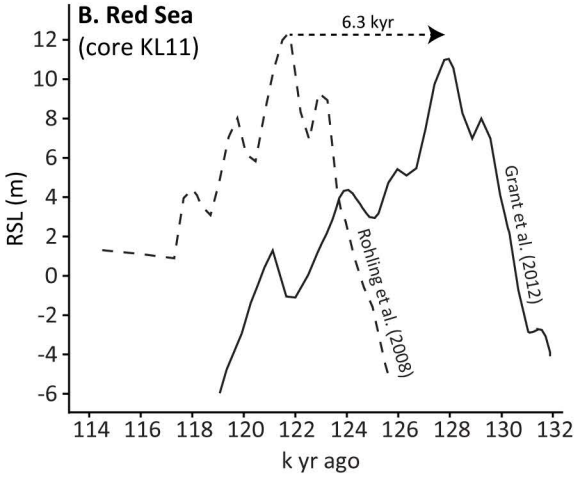
B. Red Sea
(core KL11)
6.3 kyr
Rohling et al. (2008)
Grant et al. (2012)
RSL (m)
k yr ago

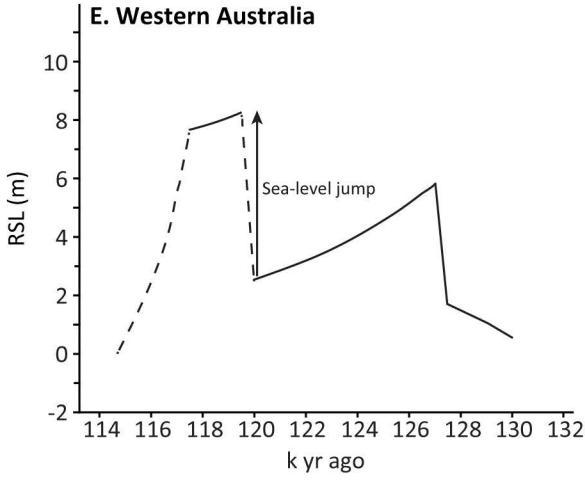
E. Western Australia
Sea-level jump
RSL (m)
k yr ago

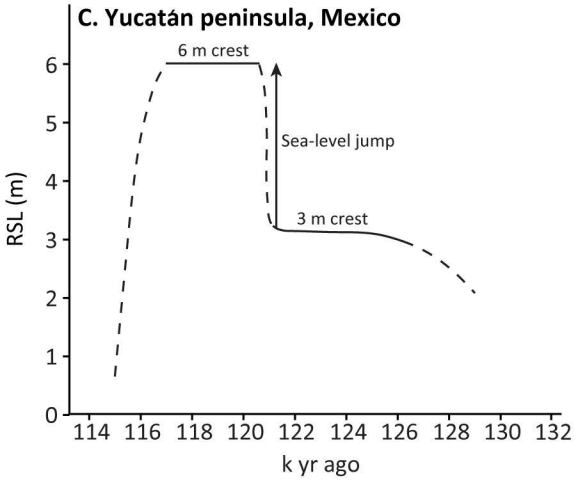
C. Yucatán peninsula, Mexico
6 m crest
Sea-level jump
3 m crest
RSL (m)
k yr ago

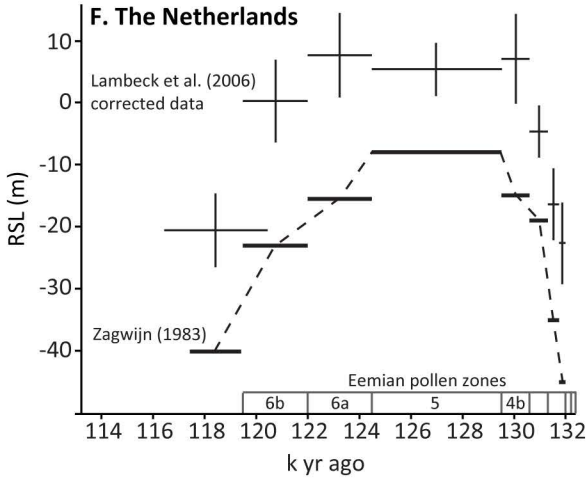
F. The Netherlands
Lambeck et al. (2006)
corrected data
Zagwijn (1983)
Eemian pollen zones
6b
6a
5
4b
RSL (m)
k yr ago

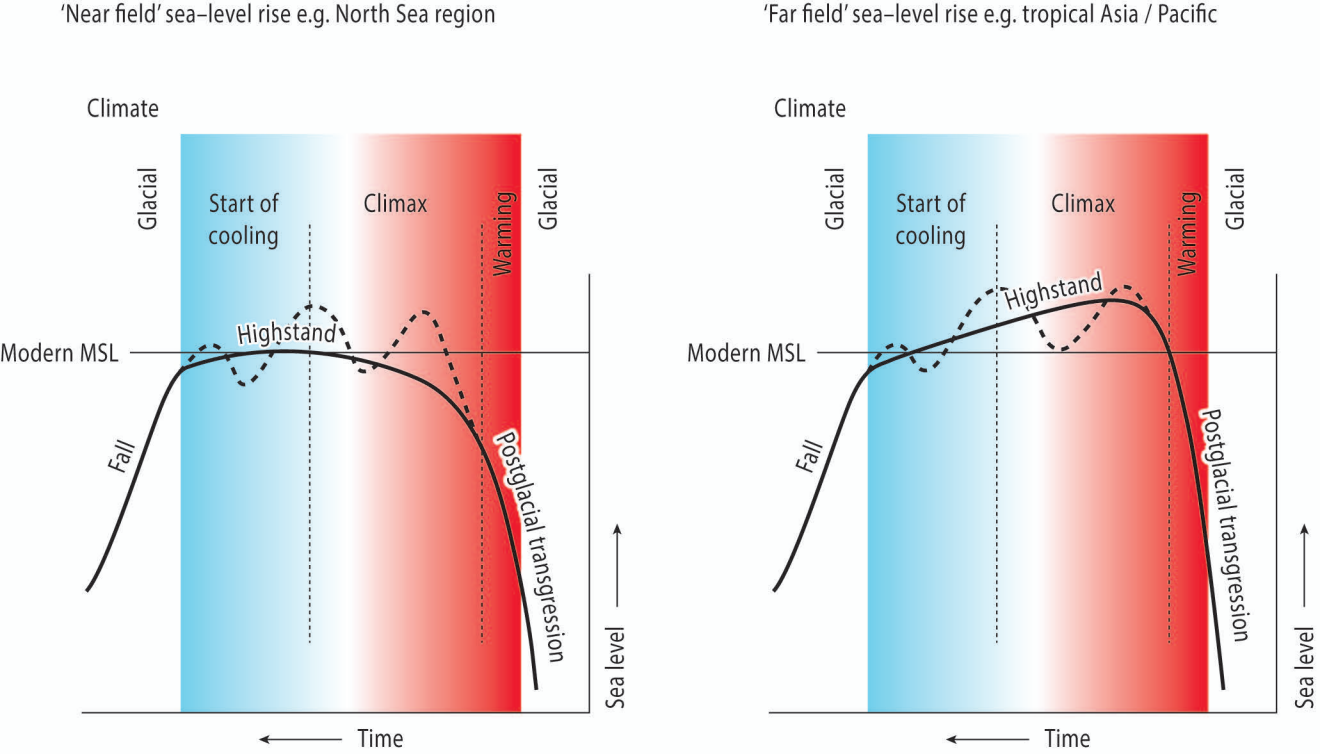
'Near field' sea–level rise e.g. North Sea region
Climate
Glacial
Start of cooling
Climax
Warming
Glacial
Modern MSL
Highstand
Fall
Postglacial transgression
Sea level
Time
'Far field' sea–level rise e.g. tropical Asia / Pacific
Climate
Glacial
Start of cooling
Climax
Warming
Glacial
Modern MSL
Highstand
Fall
Postglacial transgression
Sea level
Time

North Sea

Baltic

English Channel

White Sea

North Atlantic

Europe

Peski, Russia

Firth of Forth, Scotland

Tattershall, England

Wretton, England

Thames Estuary, England

Selsey & Stone, England

Amsterdam & Amersfoort, The Netherlands

Mommark, Denmark

Dagebüll, Germany

Sztum & Cierpięta, Poland

−5°

0°

5°

10°

15°

20°

25°

60°

55°

50°

70°

40°

−10°

30°

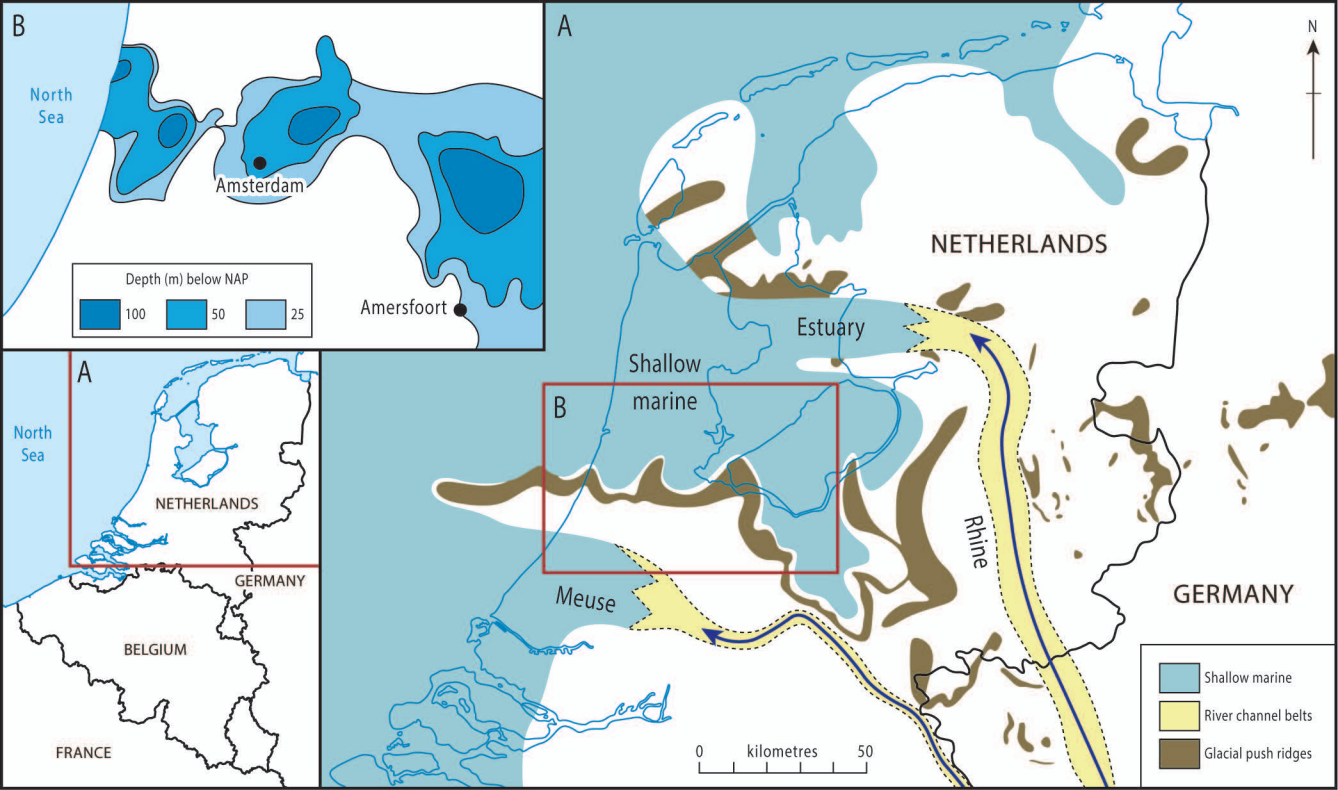
B
North Sea
Amsterdam
Depth (m) below NAP
100
50
25
Amersfoort
A
North Sea
NETHERLANDS
GERMANY
BELGIUM
FRANCE
A
B
Shallow marine
Estuary
NETHERLANDS
Rhine
Meuse
GERMANY
N
0 kilometres 50
Shallow marine
River channel belts
Glacial push ridges

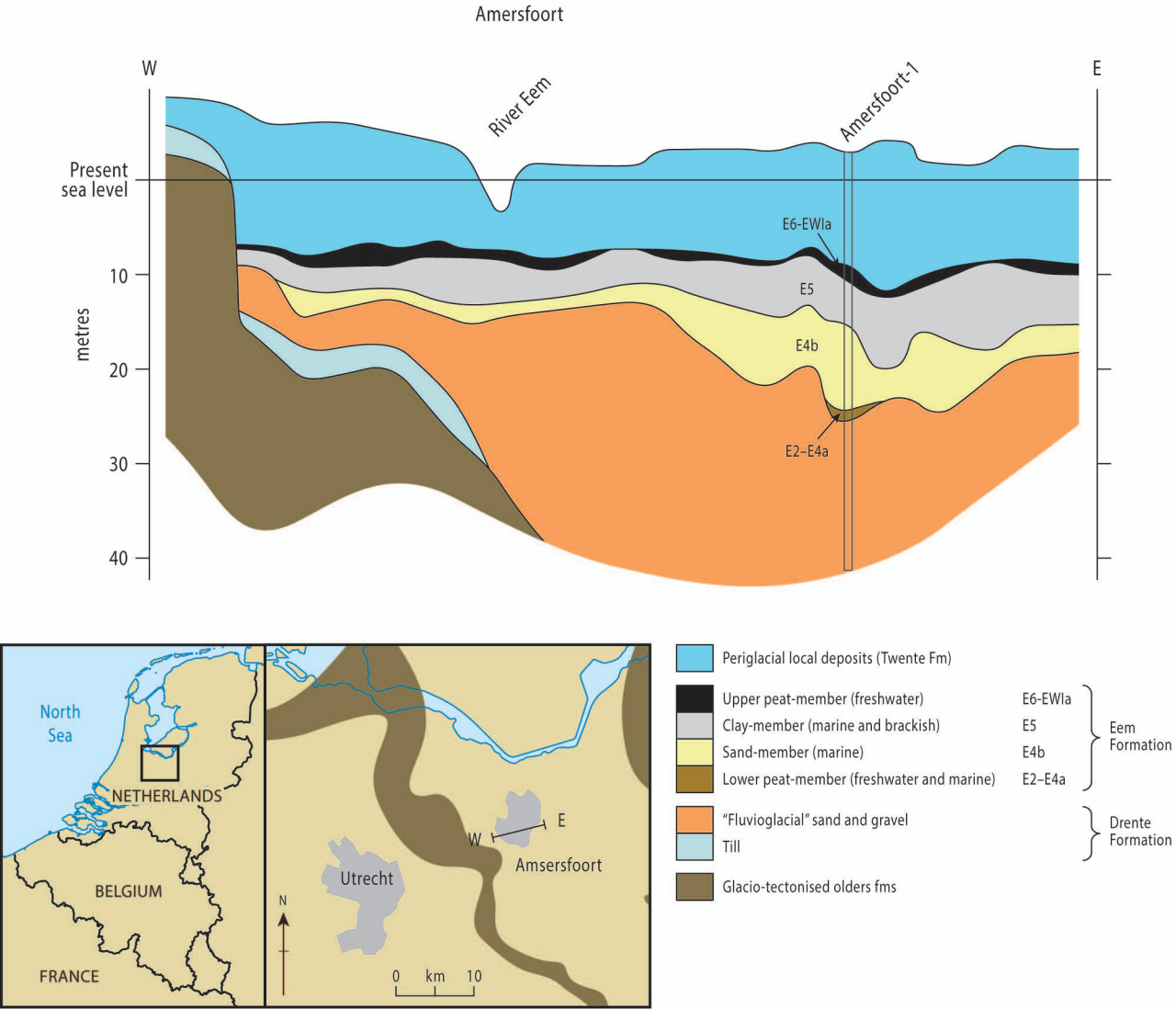
Amersfoort
W
E
River Eem
Amersfoort-1
Present sea level
metres
10
20
30
40
E6-EWIa
E5
E4b
E2–E4a
North Sea
NETHERLANDS
BELGIUM
FRANCE
Utrecht
Amersfoort
W
E
N
0 km 10
Periglacial local deposits (Twente Fm)
Upper peat-member (freshwater) E6-EWIa
Clay-member (marine and brackish) E5
Sand-member (marine) E4b
Lower peat-member (freshwater and marine) E2–E4a
Eem Formation
"Fluvioglacial" sand and gravel
Till
Drente Formation
Glacio-tectonised olders fms

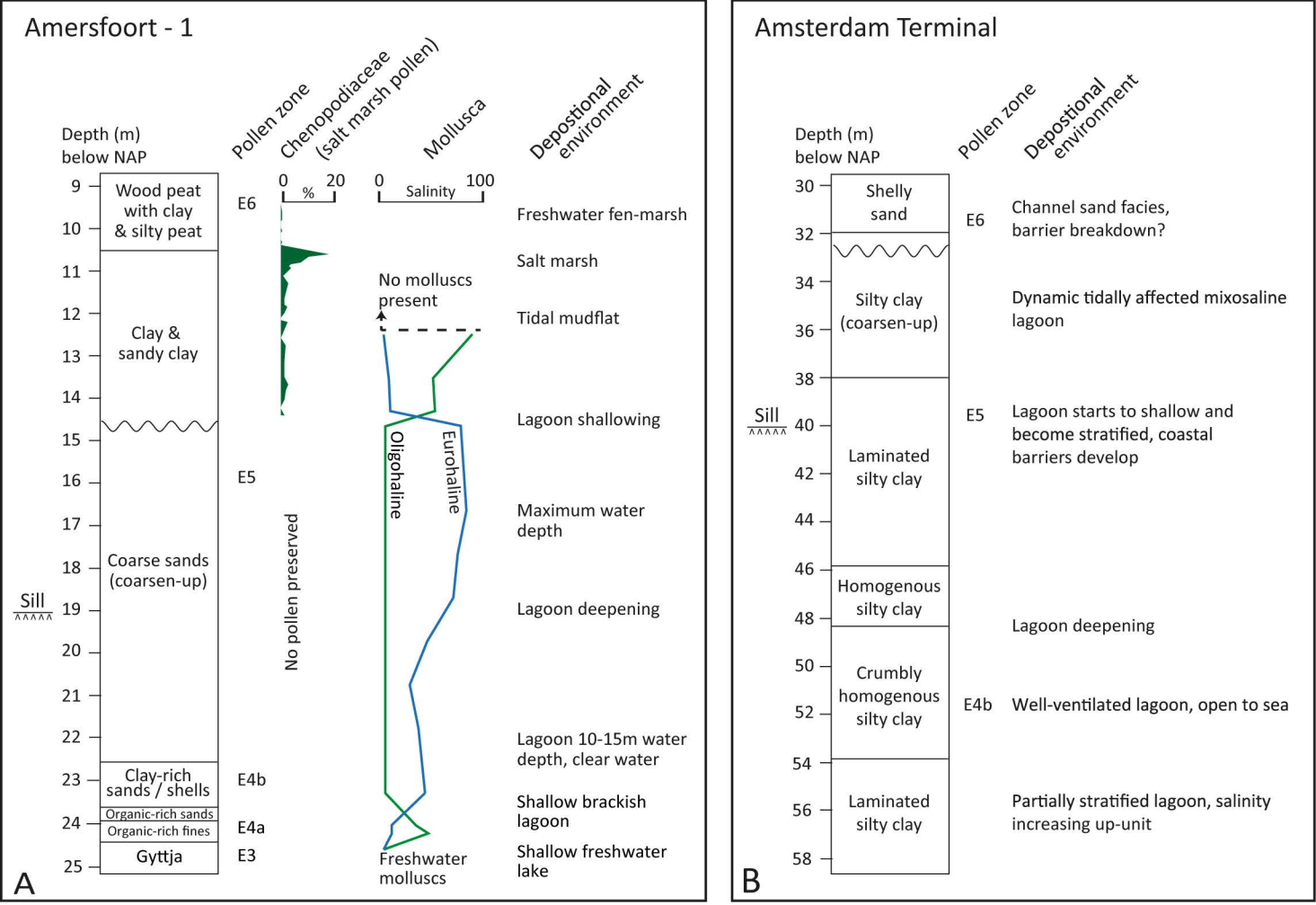
Amersfoort - 1
Depth (m) below NAP
Pollen zone
Chenopodiaceae (salt marsh pollen)
Mollusca
Depostional environment
0 % 20
0 Salinity 100
9
10
11
12
13
14
15
16
17
18
19
20
21
22
23
24
25
Wood peat with clay & silty peat
Clay & sandy clay
Coarse sands (coarsen-up)
Sill
Clay-rich sands / shells
Organic-rich sands
Organic-rich fines
Gyttja
E6
E5
E4b
E4a
E3
No pollen preserved
No molluscs present
Oligohaline
Eurohaline
Freshwater molluscs
Freshwater fen-marsh
Salt marsh
Tidal mudflat
Lagoon shallowing
Maximum water depth
Lagoon deepening
Lagoon 10-15m water depth, clear water
Shallow brackish lagoon
Shallow freshwater lake
A
Amsterdam Terminal
Depth (m) below NAP
Pollen zone
Depostional environment
30
32
34
36
38
40
42
44
46
48
50
52
54
56
58
Shelly sand
Silty clay (coarsen-up)
Laminated silty clay
Sill
Homogenous silty clay
Crumbly homogenous silty clay
Laminated silty clay
E6
E5
E4b
Channel sand facies, barrier breakdown?
Dynamic tidally affected mixosaline lagoon
Lagoon starts to shallow and become stratified, coastal barriers develop
Lagoon deepening
Well-ventilated lagoon, open to sea
Partially stratified lagoon, salinity increasing up-unit
B

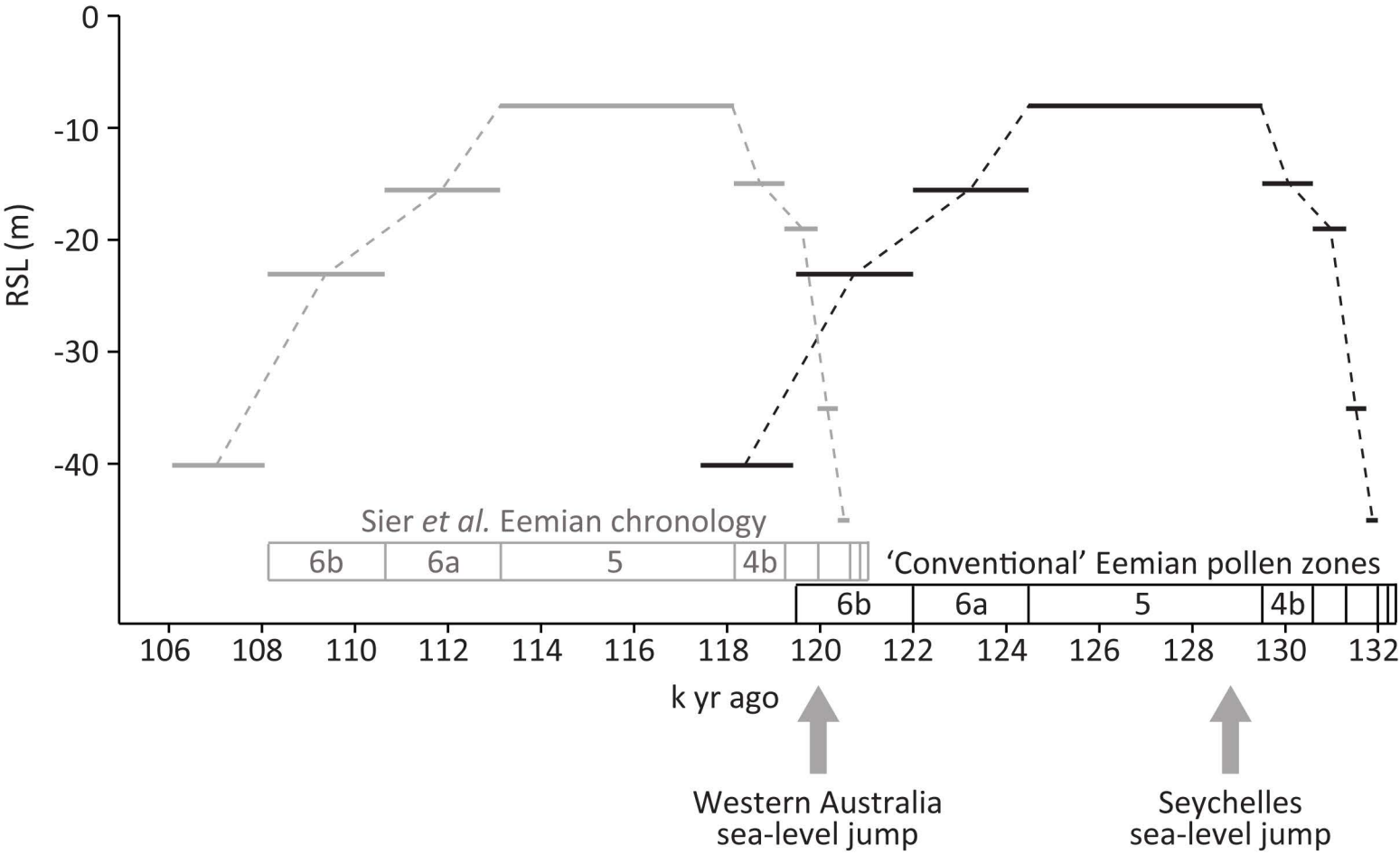
0
-10
-20
-30
-40
RSL (m)
Sier et al. Eemian chronology
6b
6a
5
4b
'Conventional' Eemian pollen zones
6b
6a
5
4b
106
108
110
112
114
116
118
120
122
124
126
128
130
132
k yr ago
Western Australia sea-level jump
Seychelles sea-level jump

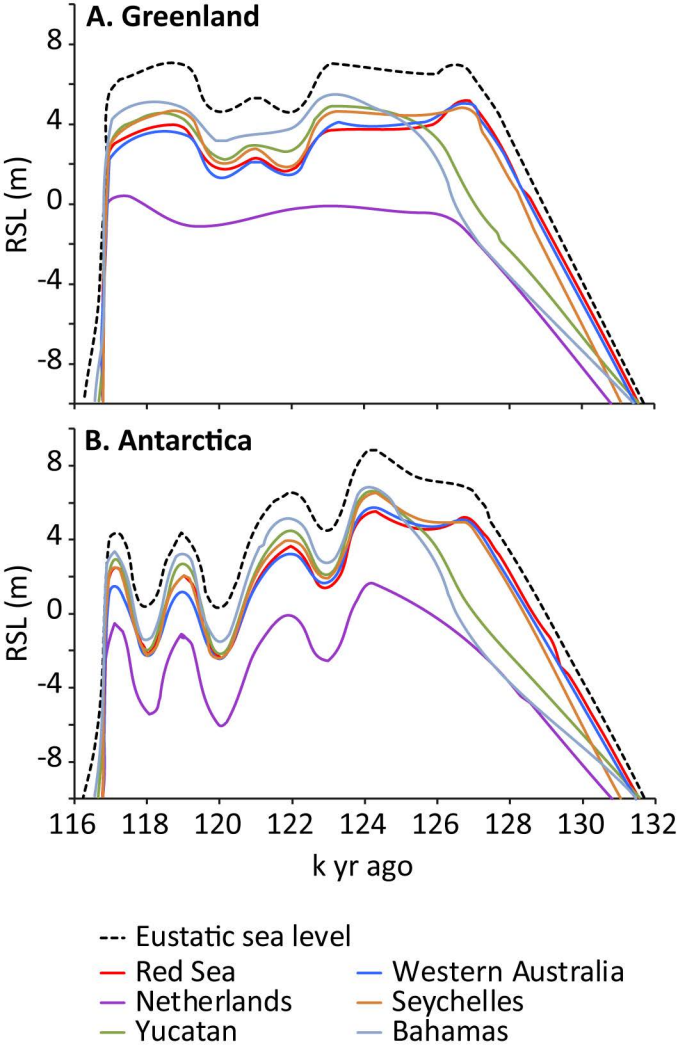
A. Greenland
B. Antarctica
RSL (m)
8
4
0
-4
-8
116
118
120
122
124
126
128
130
132
k yr ago
Eustatic sea level
Red Sea
Western Australia
Netherlands
Seychelles
Yucatan
Bahamas

Quaternary Science Reviews 2015

Near-field sea-level variability in northwest Europe and ice sheet stability during the Last Interglacial

Long, A.J., Barlow, N.L.M., Busschers, F.S., Cohen, K.M., Gehrels, W. R. & Wake, L.M.

Supplementary information Table S1

Model parameters governing deglaciation scenarios A1 and G1. Columns 2,4 and 6 titled 'Extent' refer to the time period (kyr ago) which is used to represent the extent of global ice sheets applied at each time interval. Columns 3,5 and 7 denote the scaling factor applied uniformly to the regional ice distributions at each time step. For example, at 127.00 kyr BP in model A1, Antarctica, Greenland and the Rest of the World display ice cover identical to that at 122.00 kyr BP in ICE5G - HUY2 deglaciation history (Peltier, 2004; Simpson et al. 2009). These ice extents are scaled by a factor of 1.

Loading Step (kyr ago BP)	**Antarctica**		**Greenland**		**Rest of World**	
	Extent	**Scaling Factor**	**Extent**	**Scaling Factor**	**Extent**	**Scaling Factor**
132.00	116.00	0.980	116.00	0.980	116.00	0.980
127.00	122.00	1.000	122.00	1.000	122.00	1.000
126.00	122.00	1.000	122.00	1.000	122.00	1.000
125.00	122.00	0.999	122.00	1.000	122.00	1.000
124.00	122.00	0.998	122.00	1.000	122.00	1.000
123.00	122.00	1.020	122.00	1.000	122.00	1.000
122.00	122.00	1.000	122.00	1.000	122.00	1.000
121.00	122.00	1.020	122.00	1.000	122.00	1.000
120.00	122.00	1.090	122.00	1.000	122.00	1.000
119.00	122.00	1.030	122.00	1.000	122.00	1.000
118.00	122.00	1.100	122.00	1.000	122.00	1.000
117.00	116.00	1.000	122.00	1.000	122.00	1.000
116.00	116.00	1.000	115.00	1.000	116.00	1.000
Model G1						
Loading Step (kyr ago BP)	**Antarctica**		**Greenland**		**Rest of World**	
	Extent	**Scaling Factor**	**Extent**	**Scaling Factor**	**Extent**	**Scaling Factor**

132.00	116.00	0.980	116.00	0.980	116.00	0.980
127.00	122.00	1.000	122.00	1.000	122.00	1.000
126.00	122.00	1.000	122.00	0.900	122.00	1.000
125.00	122.00	1.000	122.00	0.700	122.00	1.000
124.00	122.00	1.000	122.00	0.500	122.00	1.000
123.00	122.00	1.000	122.00	0.200	122.00	1.000
122.00	122.00	1.000	116.00	1.500	122.00	1.000
121.00	122.00	1.000	116.00	1.050	122.00	1.000
120.00	122.00	1.000	116.00	1.500	122.00	1.000
119.00	122.00	1.000	122.00	0.200	122.00	1.000
118.00	122.00	1.000	122.00	1.000	122.00	1.000
117.00	122.00	1.000	116.00	1.000	122.00	1.000
116.00	116.00	1.000	116.00	1.000	116.00	1.000

Package 1

The figures contained in PDF packages **FigureS1.pdf** and **FigureS2.pdf** show plots of global relative sea level (RSL) and global sea level trends for the time period between 132 kyr BP and 116 kyr BP for deglaciation histories A1 and G1 respectively. Snapshots of global relative sea level are taken at the times listed in Table S1, whereas sea level trends correspond to the rate of change of relative sea level from the preceding time slice. For this reason, no corresponding sea-level trends accompany the plot of global relative sea level for 132 kyr BP.

FigureS1.pdf: Global relative sea level and sea level trends for deglaciation history A1.
FigureS2.pdf: Global relative sea level and sea level trends for deglaciation history G1.

Package 2

PDF Package 2 contains plots of global ice extent and changes in ice load between the time steps detailed in Table S1. The ice loads applied at each time step in Table S1 correspond to the change in ice thickness with respect to the previous time step. For example, the ice load applied at 122 kyr BP reflects the change in global ice thickness from 123 kyr to 122 kyr BP. For this reason, no corresponding change in ice load accompanies the plot of ice extent for 132 kyr BP.

FigureS3.pdf: Global ice extent and loading changes for deglaciation history A1.
FigureS4.pdf: Global ice extent and loading changes for deglaciation history G1.

Package 3

Package 3 contains two animations of global ice extent and corresponding relative sea level change for deglaciation histories A1 and G1.

AnimationS1.avi: Thirteen-frame Audio Video Interleaved (.avi) animation of global ice extent and relative sea level for the period 132 – 116 kyr BP for experiment A1.
AnimationS2.avi: Thirteen-frame Audio Video Interleaved (.avi) animation of global ice extent and relative sea level for the period 132 – 116 kyr BP for experiment G1.

RSL at time 132 kyr BP for Antarctica experiment

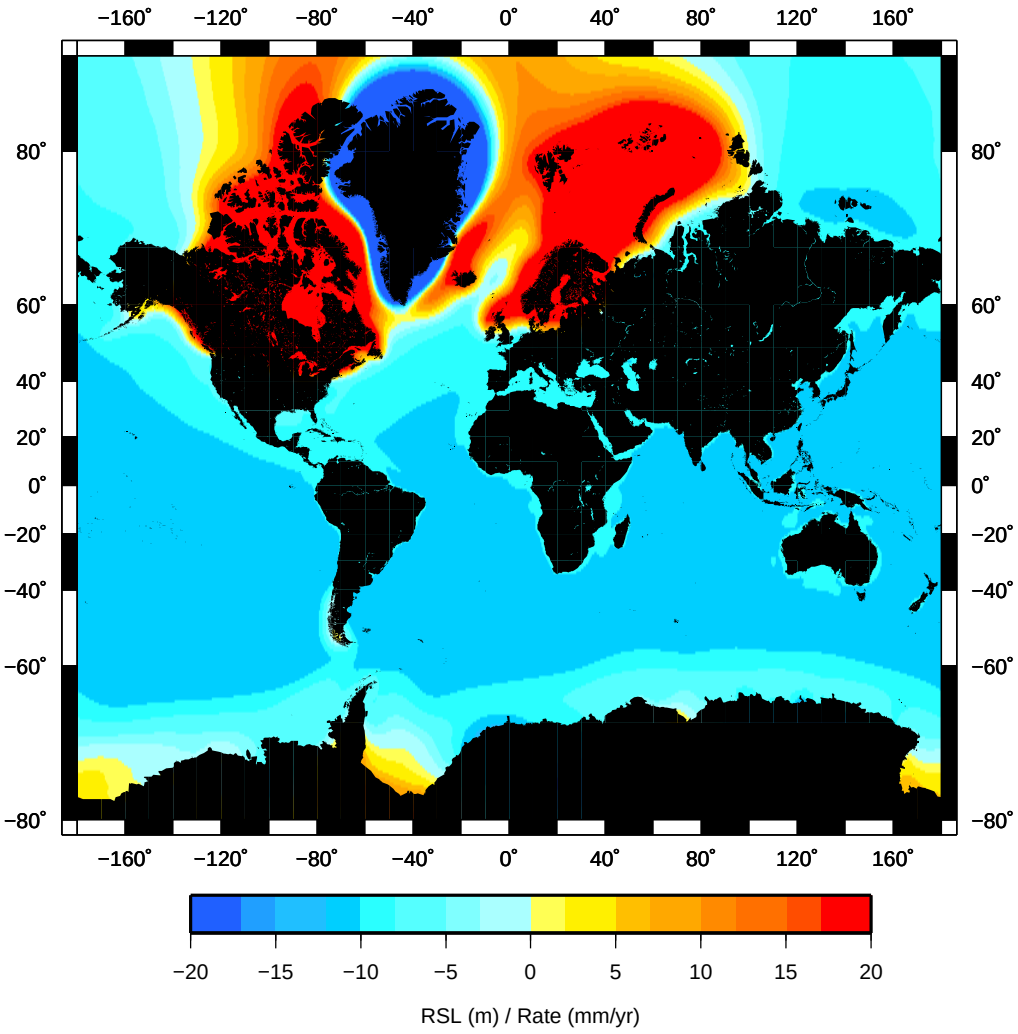

RSL (upper) and sea−level trend (lower) at time 127 kyr BP for Antarctica experiment

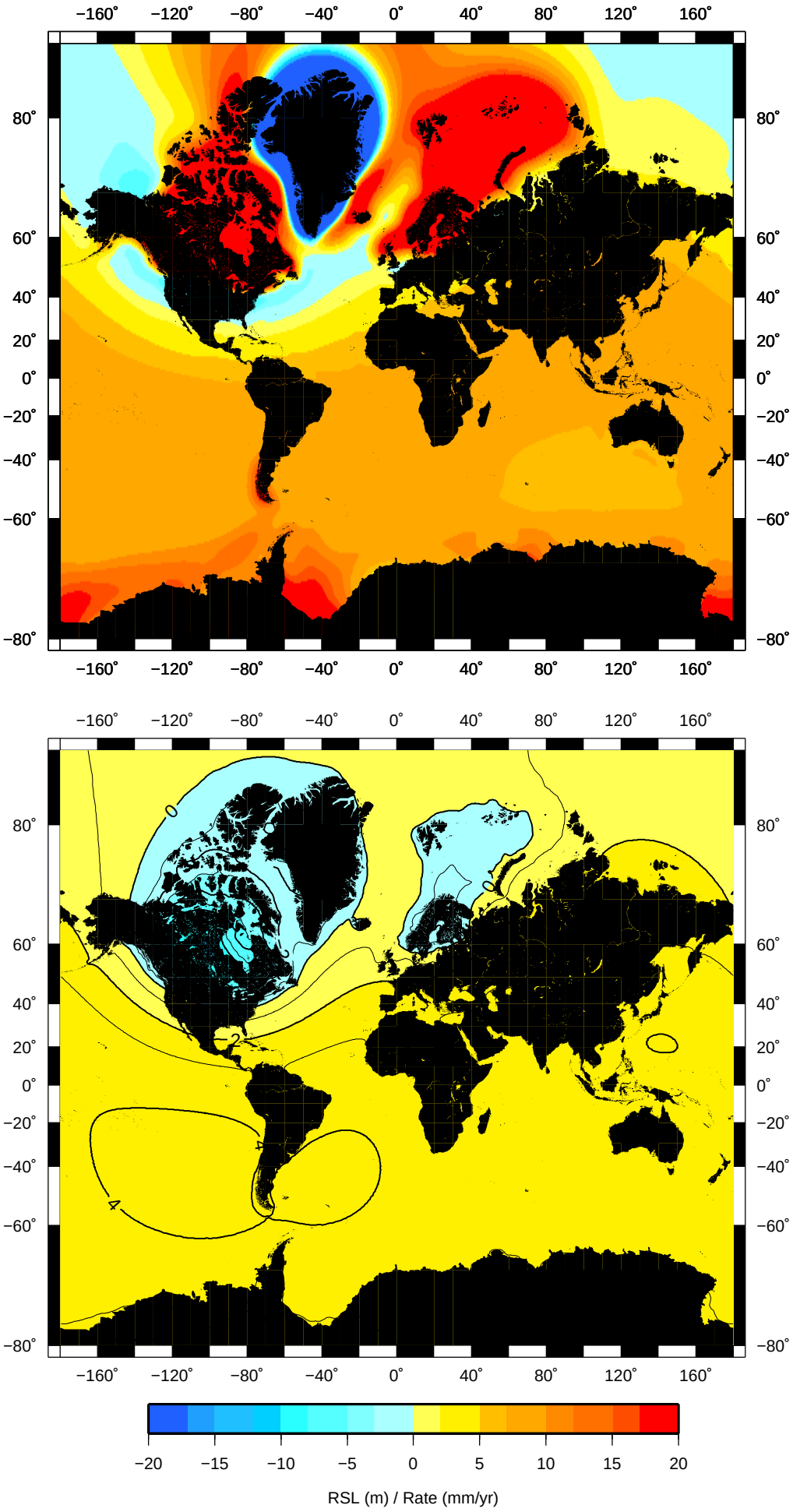

RSL (upper) and sea−level trend (lower) at time 126 kyr BP for Antarctica experiment

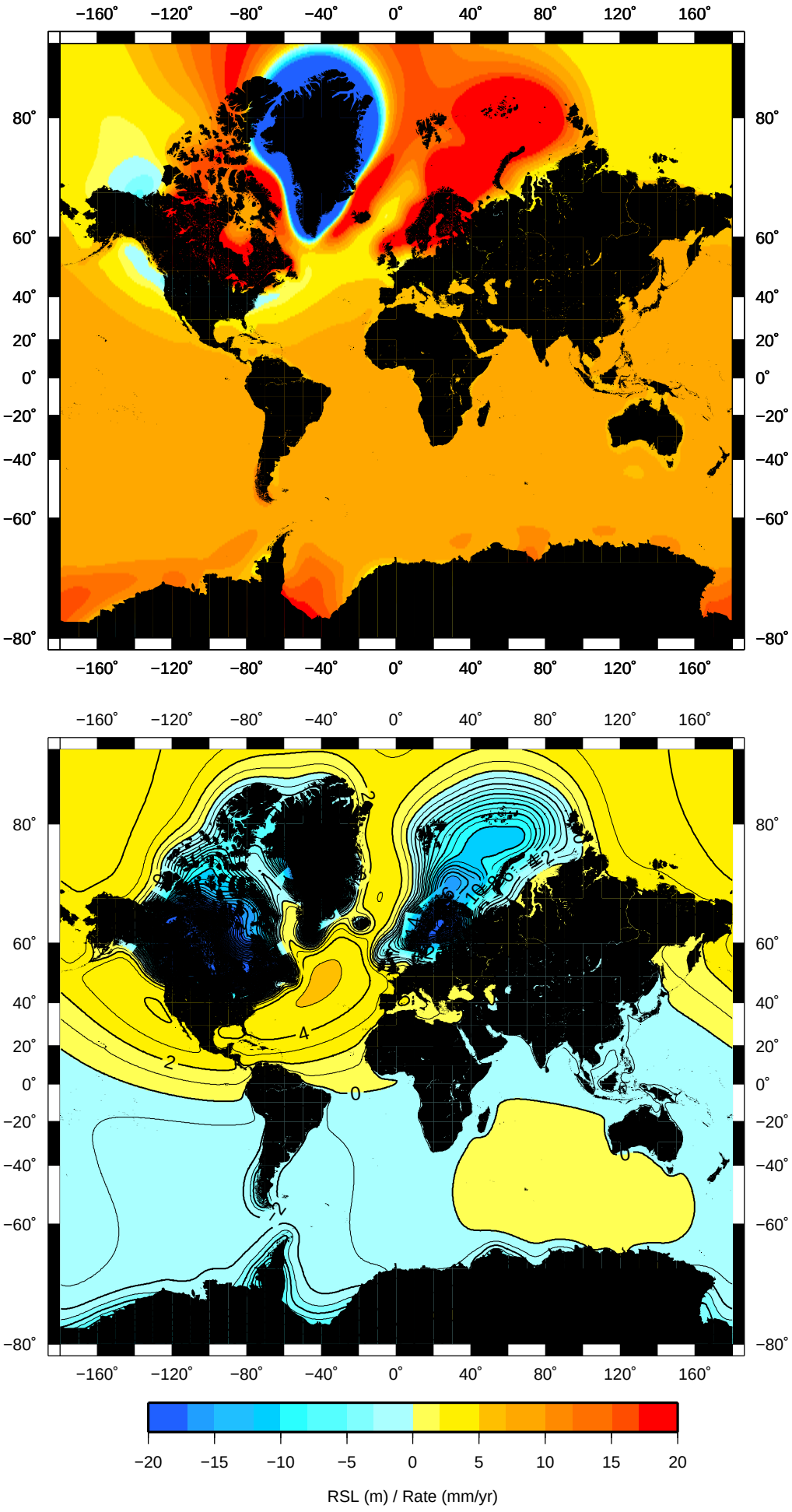

RSL (upper) and sea−level trend (lower) at time 125 kyr BP for Antarctica experiment

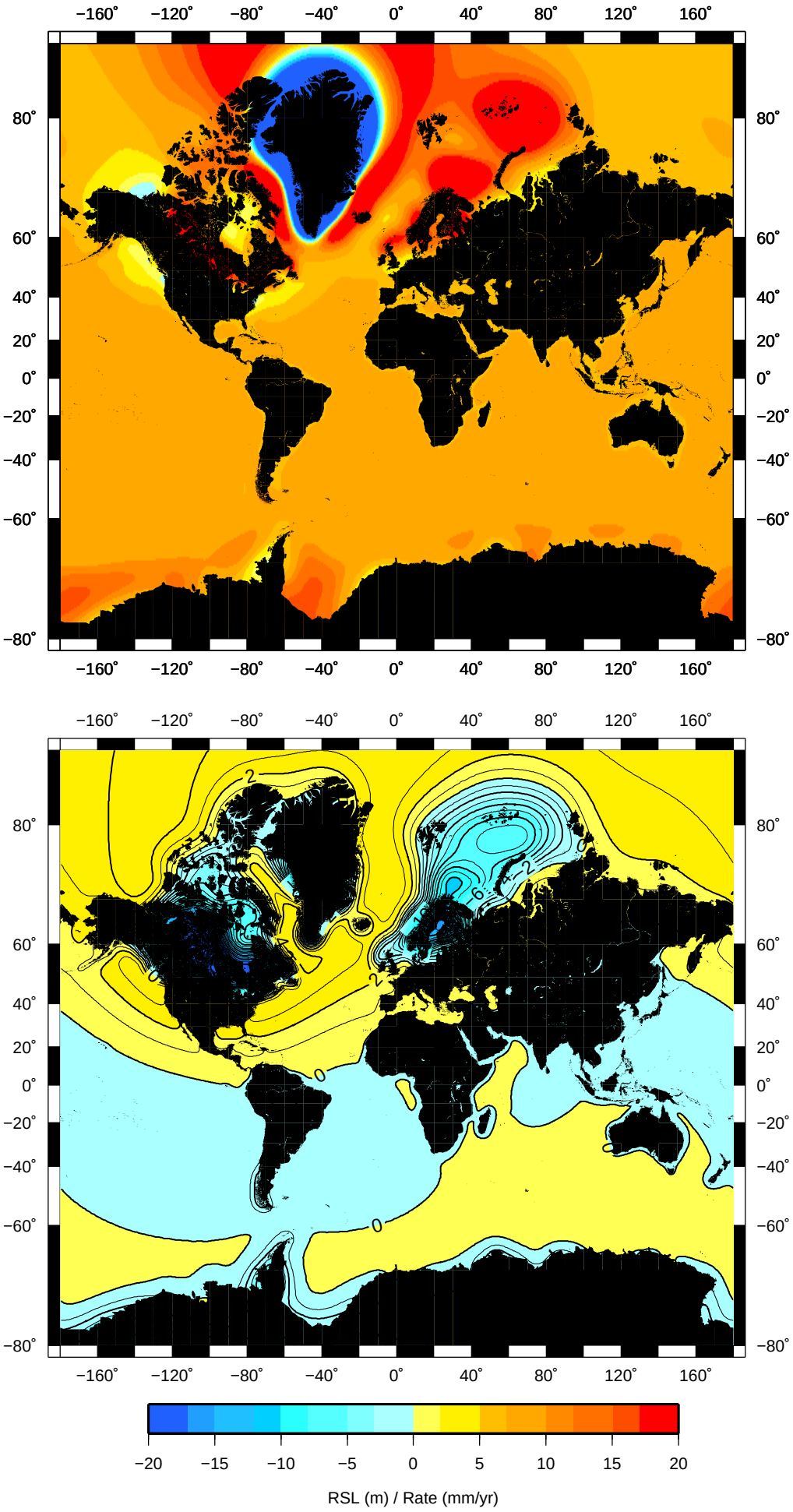

RSL (upper) and sea−level trend (lower) at time 124 kyr BP for Antarctica experiment

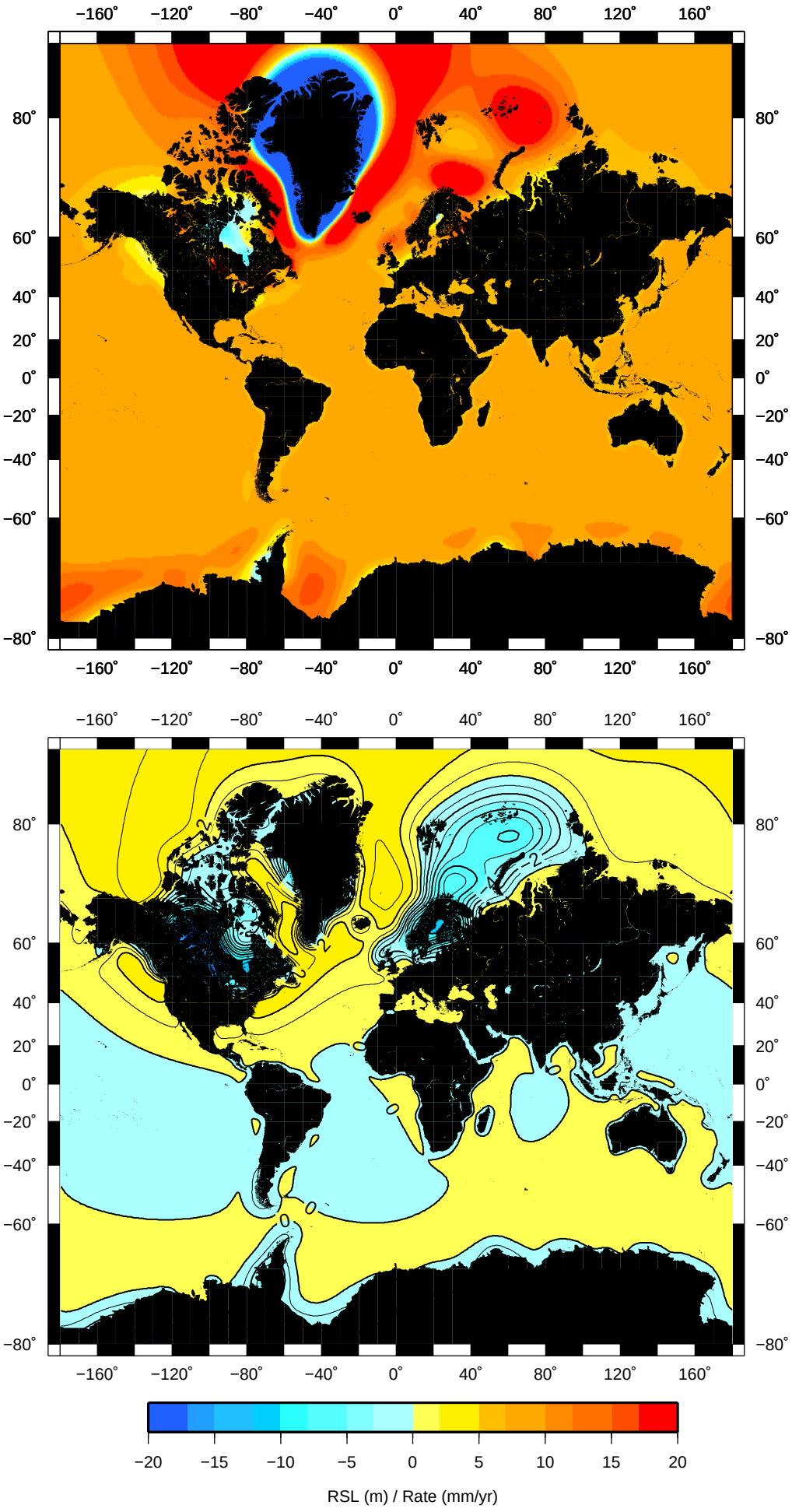

RSL (upper) and sea−level trend (lower) at time 123 kyr BP for Antarctica experiment

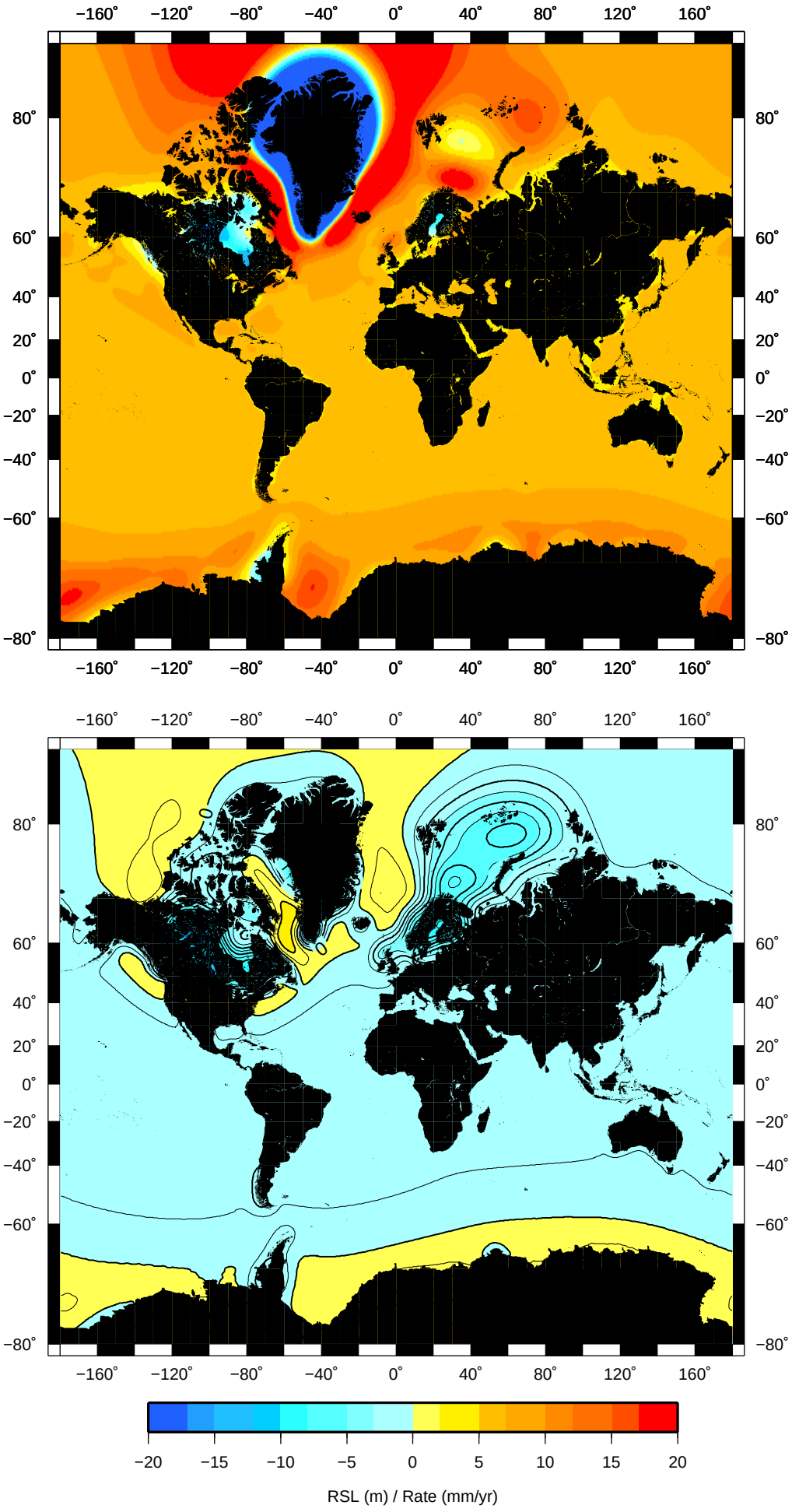

RSL (upper) and sea−level trend (lower) at time 122 kyr BP for Antarctica experiment

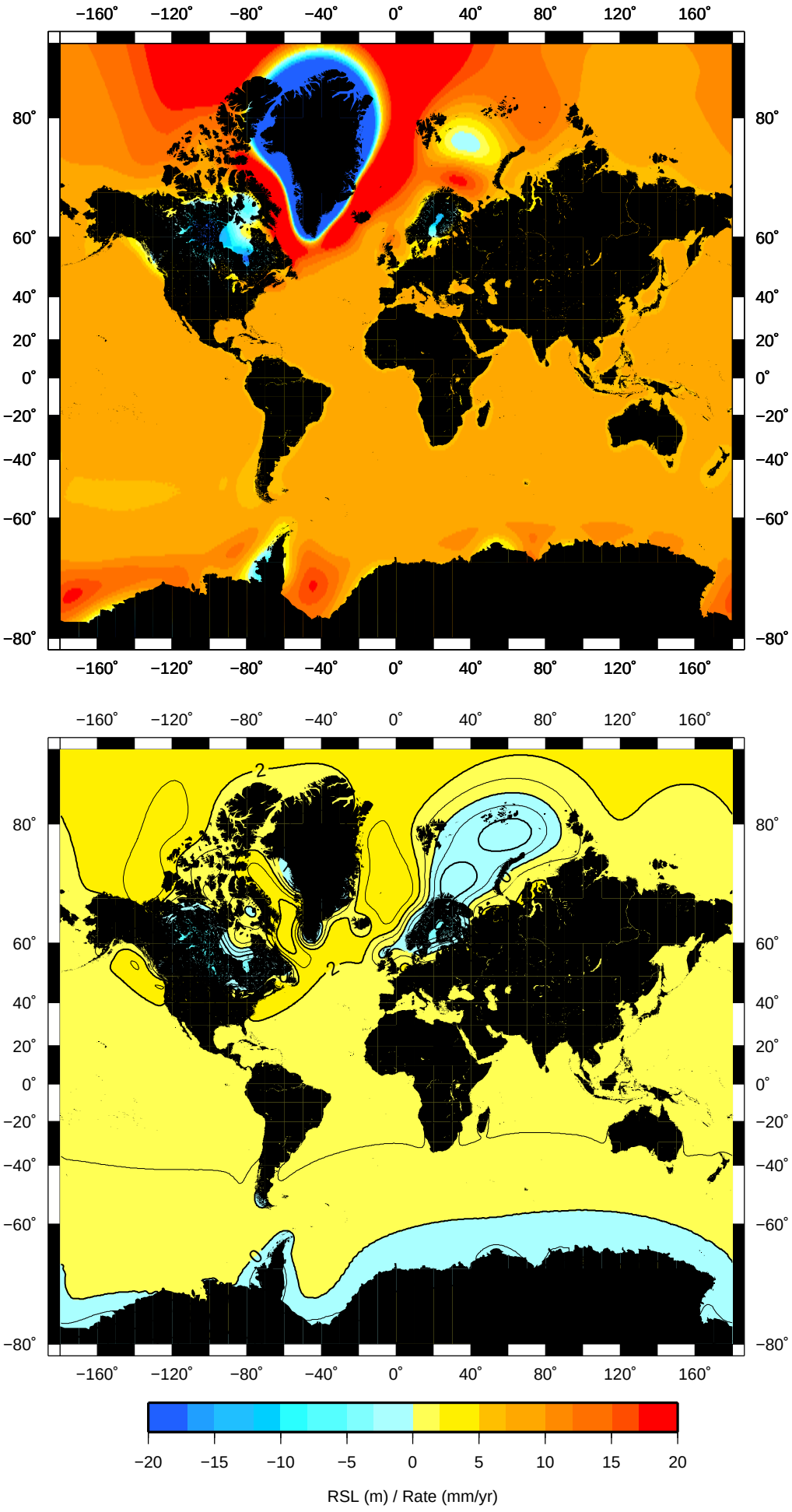

RSL (upper) and sea−level trend (lower) at time 121 kyr BP for Antarctica experiment

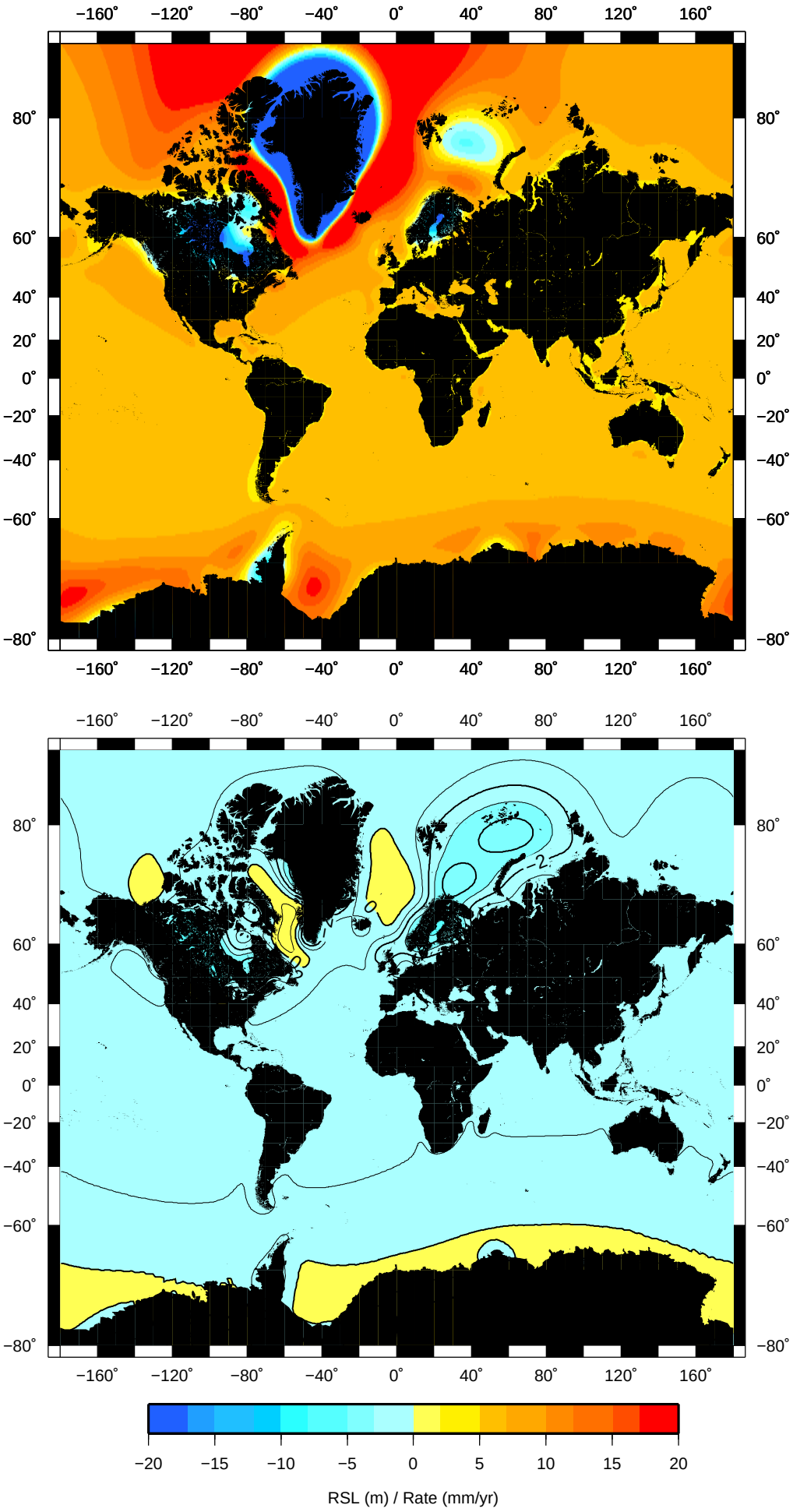

RSL (upper) and sea−level trend (lower) at time 120 kyr BP for Antarctica experiment

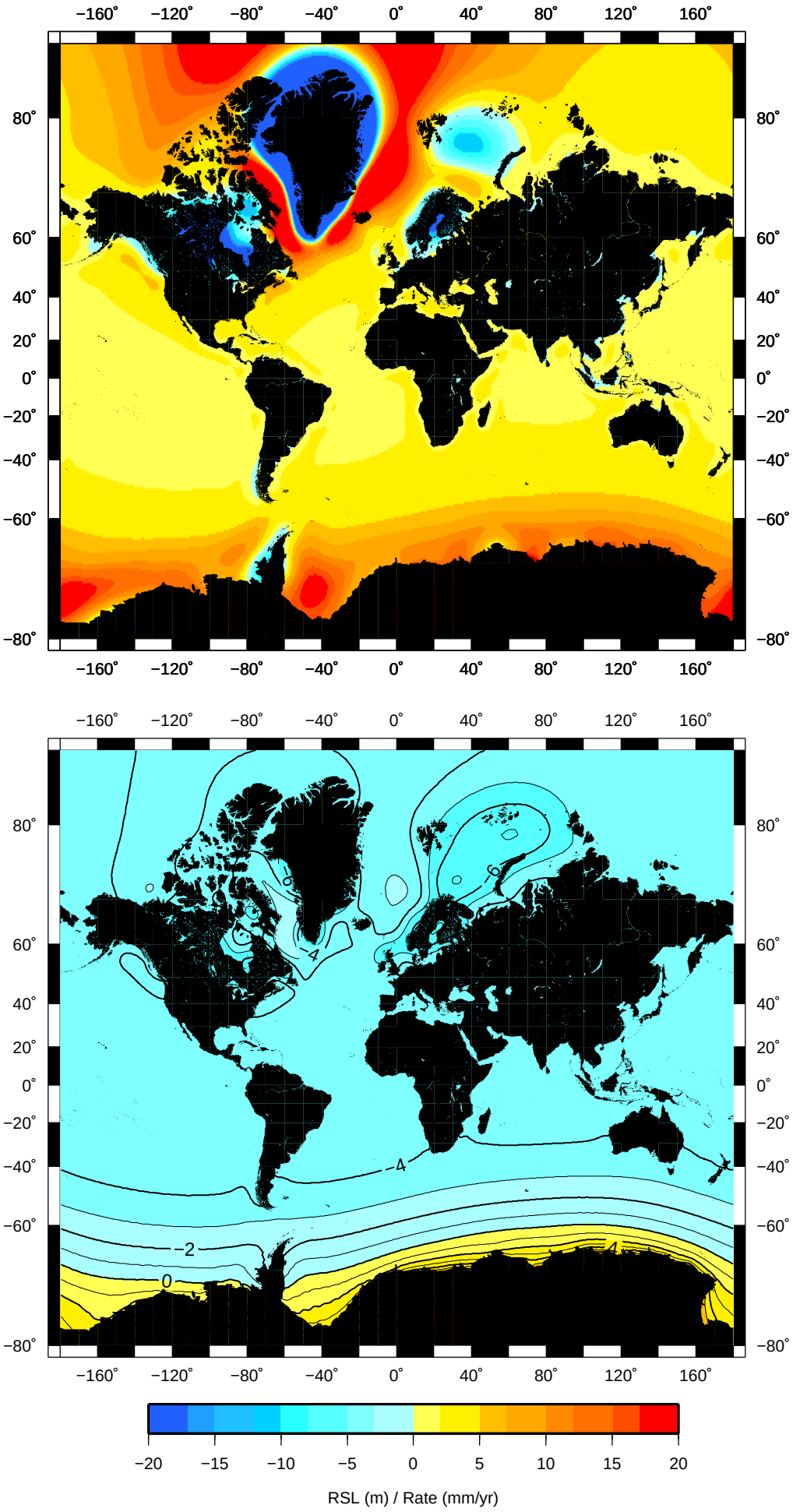

RSL (upper) and sea−level trend (lower) at time 119 kyr BP for Antarctica experiment

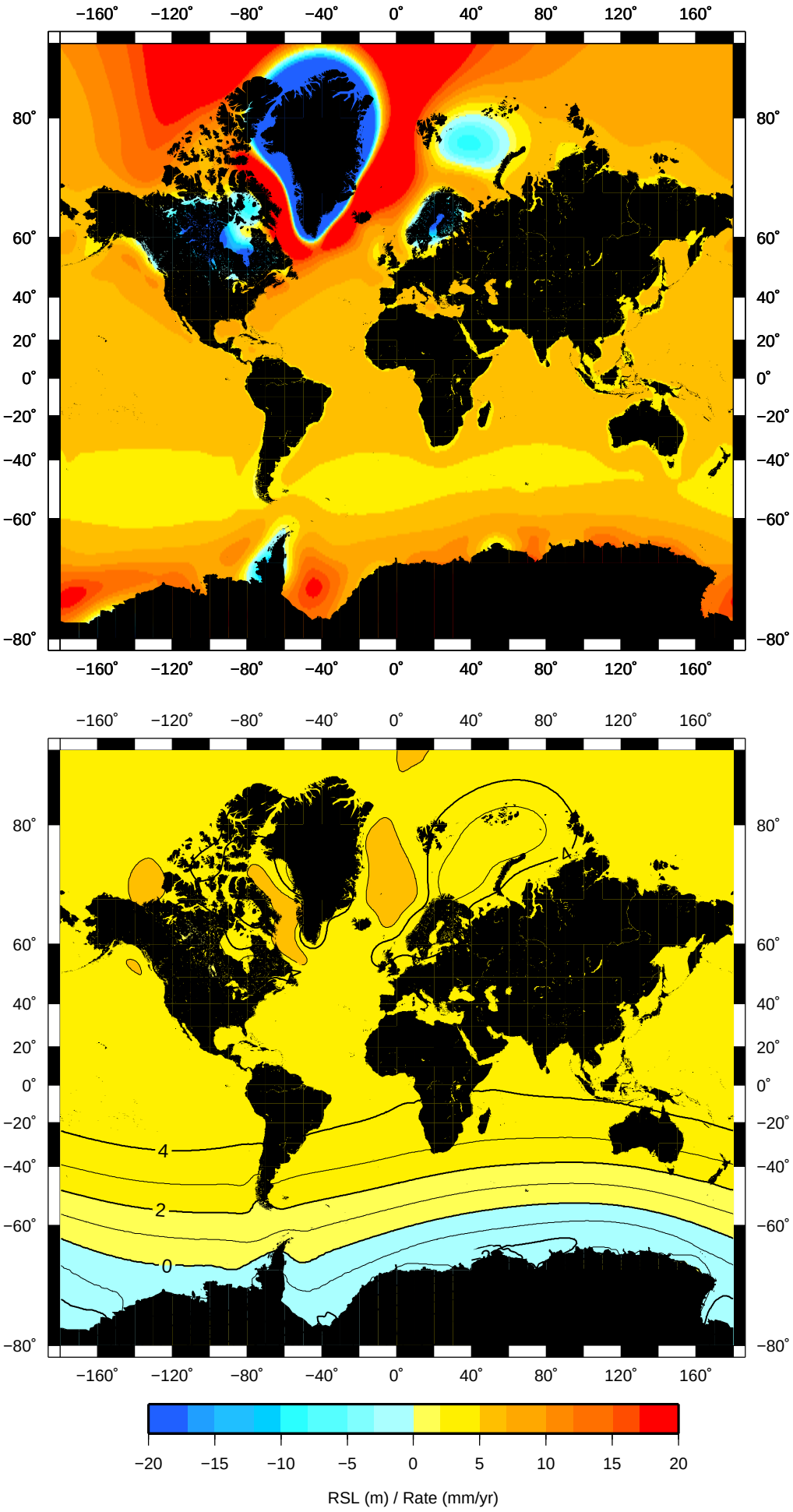

RSL (upper) and sea−level trend (lower) at time 118 kyr BP for Antarctica experiment

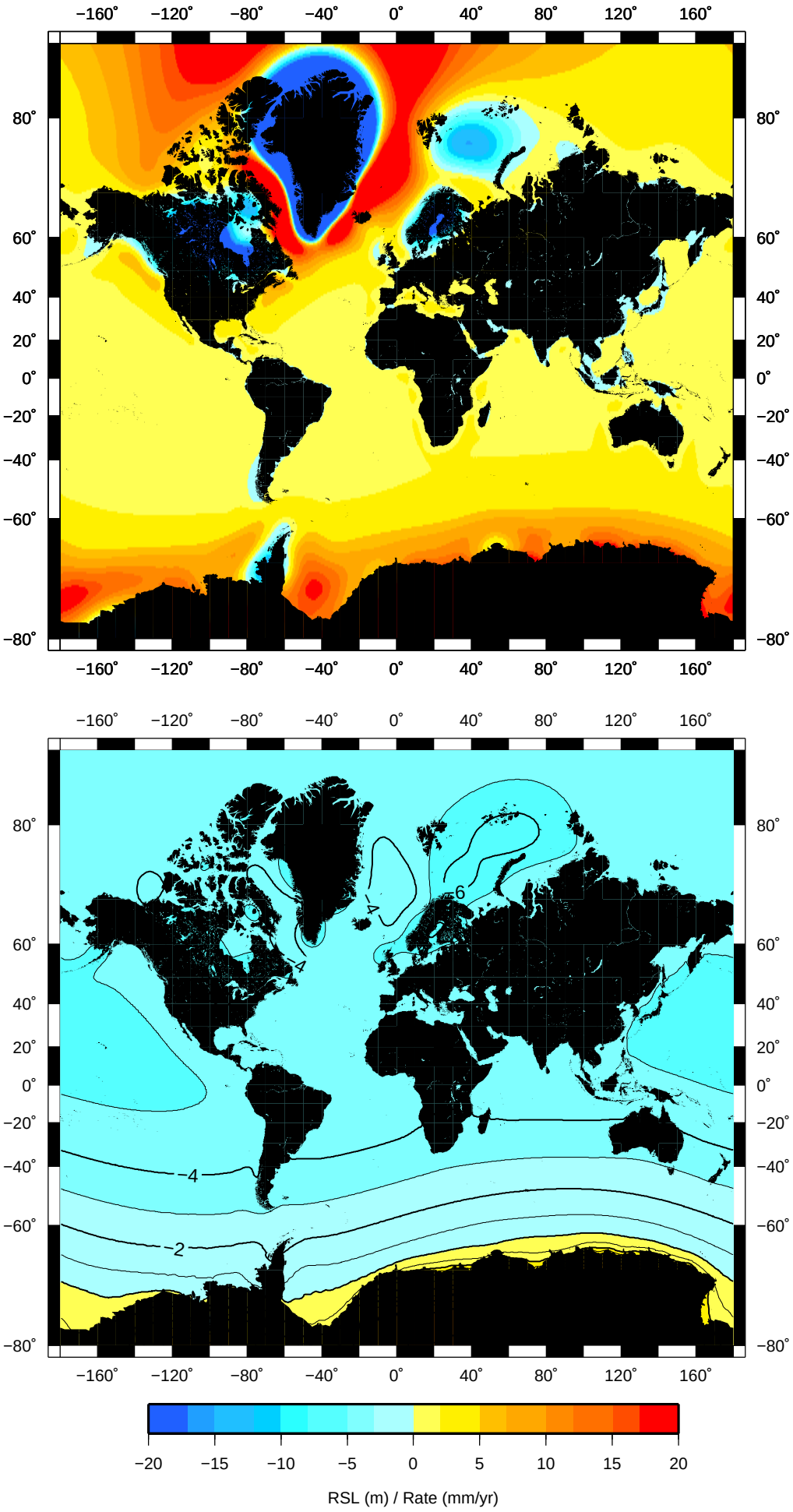

RSL (upper) and sea−level trend (lower) at time 117 kyr BP for Antarctica experiment

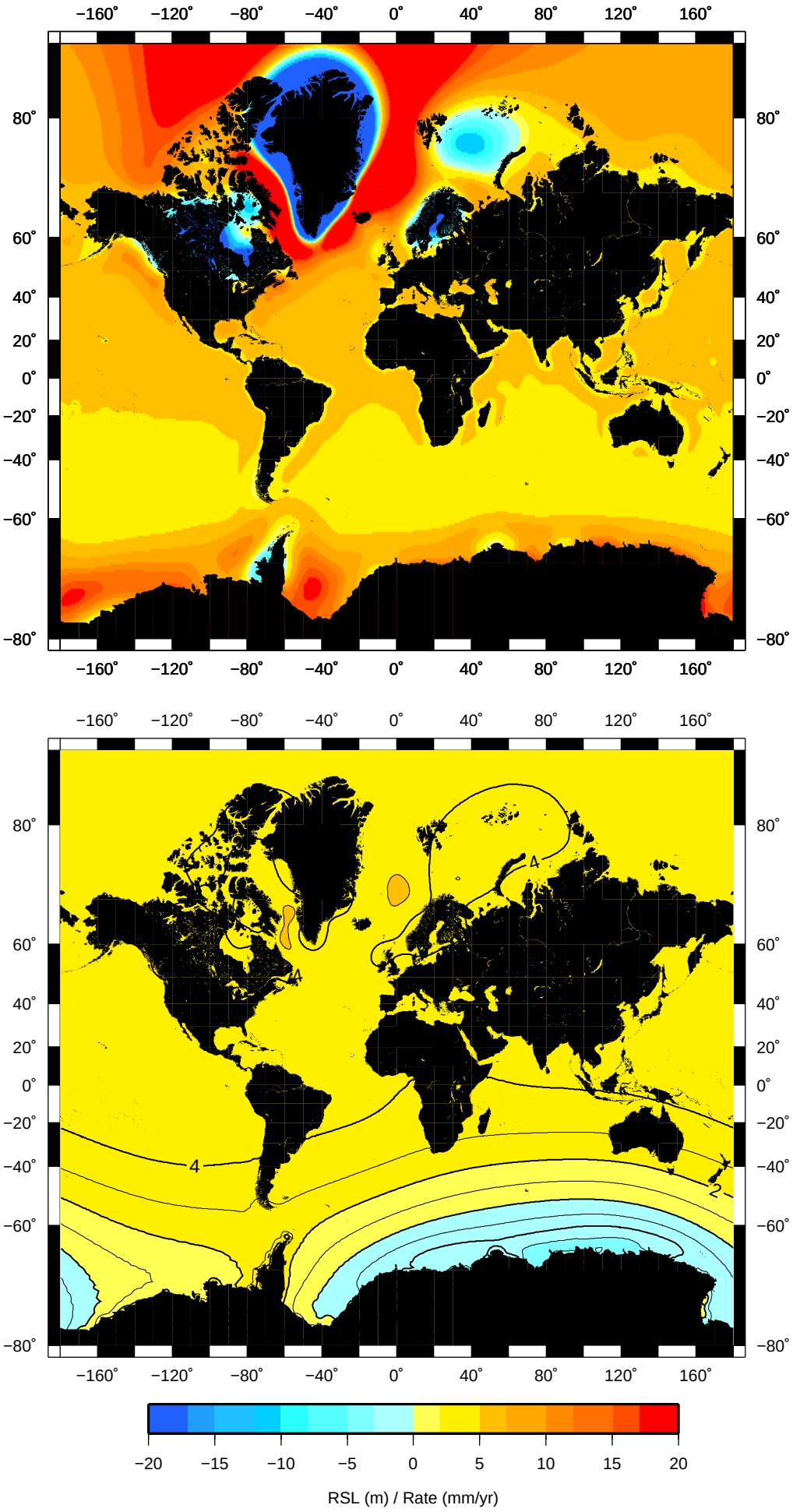

RSL (upper) and sea−level trend (lower) at time 116 kyr BP for Antarctica experiment

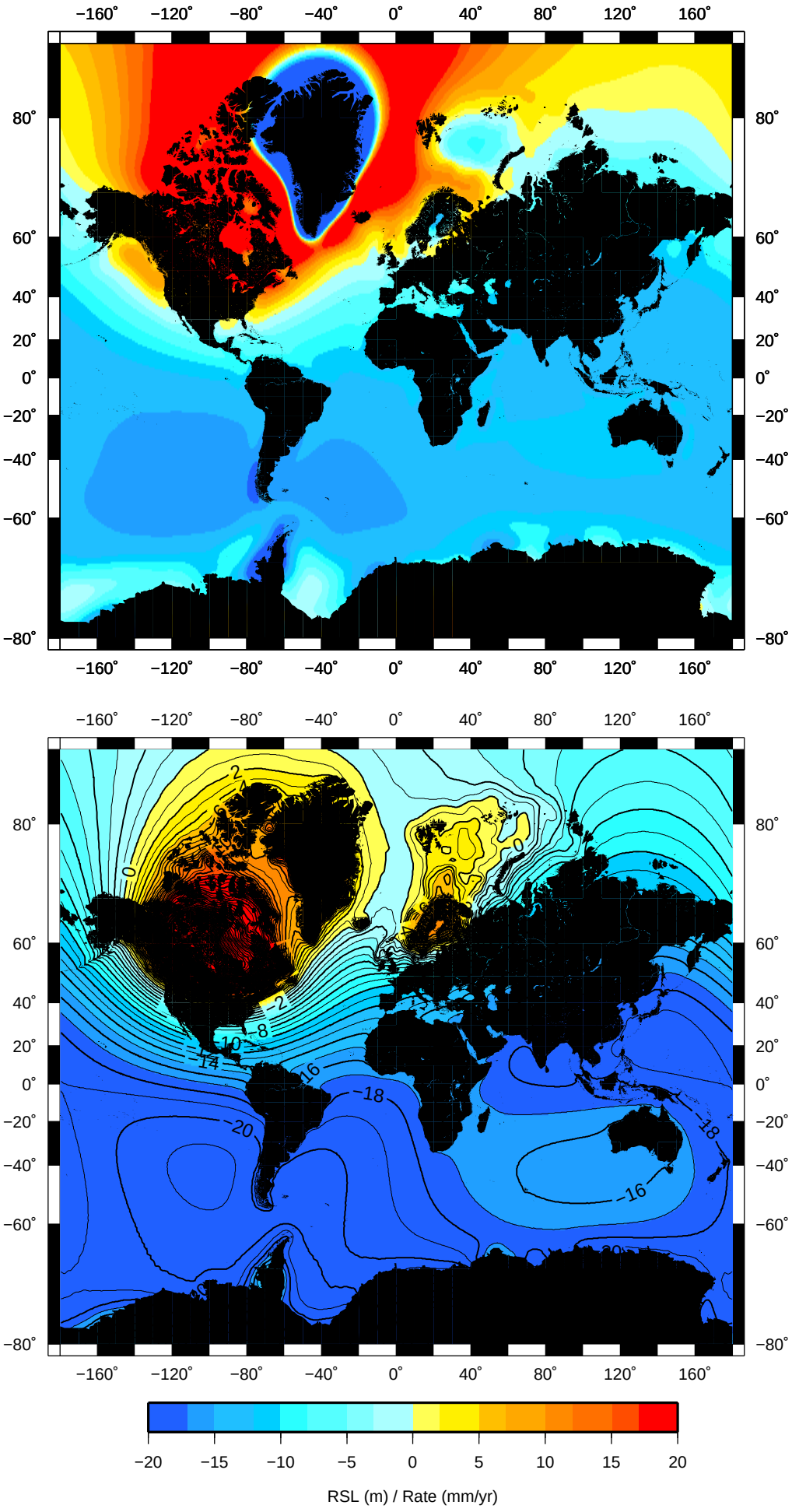

RSL at time 132 kyr BP for Greenland experiment

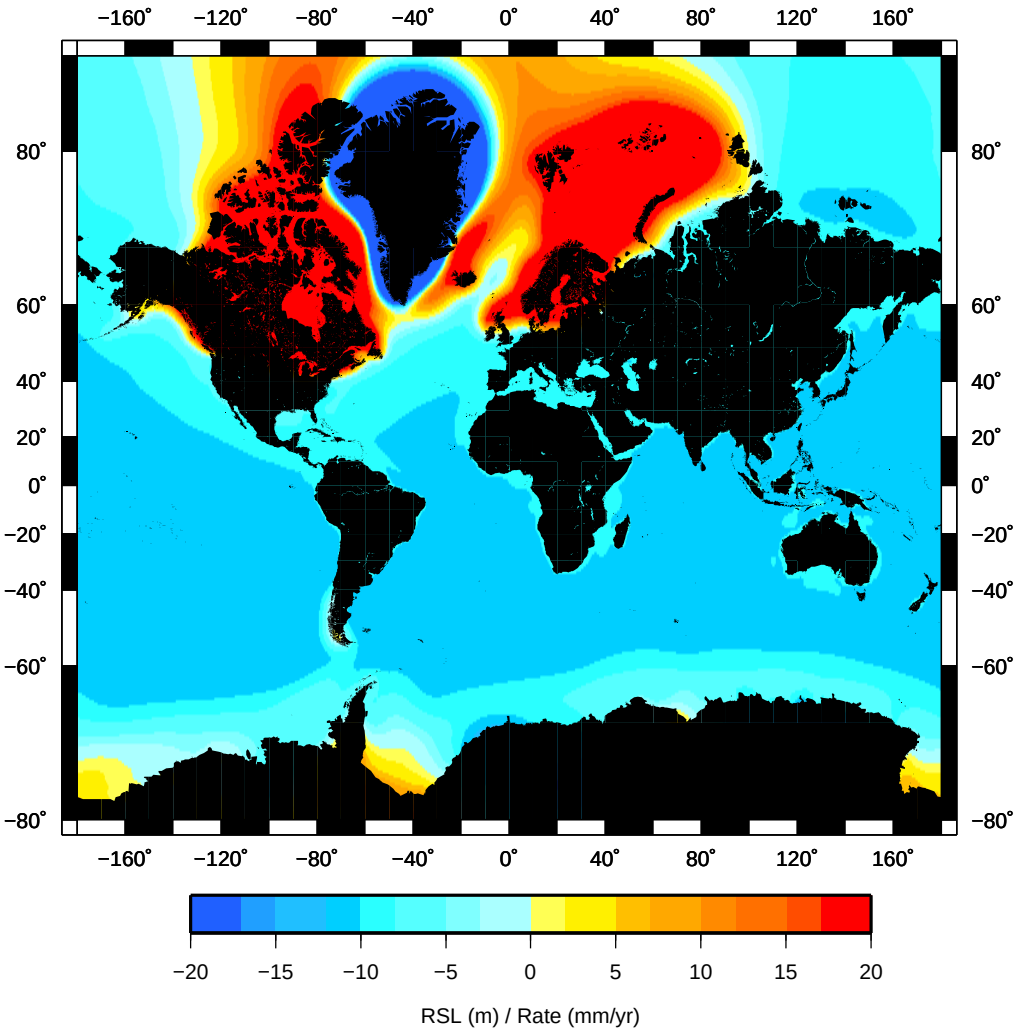

RSL (upper) and sea−level trend (lower) at time 127 kyr BP for Greenland experiment

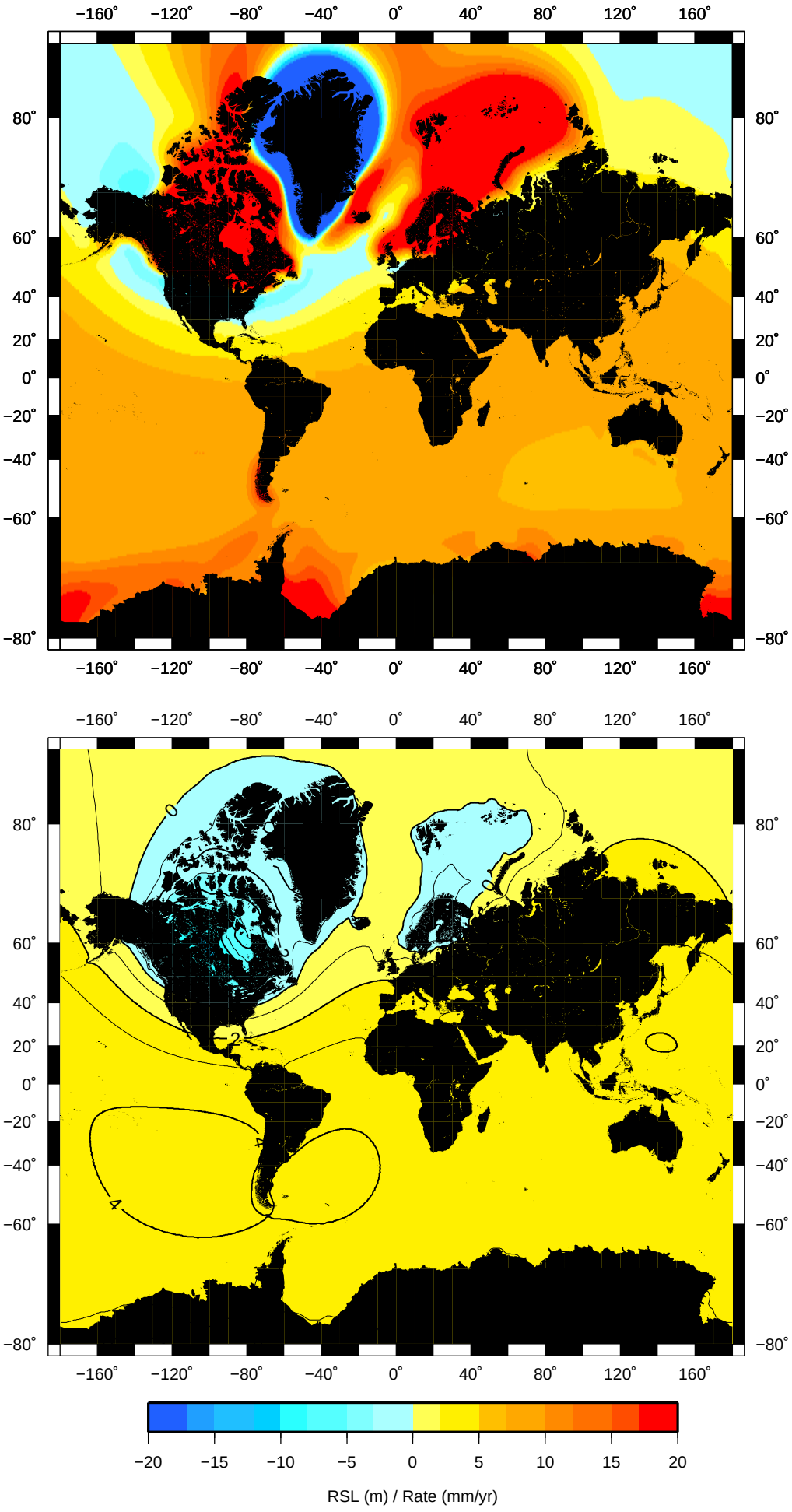

RSL (upper) and sea−level trend (lower) at time 126 kyr BP for Greenland experiment

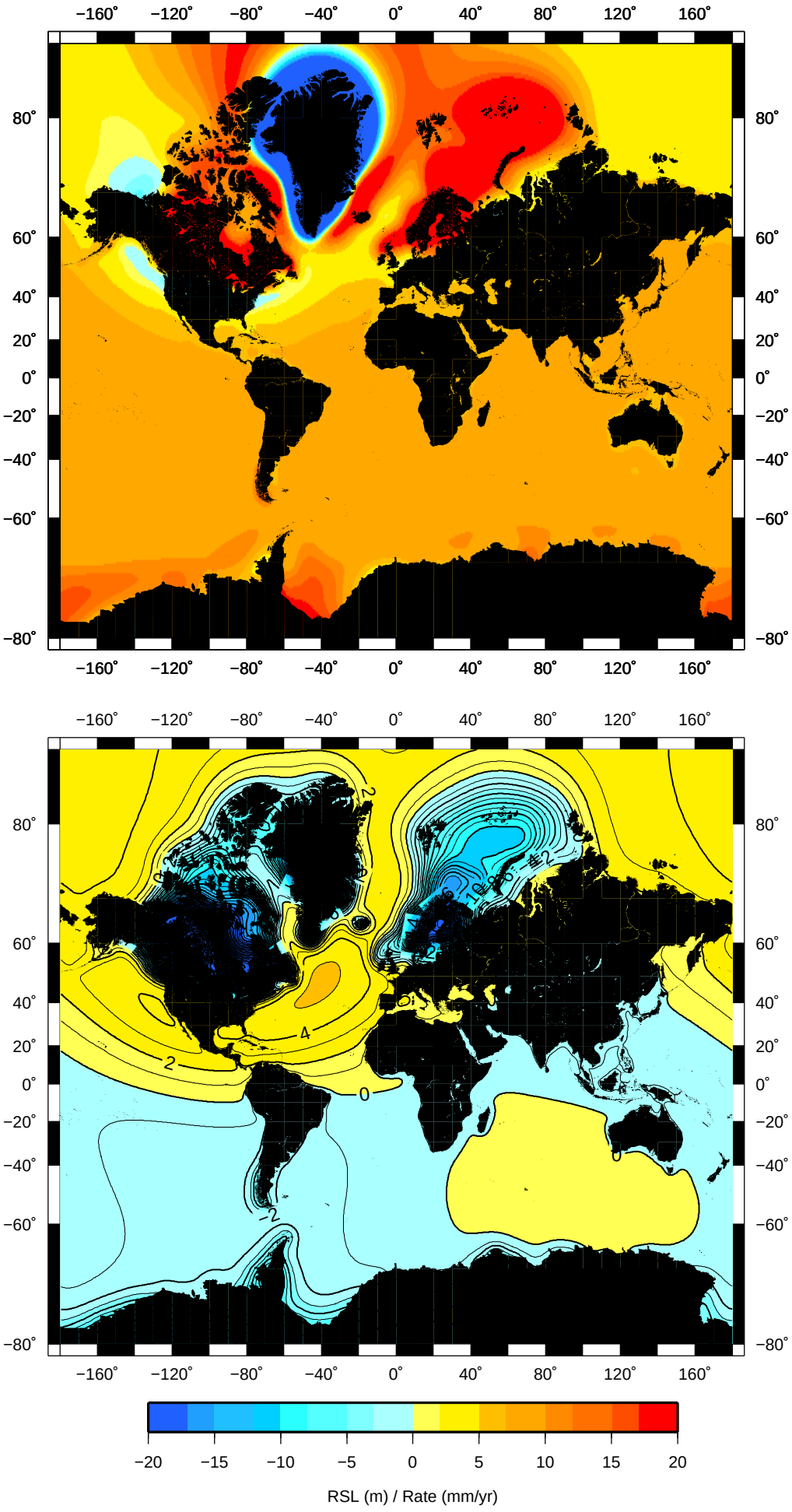

RSL (upper) and sea−level trend (lower) at time 125 kyr BP for Greenland experiment

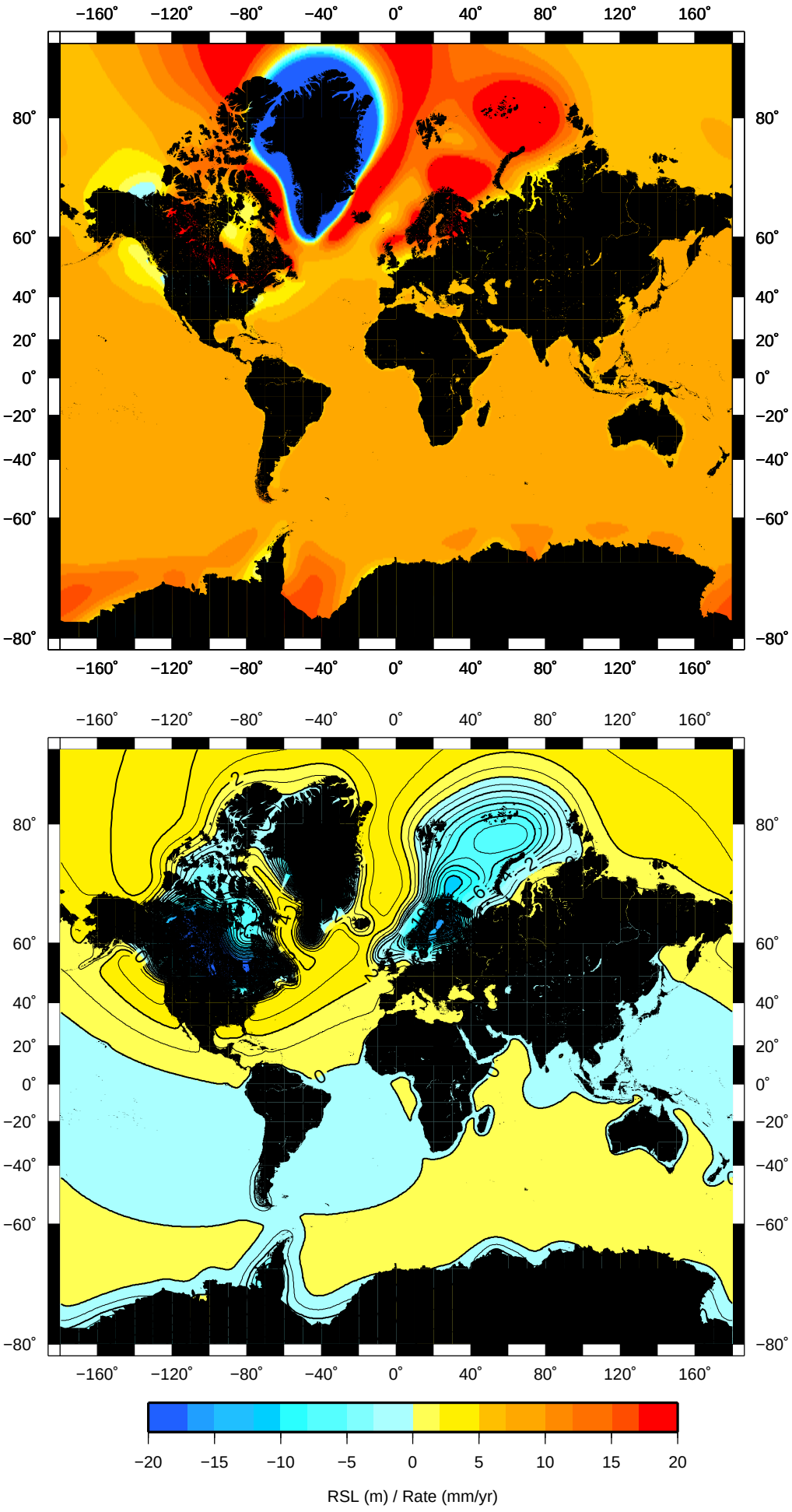

RSL (upper) and sea−level trend (lower) at time 124 kyr BP for Greenland experiment

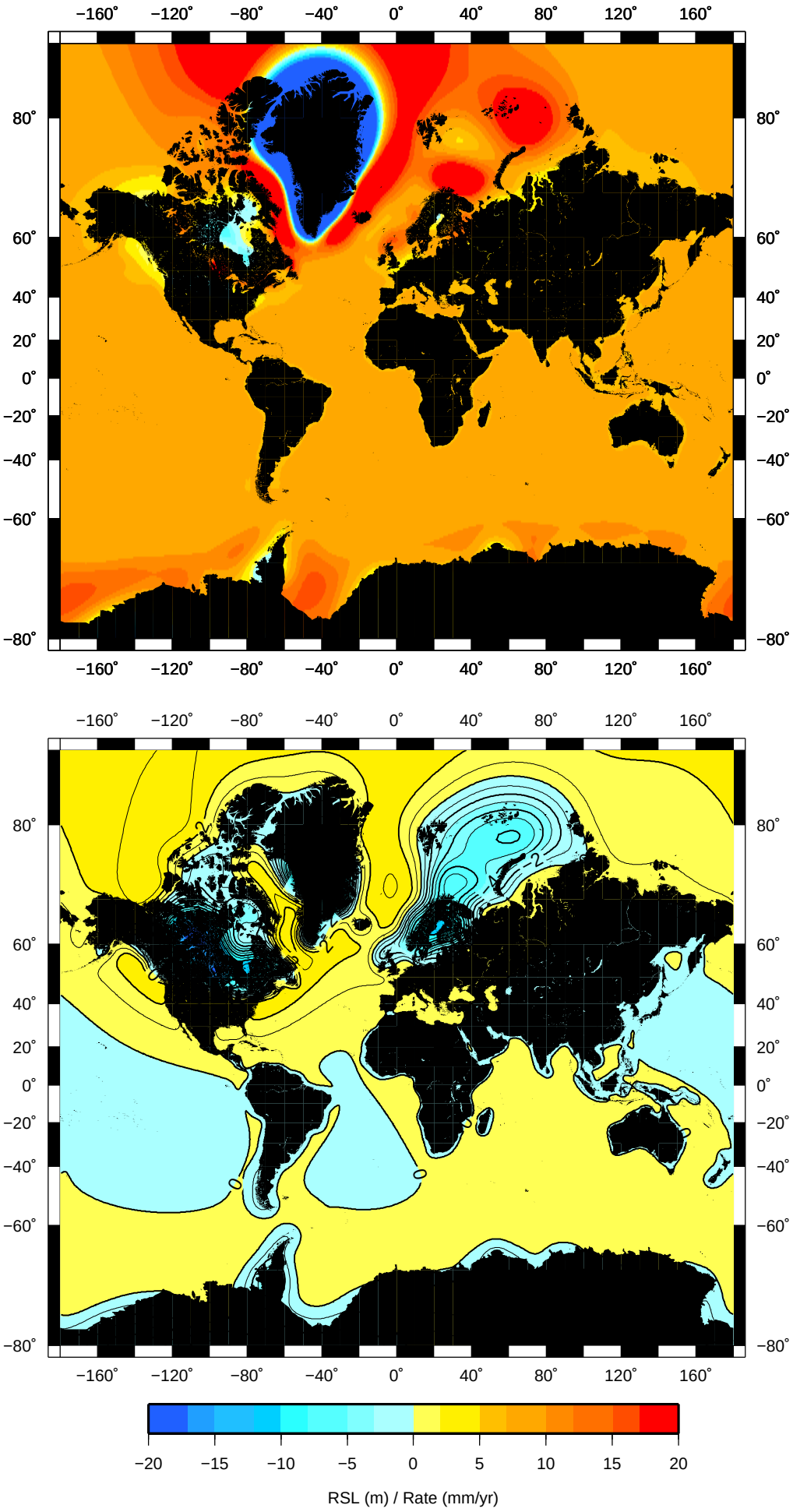

RSL (upper) and sea−level trend (lower) at time 123 kyr BP for Greenland experiment

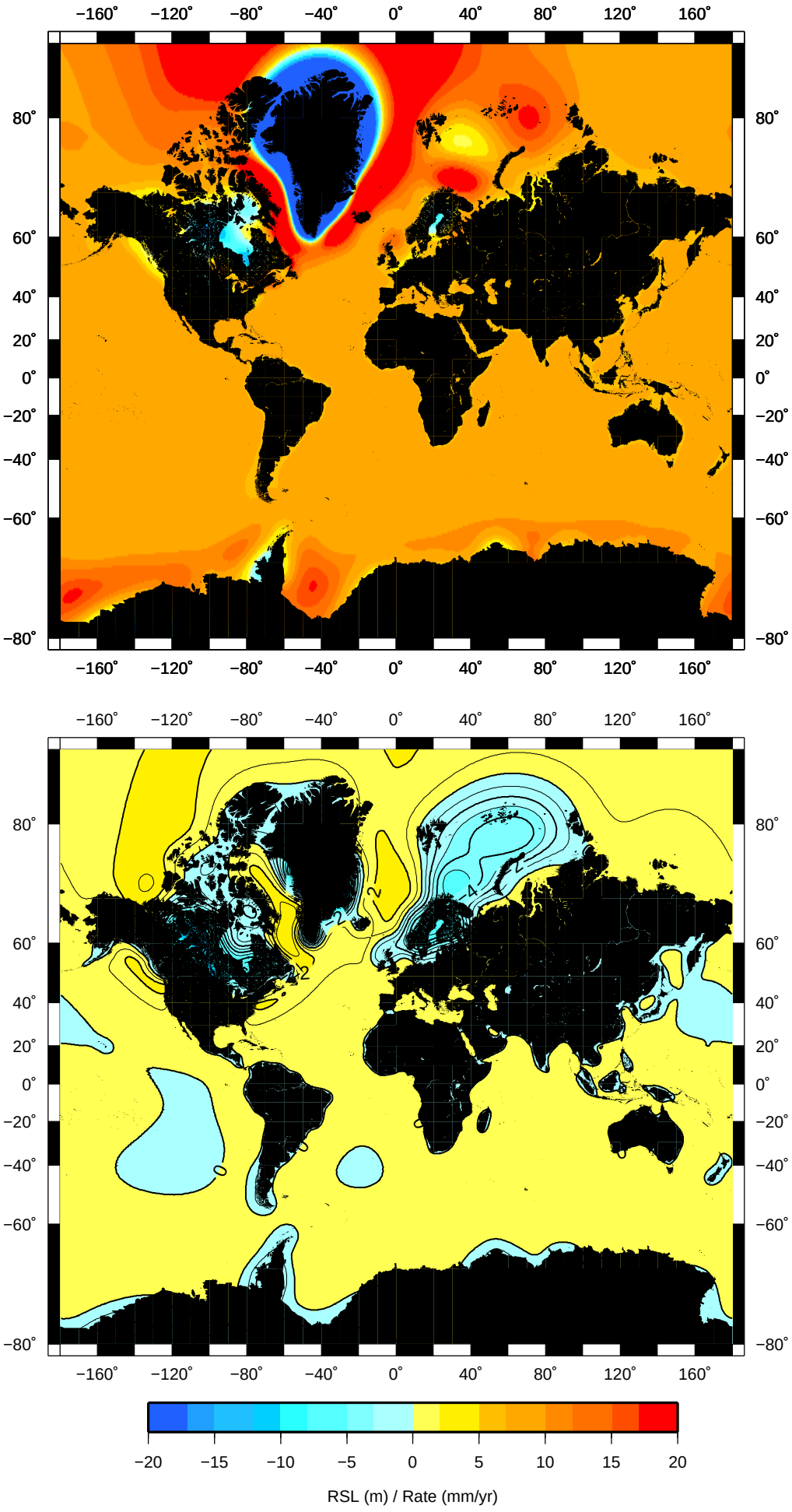

RSL (upper) and sea−level trend (lower) at time 122 kyr BP for Greenland experiment

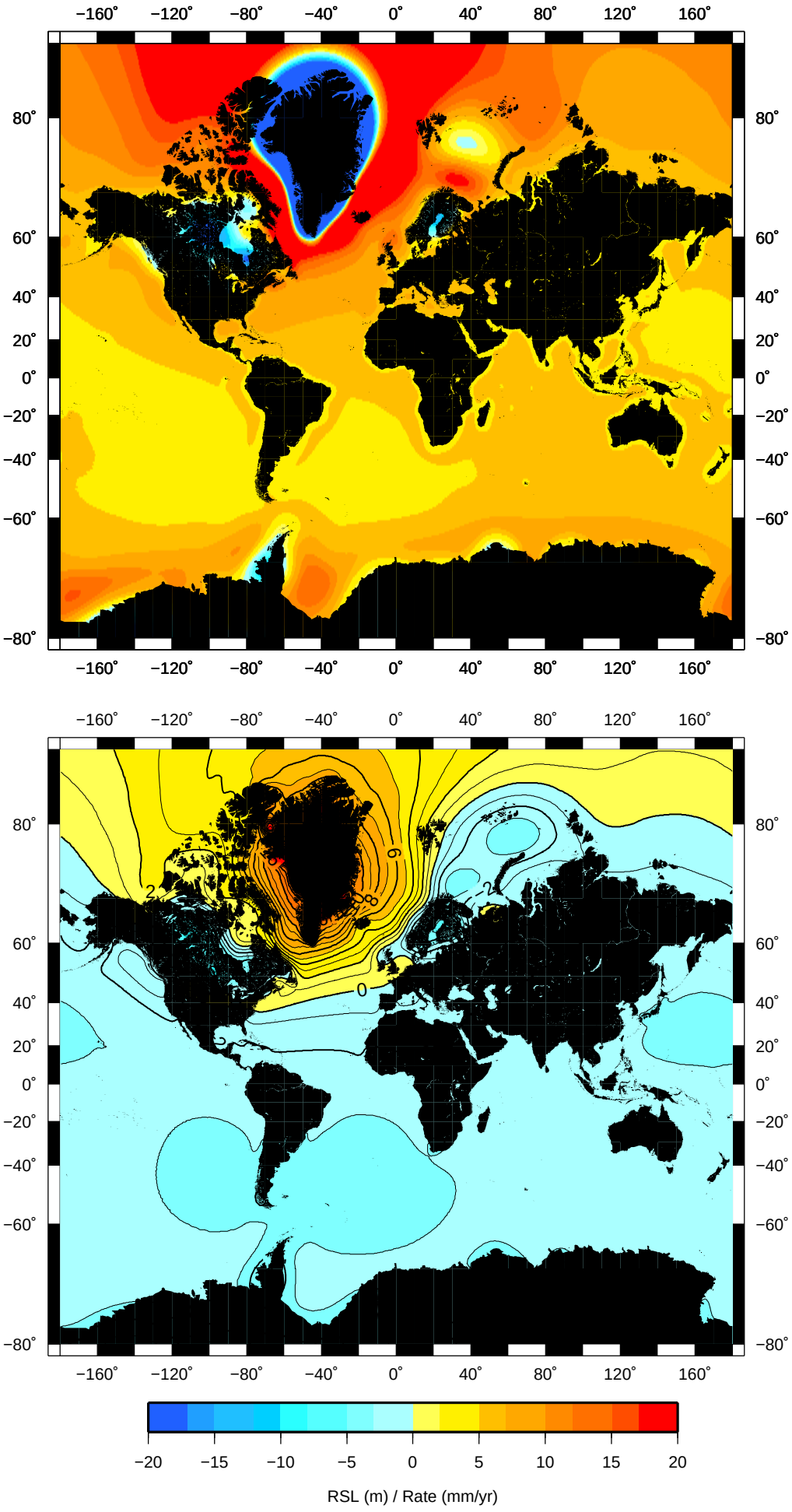

RSL (upper) and sea−level trend (lower) at time 121 kyr BP for Greenland experiment

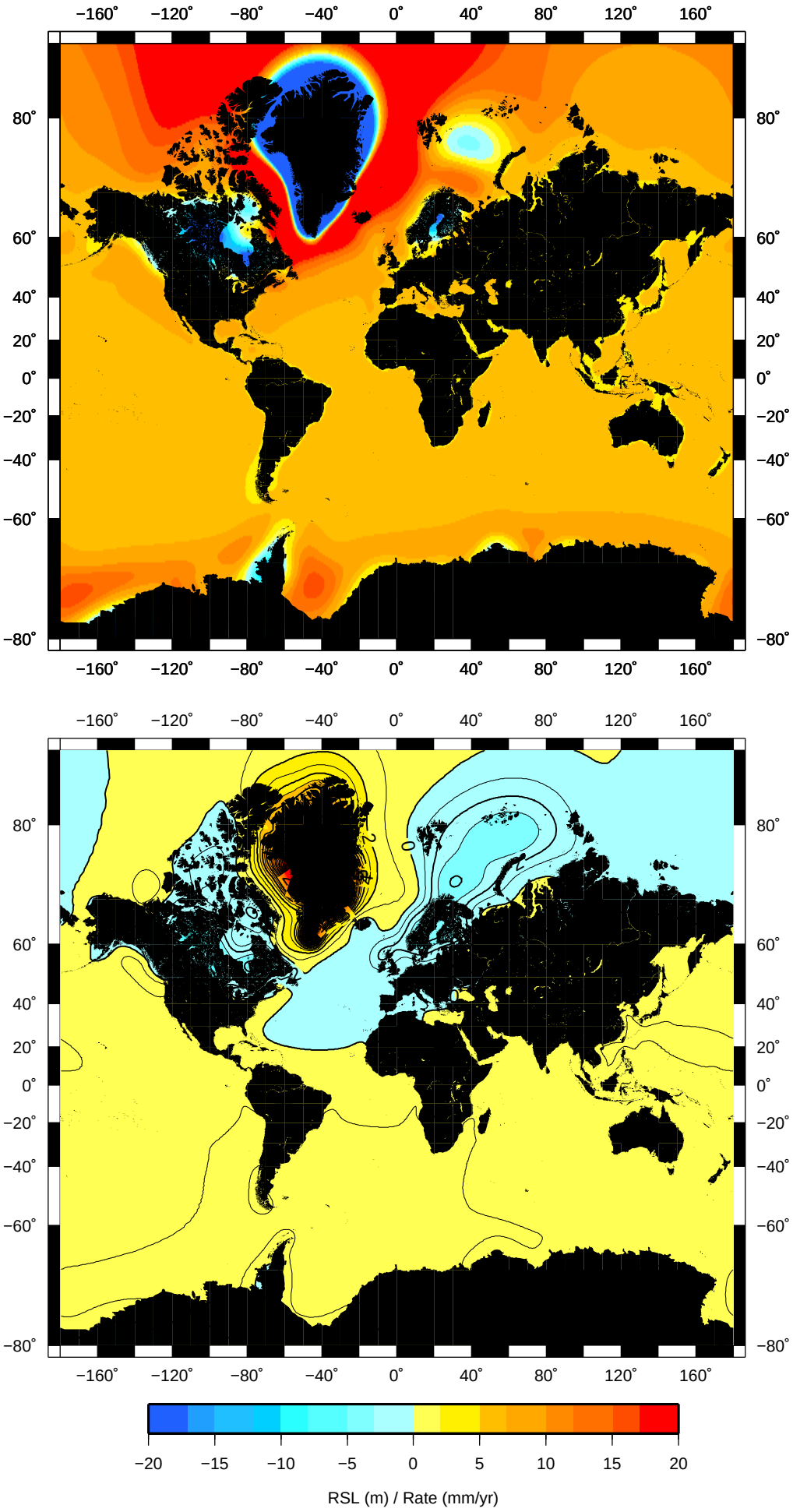

RSL (upper) and sea−level trend (lower) at time 120 kyr BP for Greenland experiment

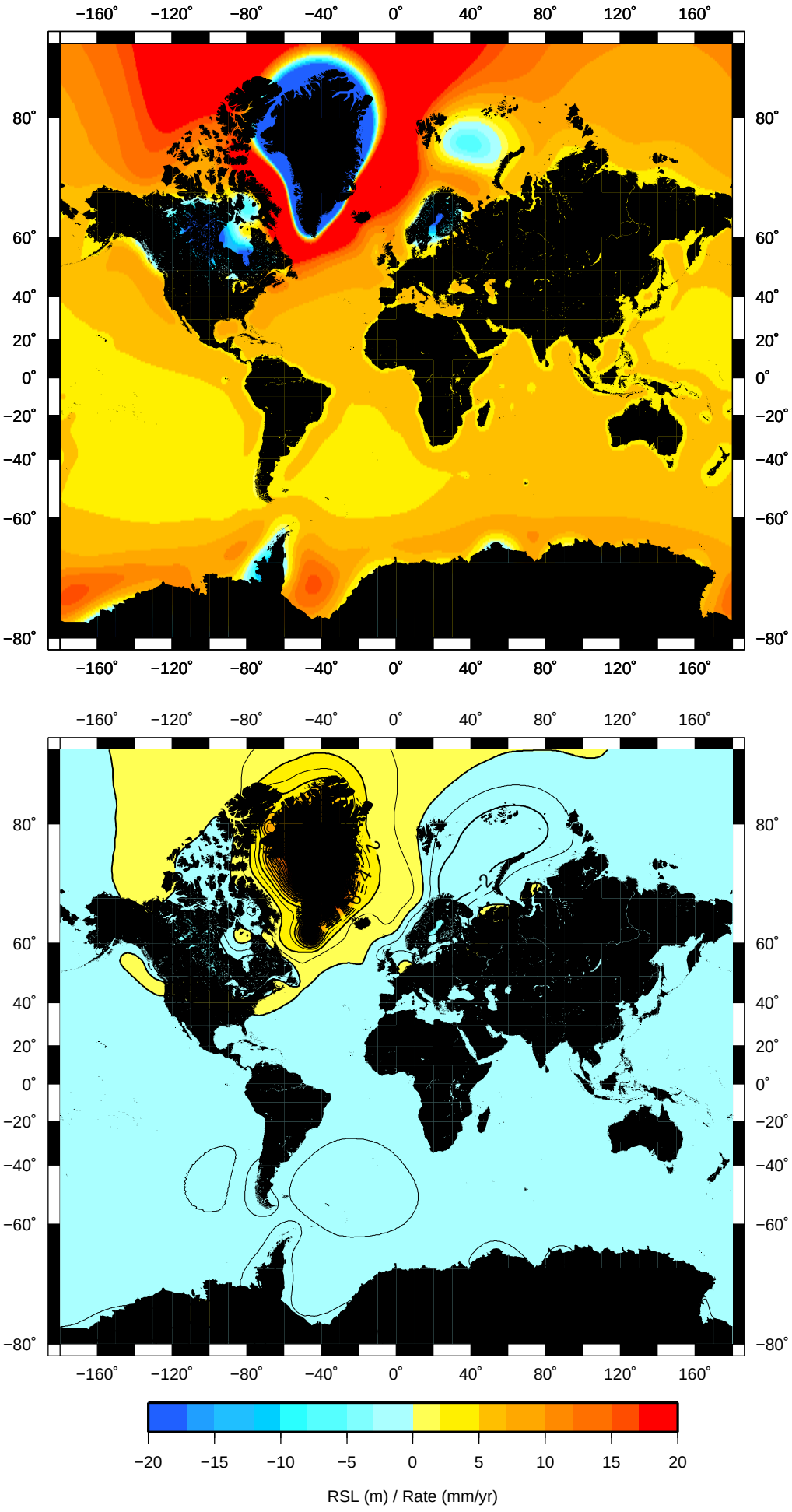

RSL (upper) and sea−level trend (lower) at time 119 kyr BP for Greenland experiment

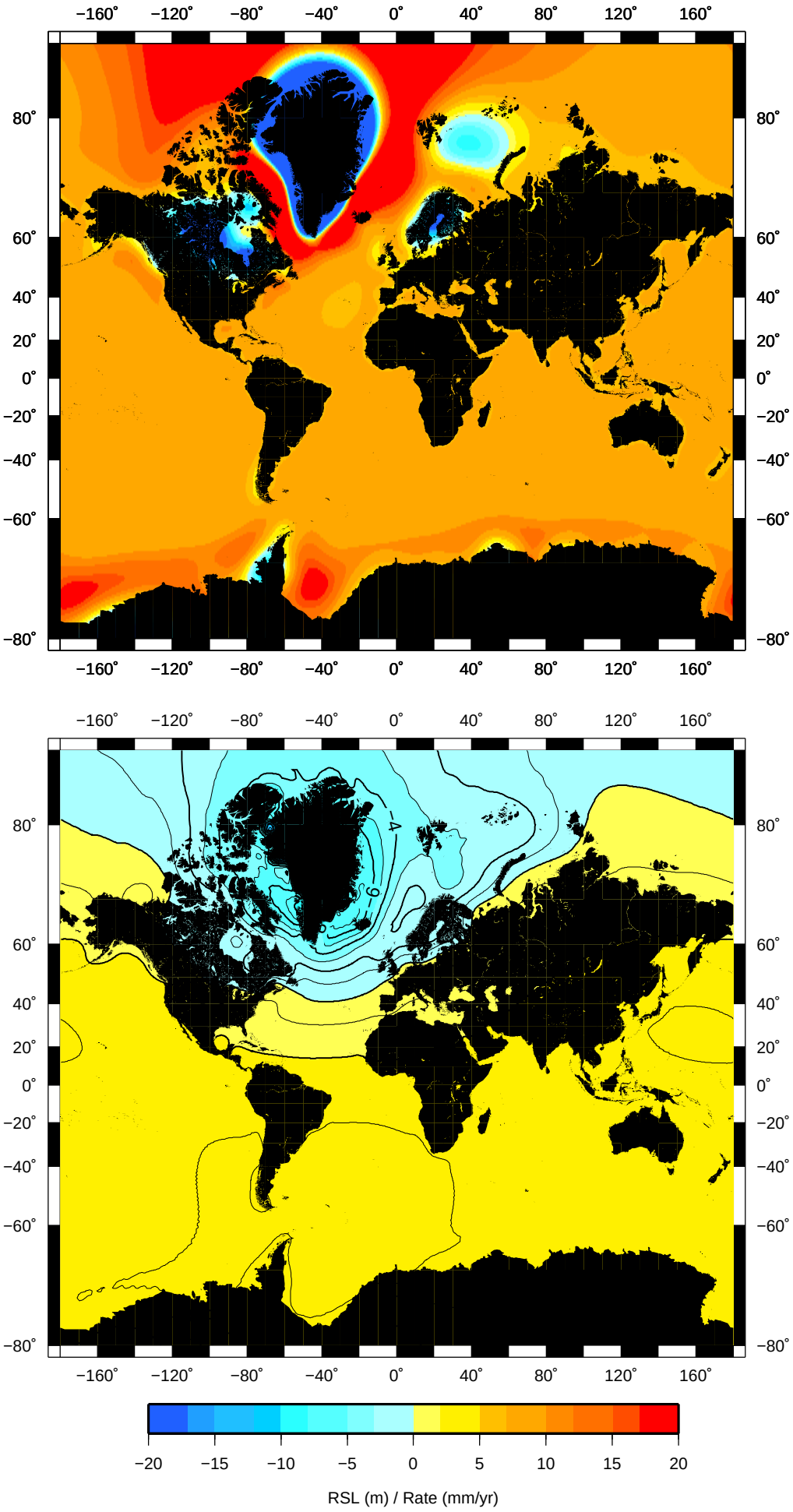

RSL (upper) and sea−level trend (lower) at time 118 kyr BP for Greenland experiment

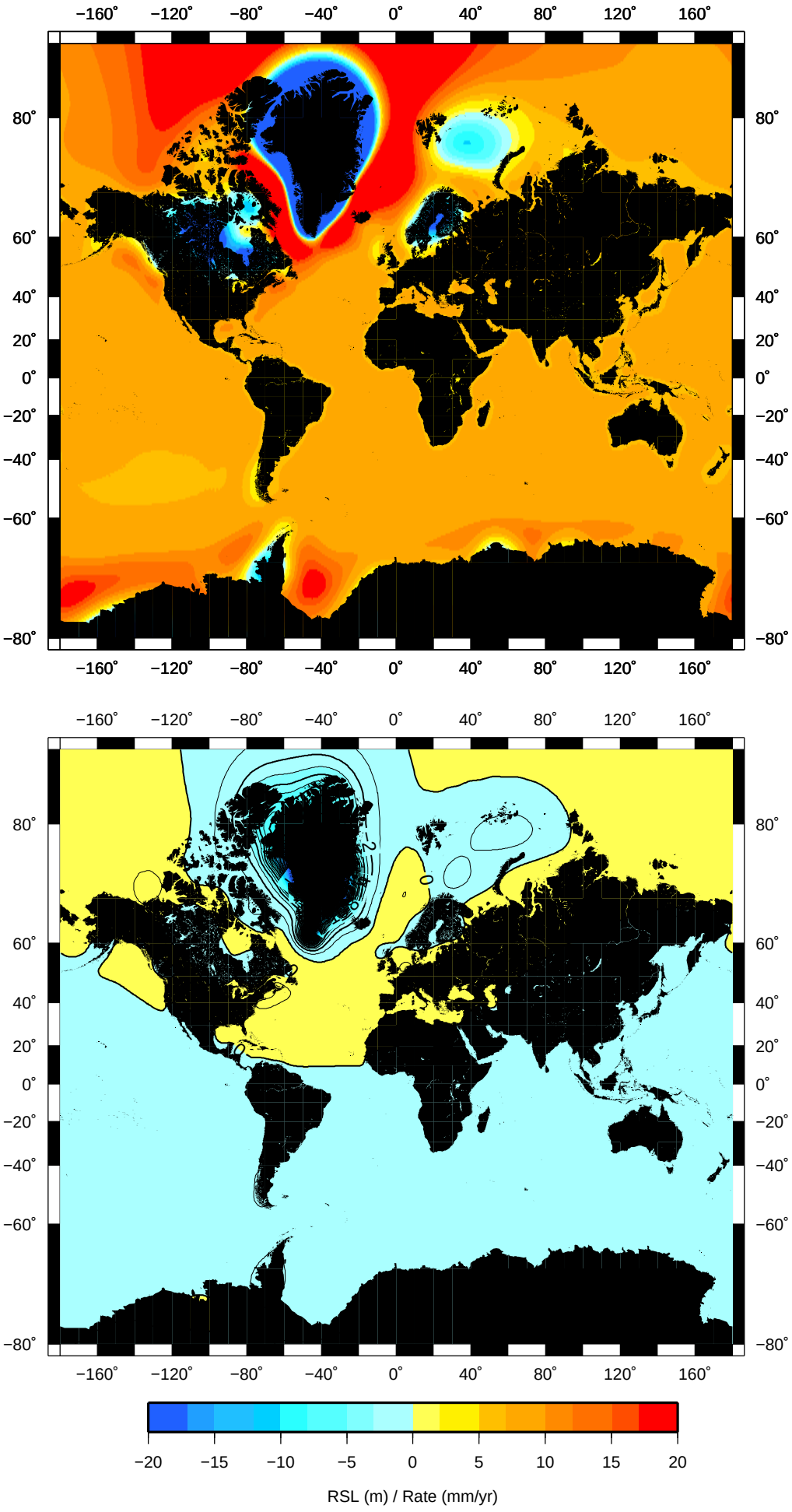

RSL (upper) and sea−level trend (lower) at time 117 kyr BP for Greenland experiment

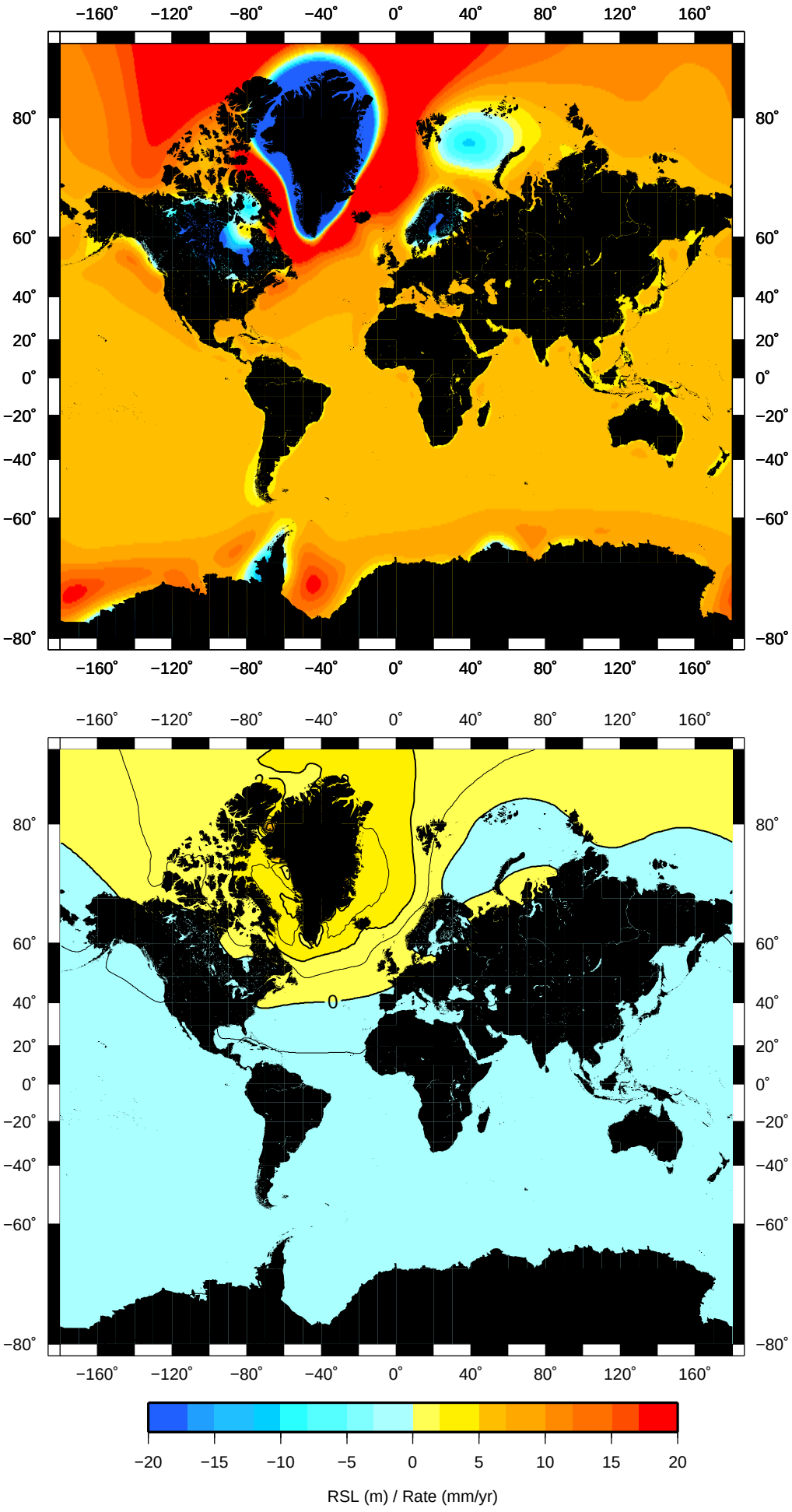

RSL (upper) and sea−level trend (lower) at time 116 kyr BP for Greenland experiment

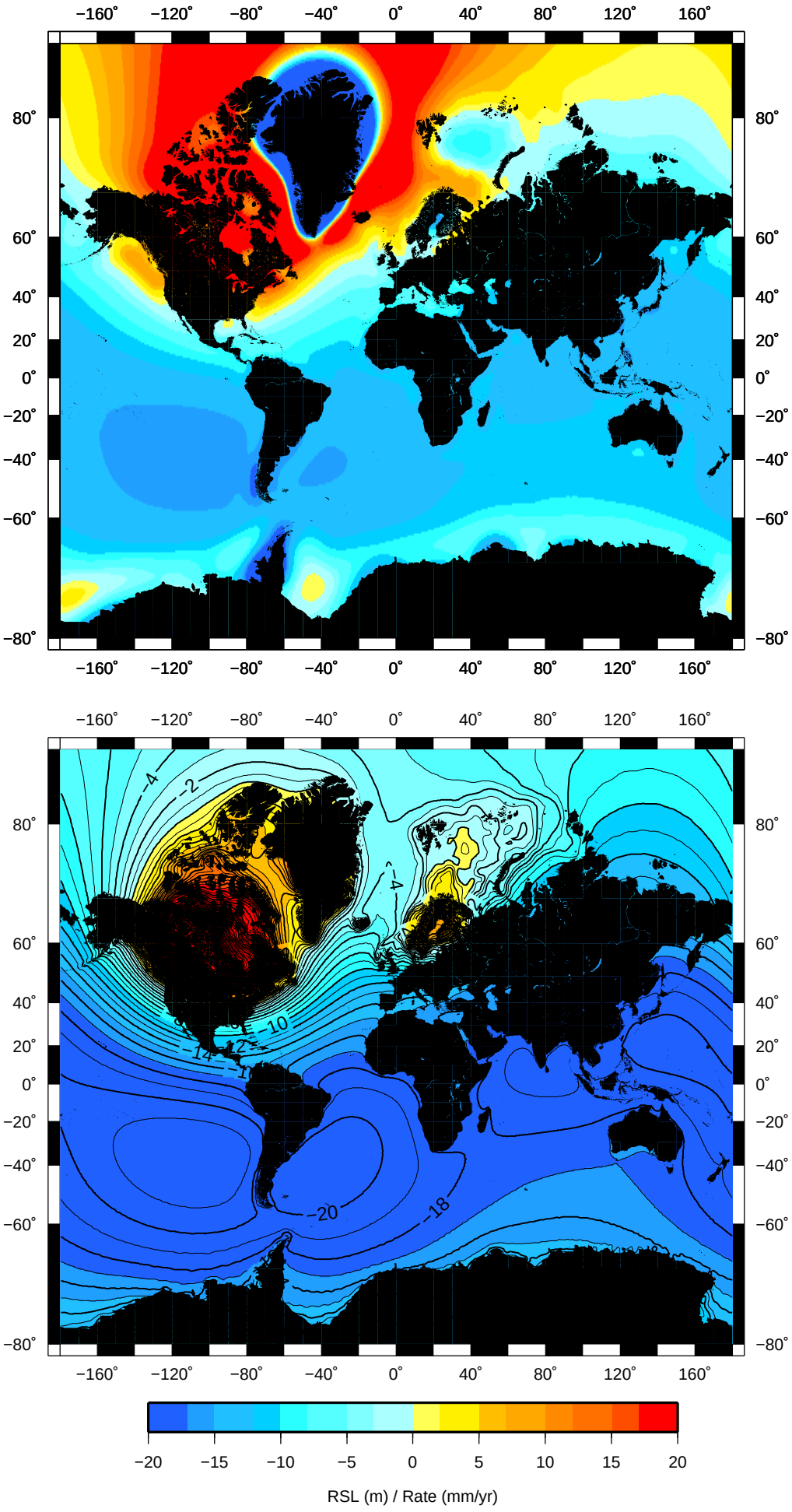

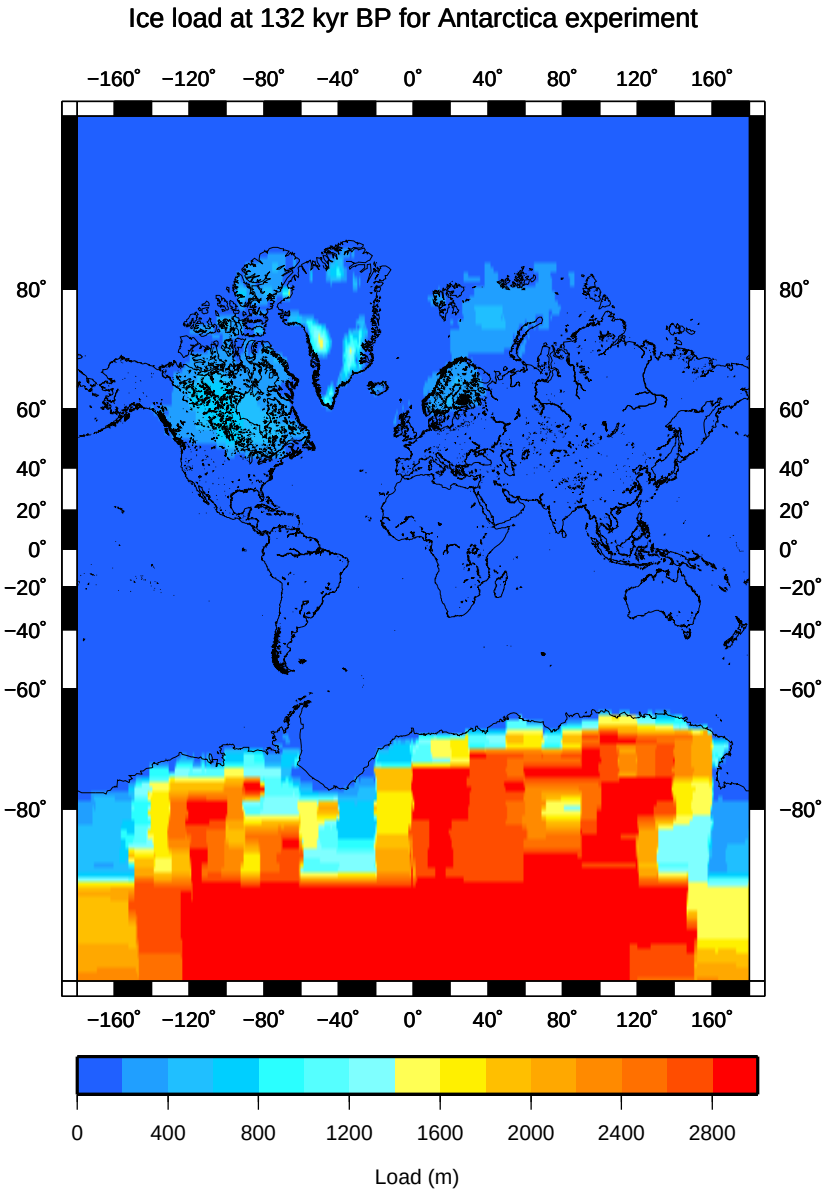
Ice load at 132 kyr BP for Antarctica experiment
−160° −120° −80° −40° 0° 40° 80° 120° 160°
80° 60° 40° 20° 0° −20° −40° −60° −80°
0 400 800 1200 1600 2000 2400 2800
Load (m)

Ice load at 127 kyr BP for Antarctica experiment

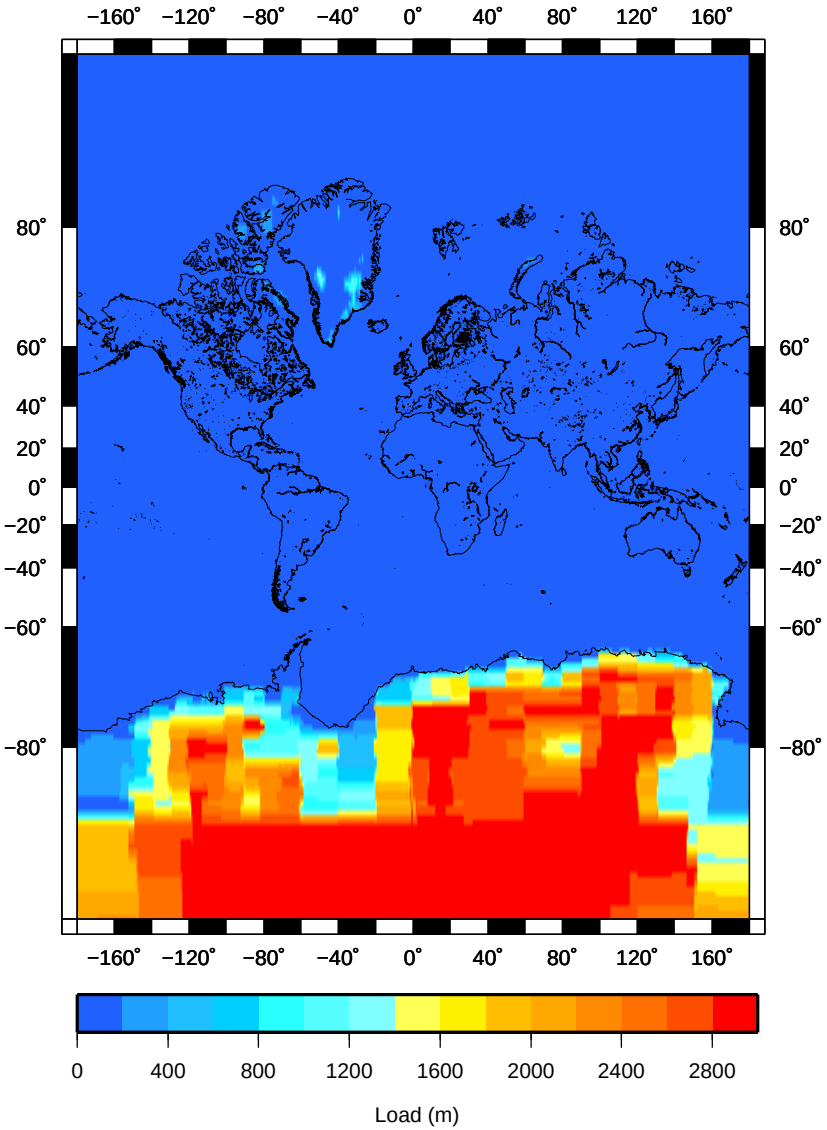

Change in ice load at 127 kyr BP for Antarctica experiment

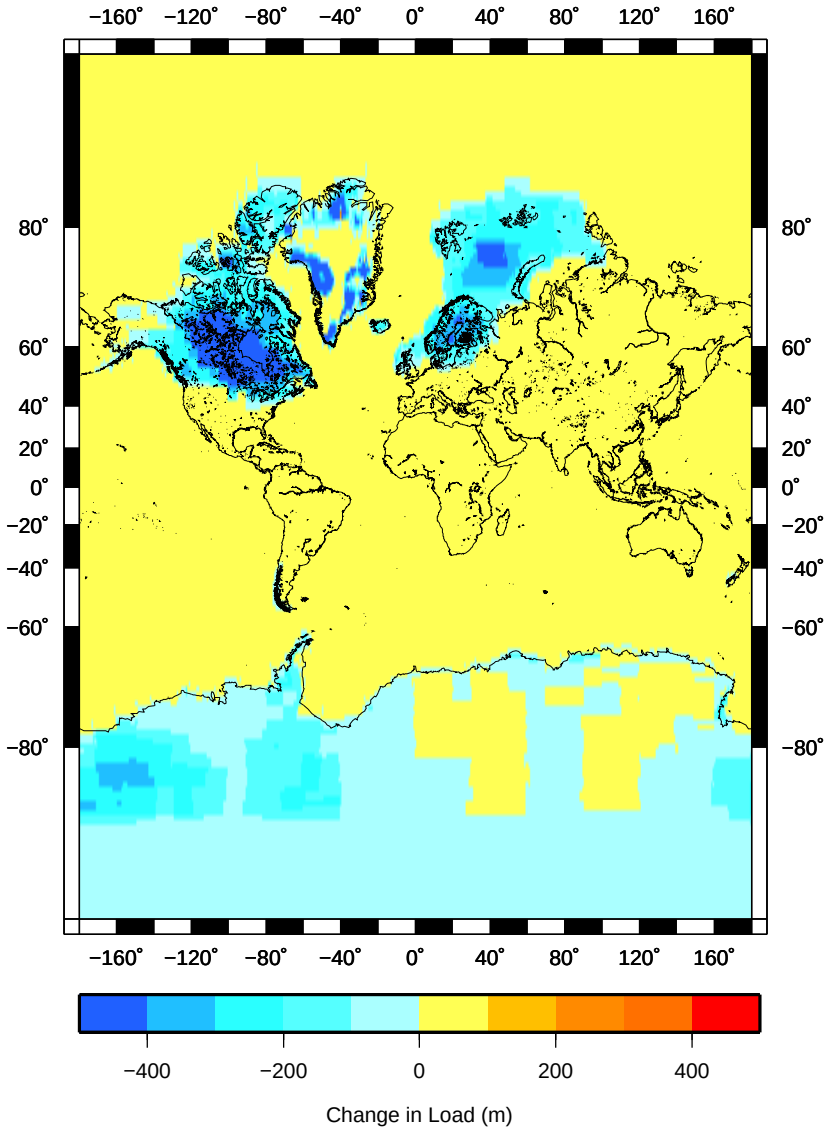

Ice load at 126 kyr BP for Antarctica experiment

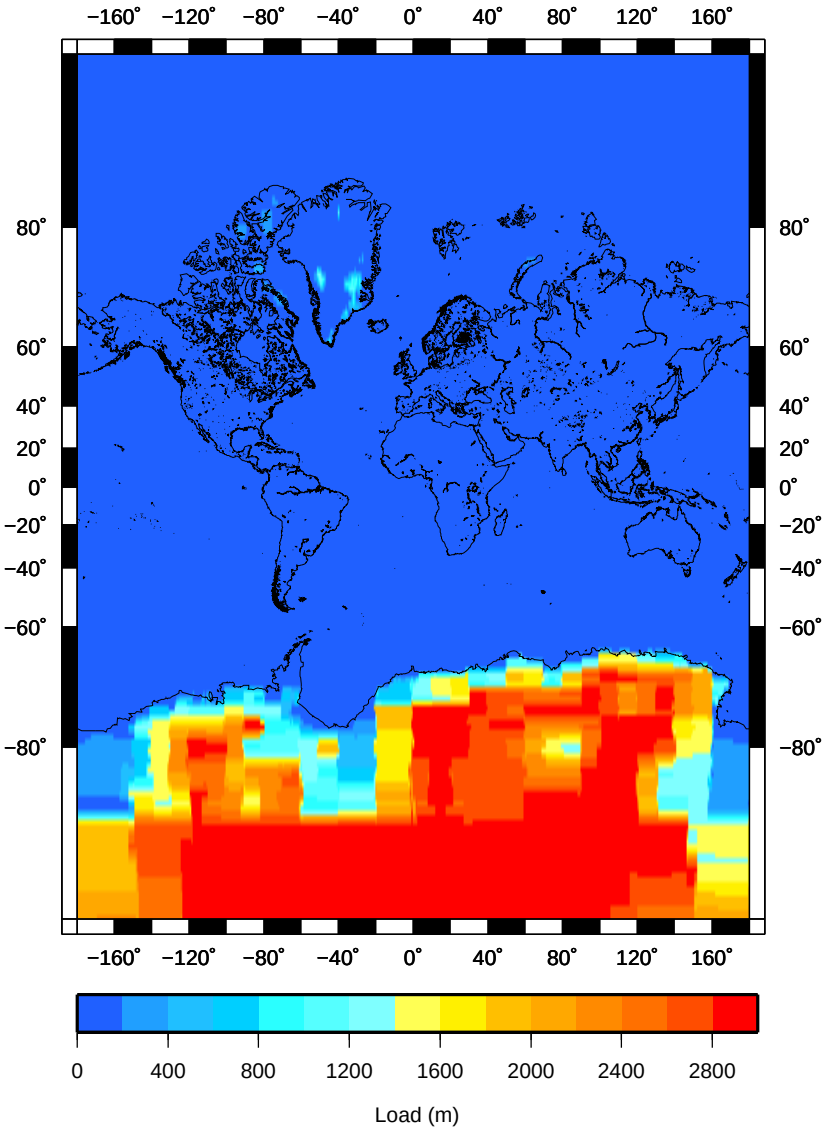

Change in ice load at 126 kyr BP for Antarctica experiment

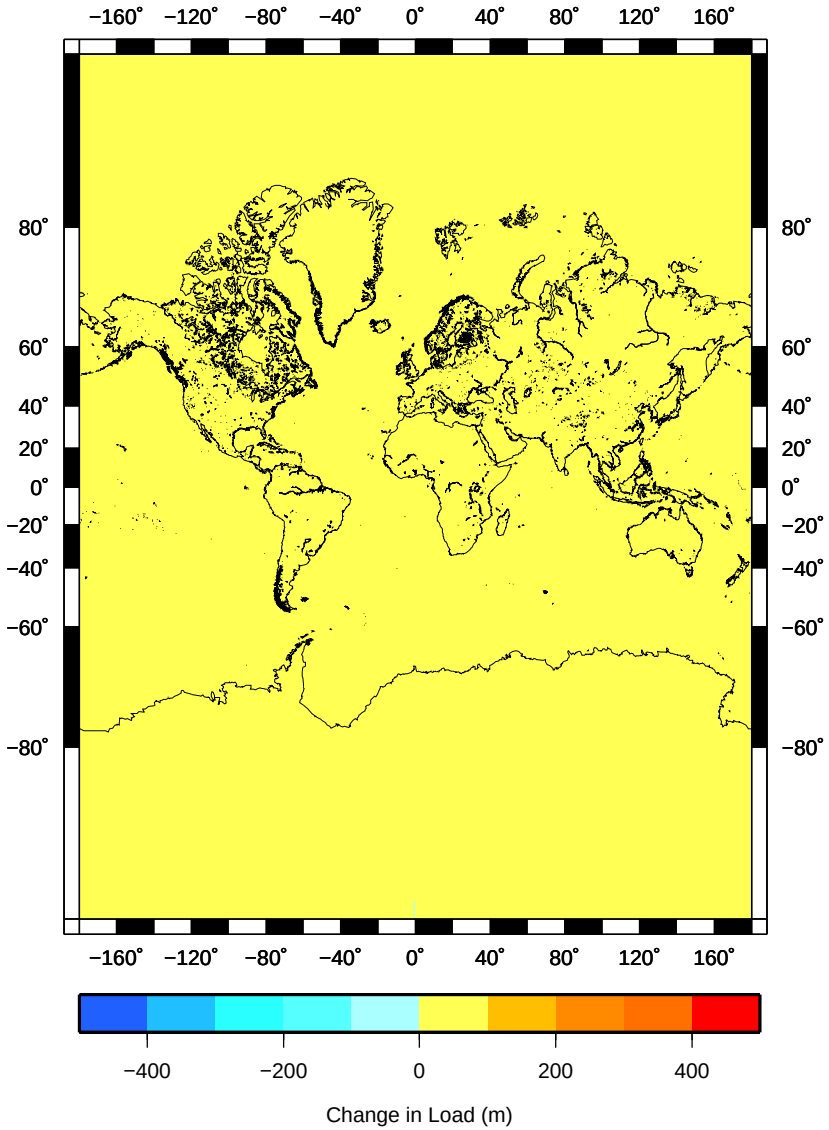

Ice load at 125 kyr BP for Antarctica experiment

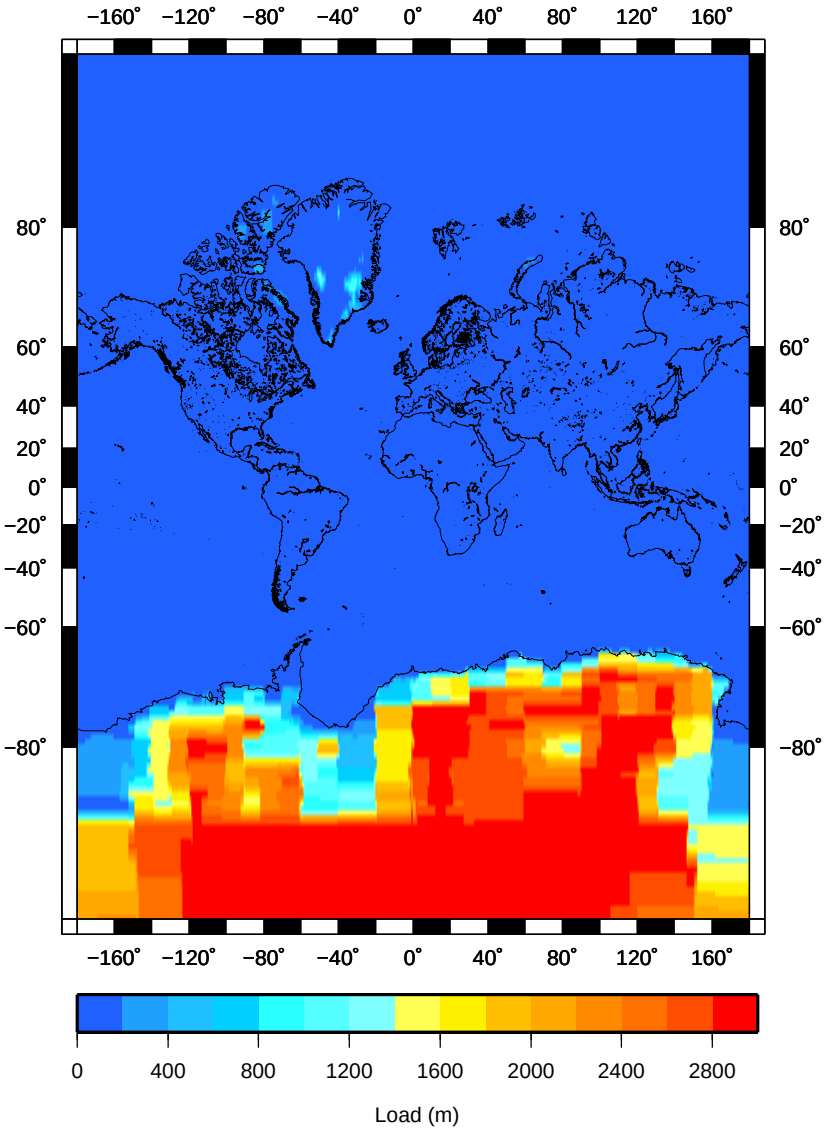

Change in ice load at 125 kyr BP for Antarctica experiment

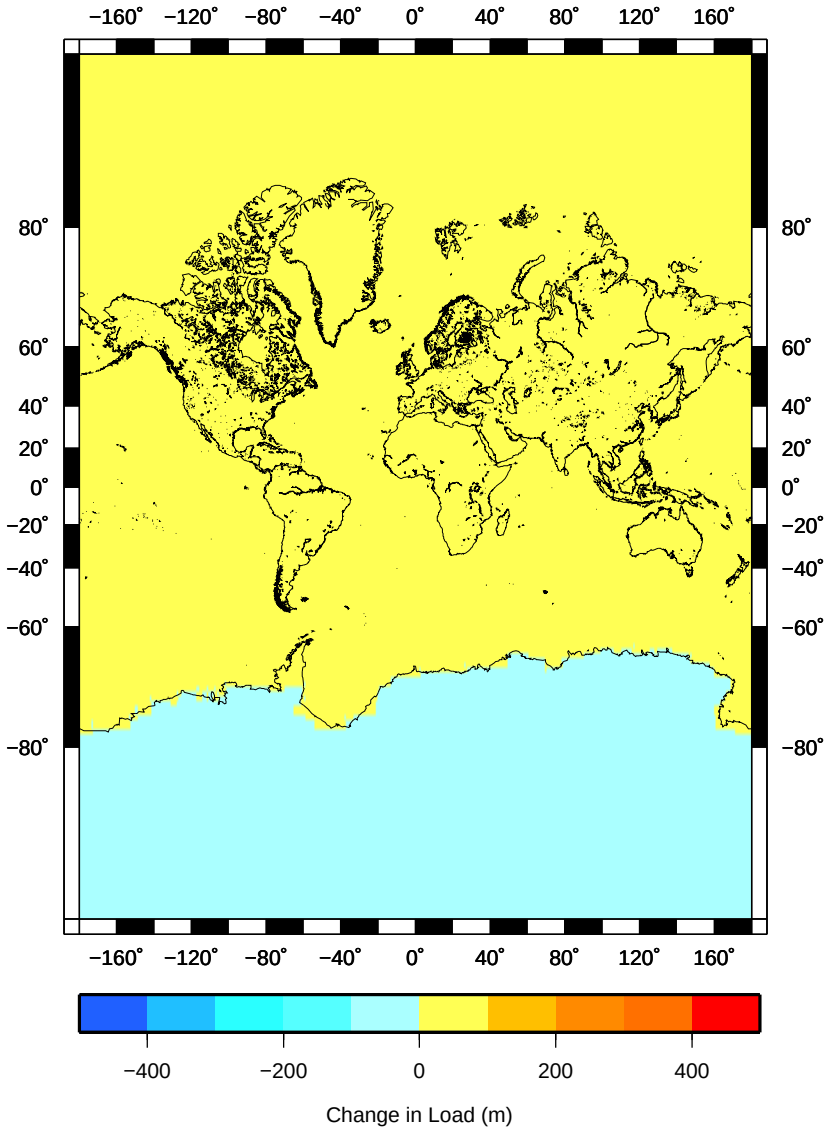

Ice load at 124 kyr BP for Antarctica experiment

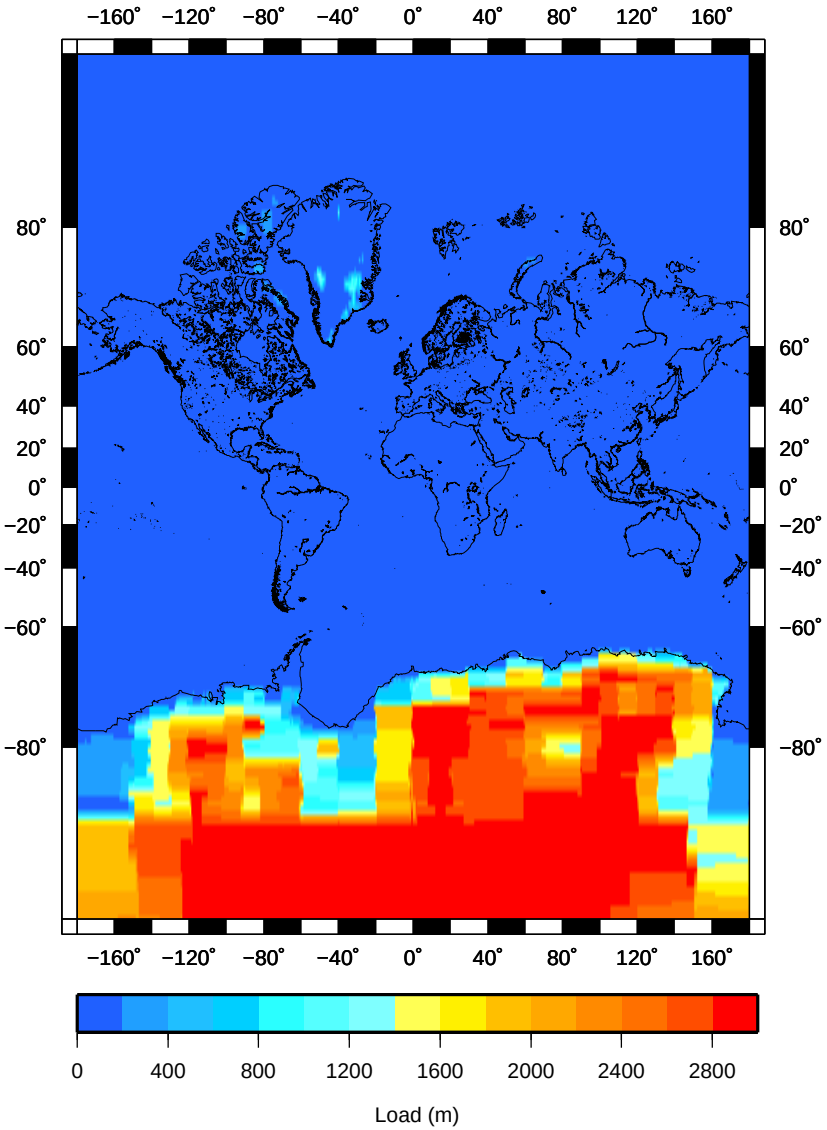

Change in ice load at 124 kyr BP for Antarctica experiment

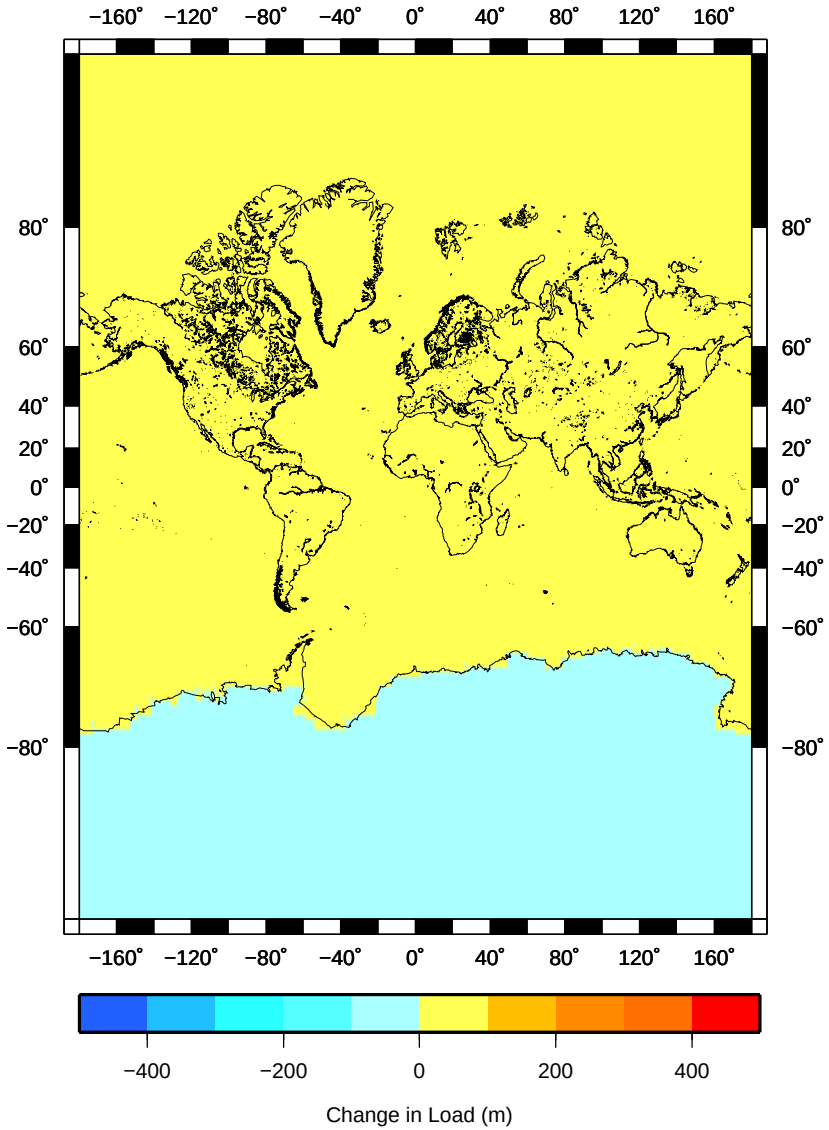

Ice load at 123 kyr BP for Antarctica experiment

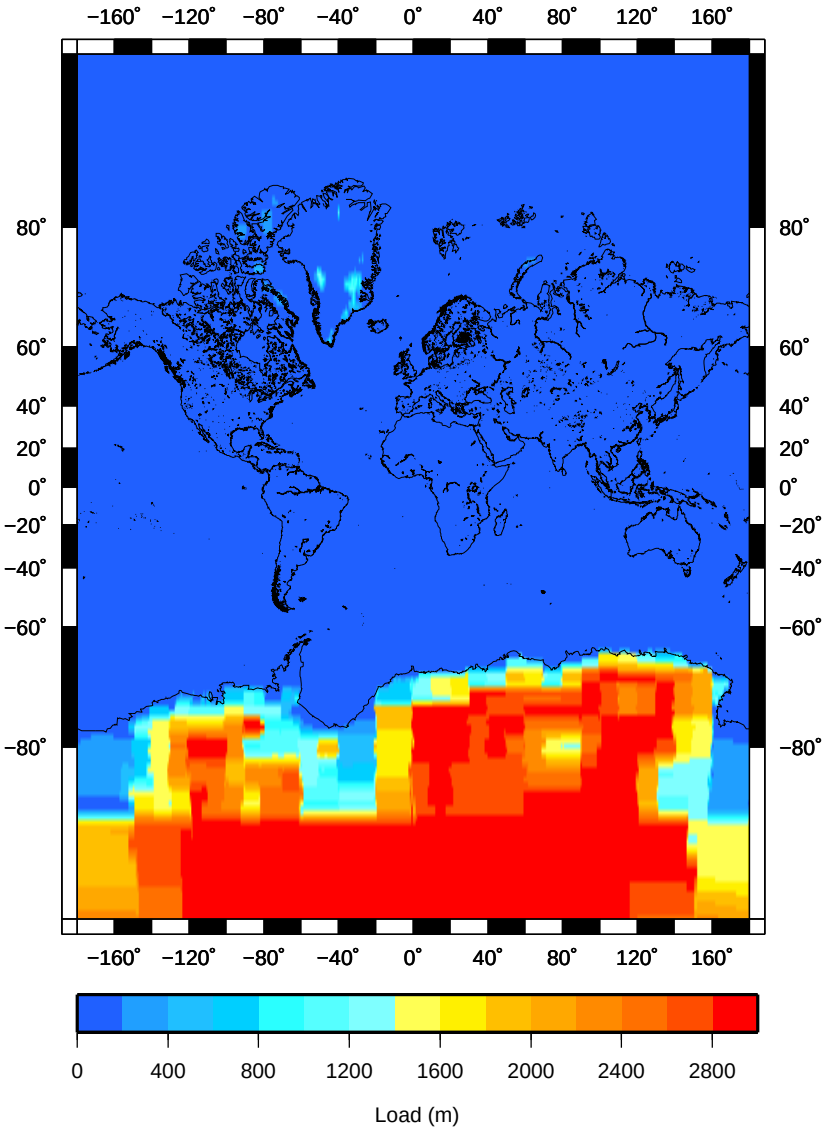

Change in ice load at 123 kyr BP for Antarctica experiment

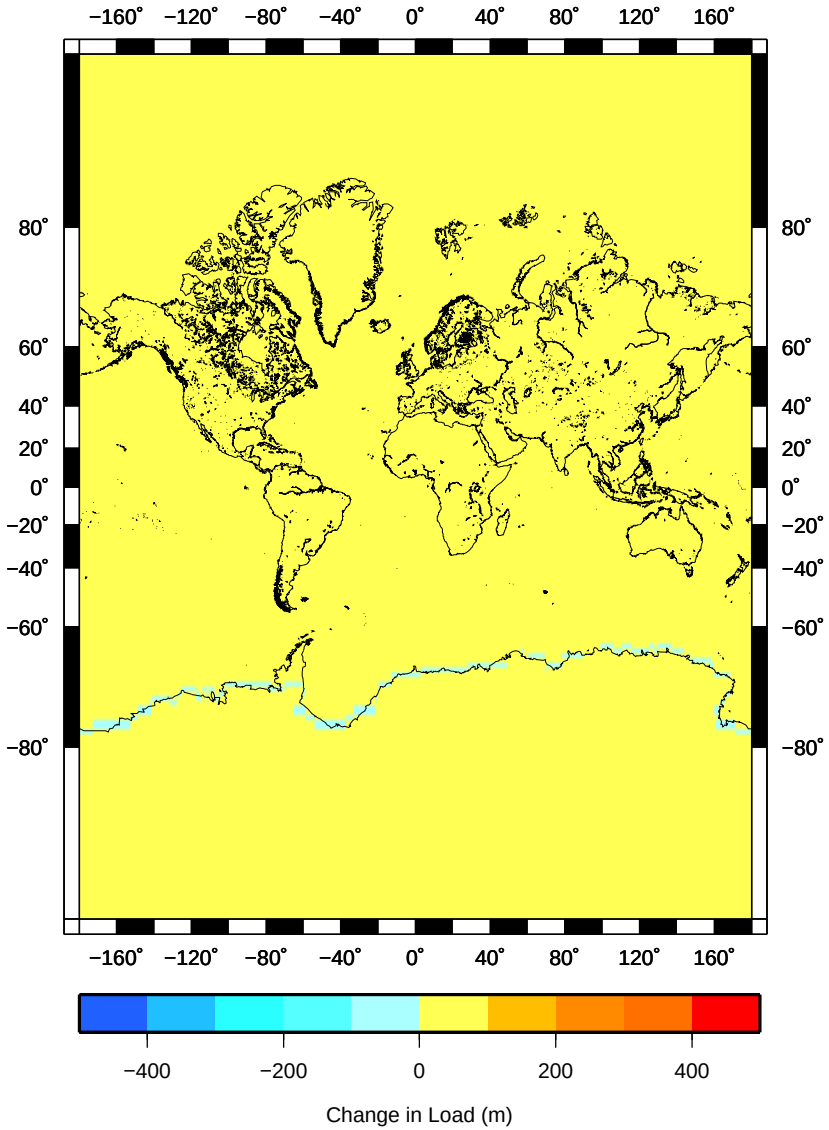

Ice load at 122 kyr BP for Antarctica experiment

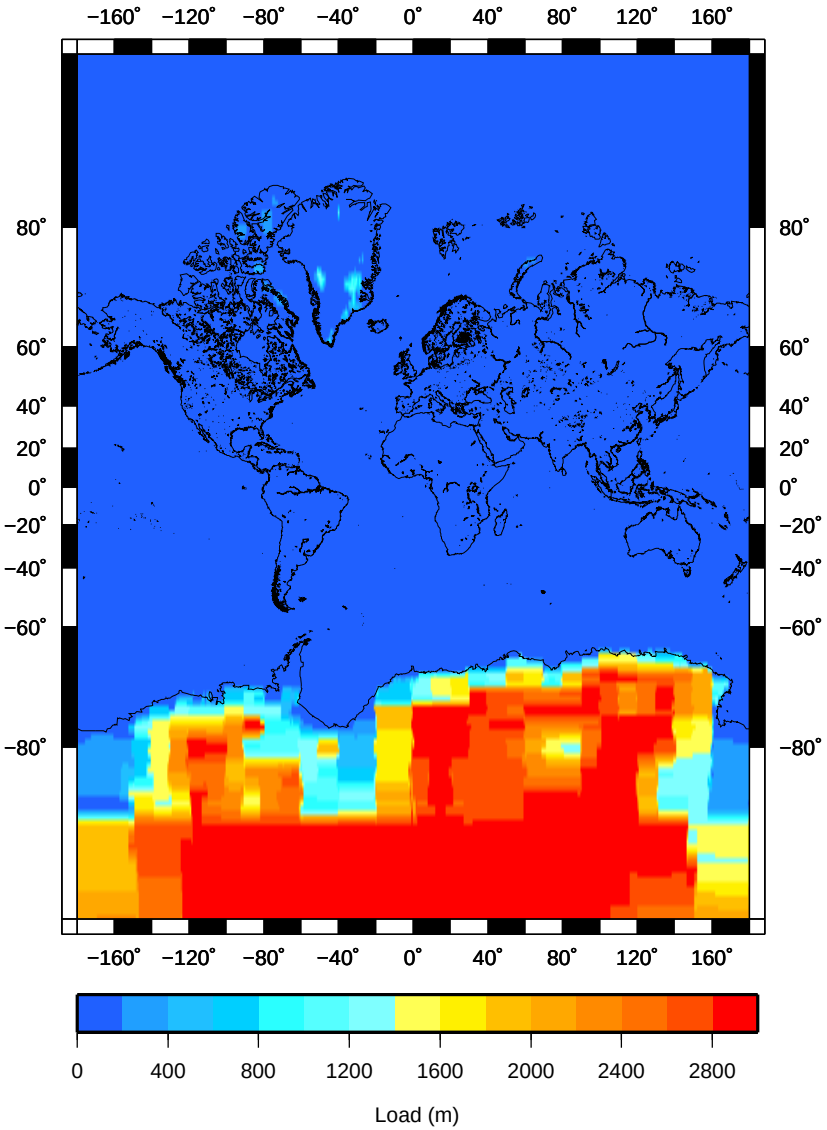

Change in ice load at 122 kyr BP for Antarctica experiment

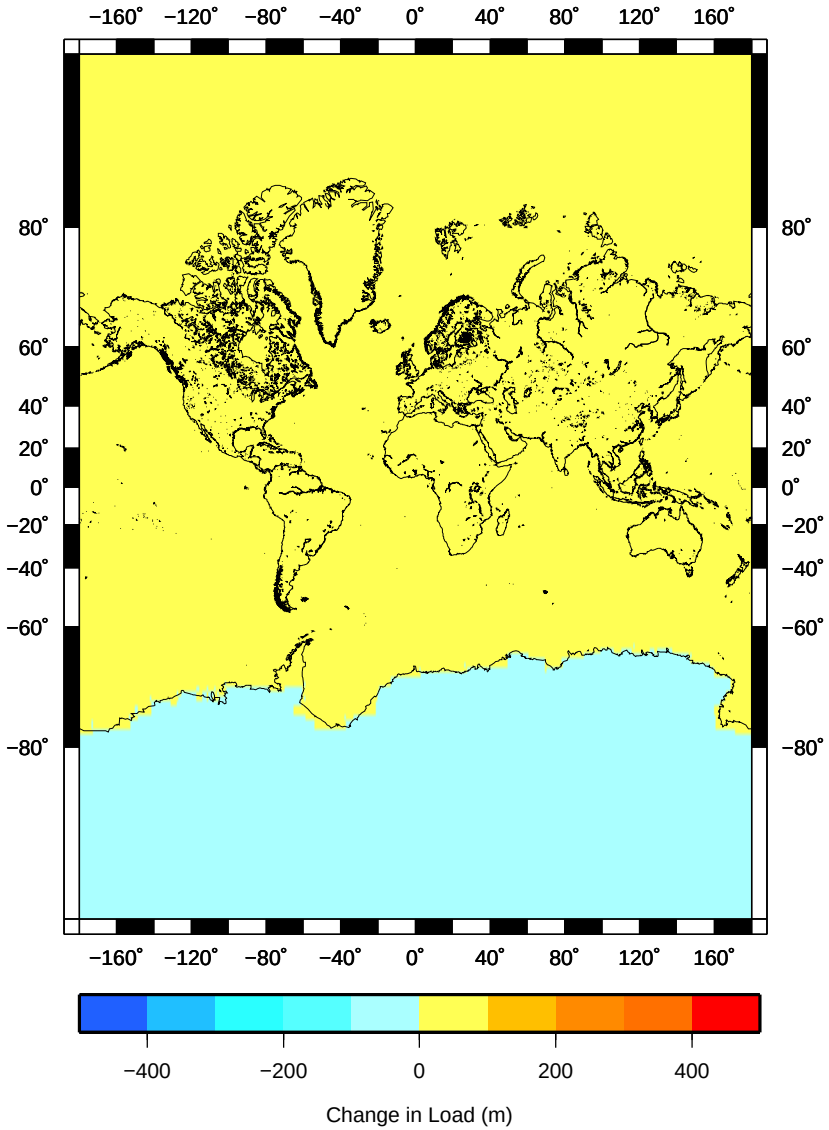

Ice load at 121 kyr BP for Antarctica experiment

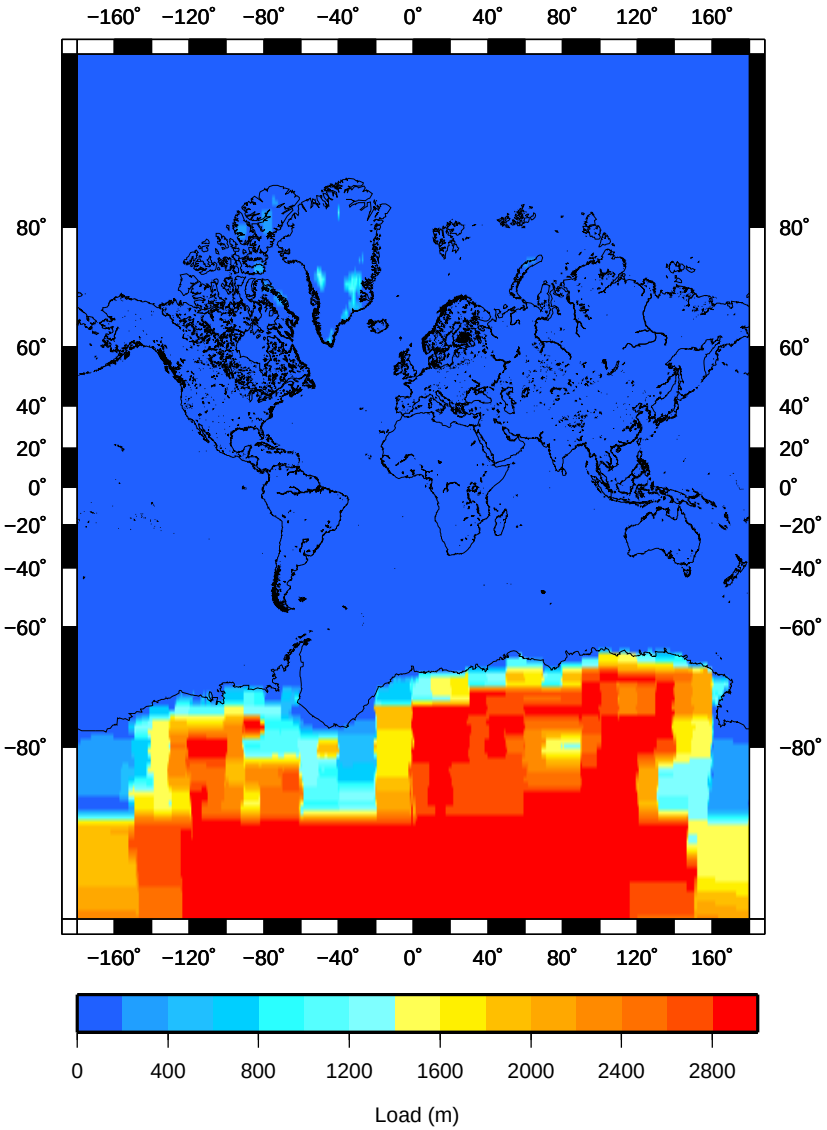

Change in ice load at 121 kyr BP for Antarctica experiment

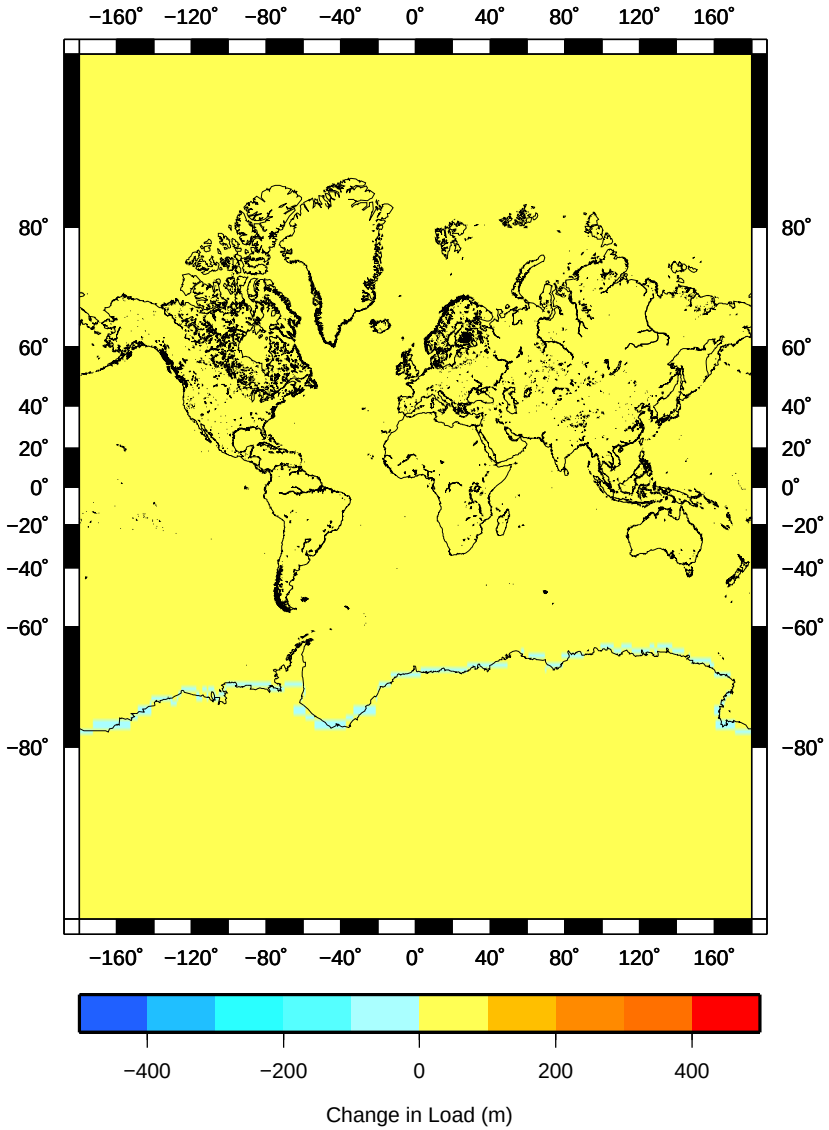

Ice load at 120 kyr BP for Antarctica experiment

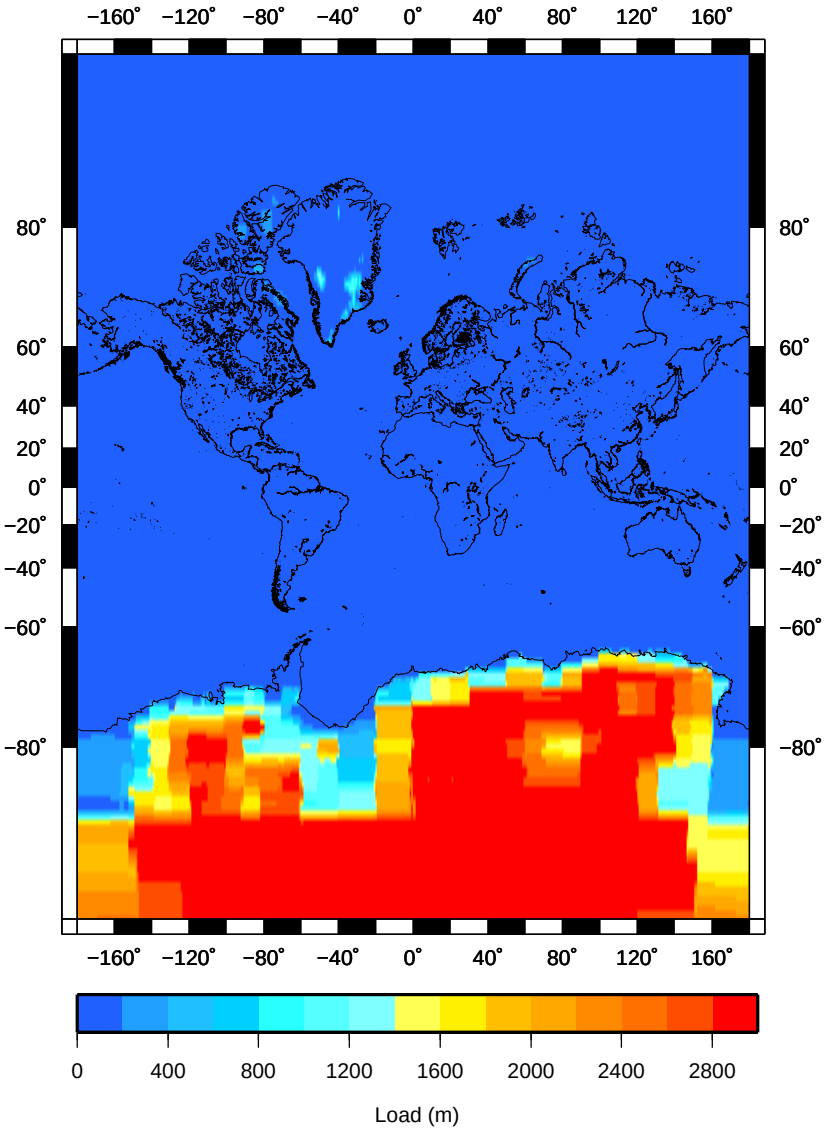

Change in ice load at 120 kyr BP for Antarctica experiment

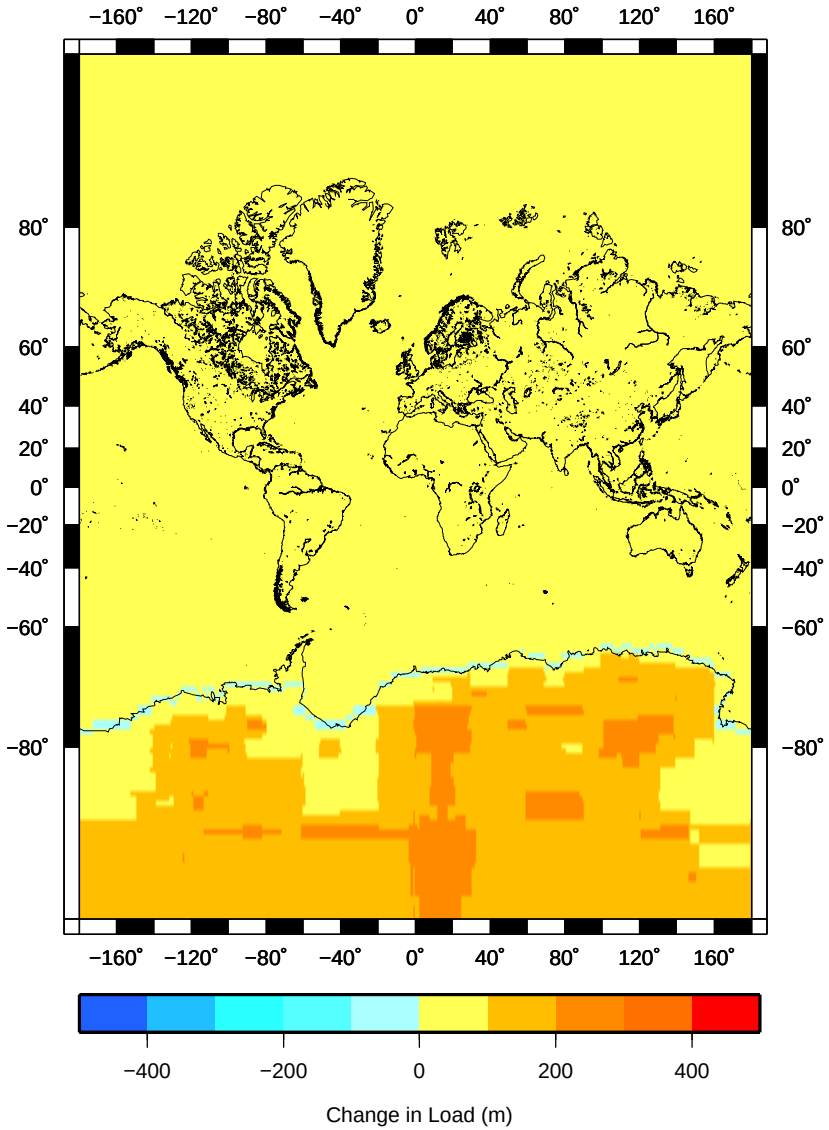

Ice load at 119 kyr BP for Antarctica experiment

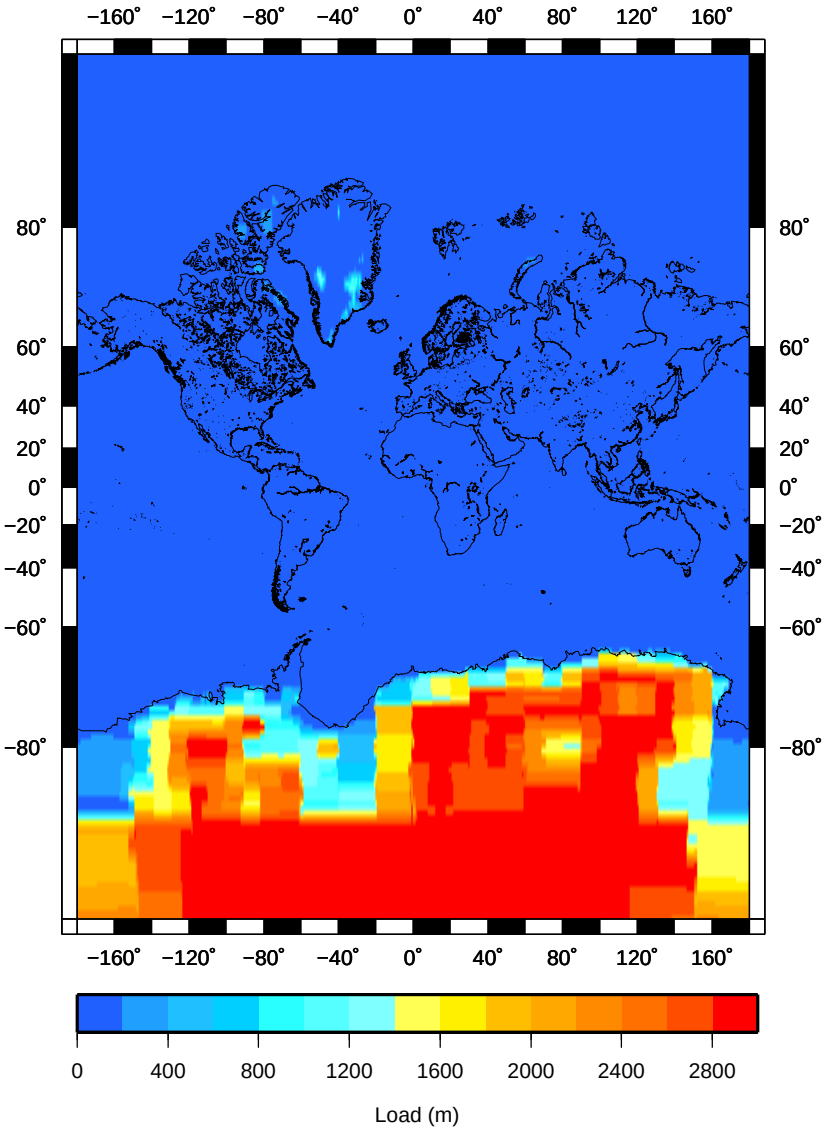

Change in ice load at 119 kyr BP for Antarctica experiment

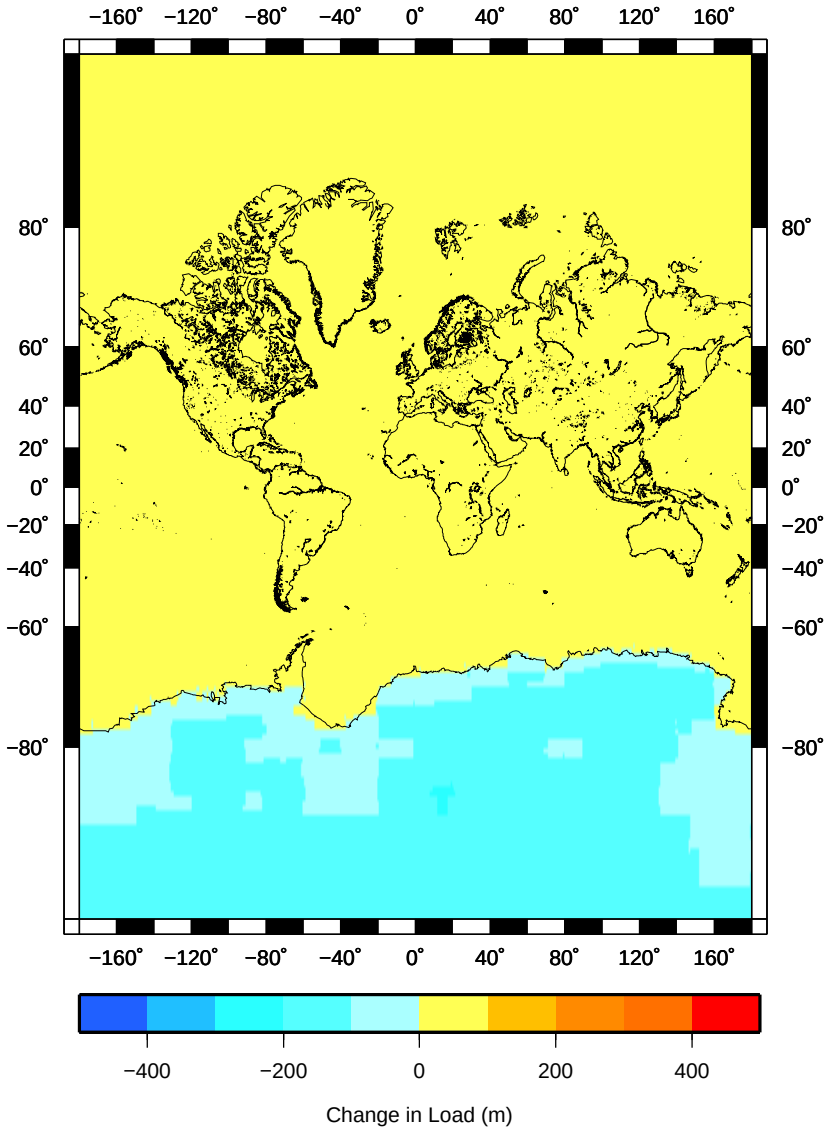

Ice load at 118 kyr BP for Antarctica experiment

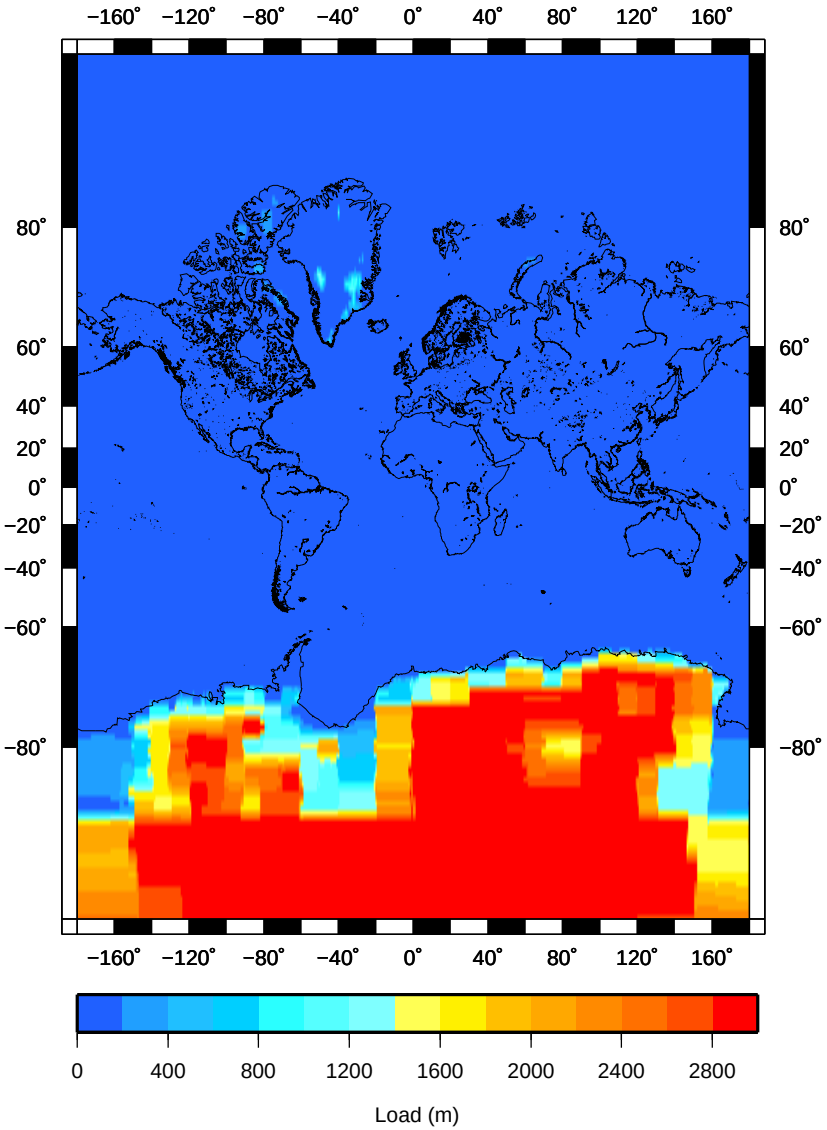

Change in ice load at 118 kyr BP for Antarctica experiment

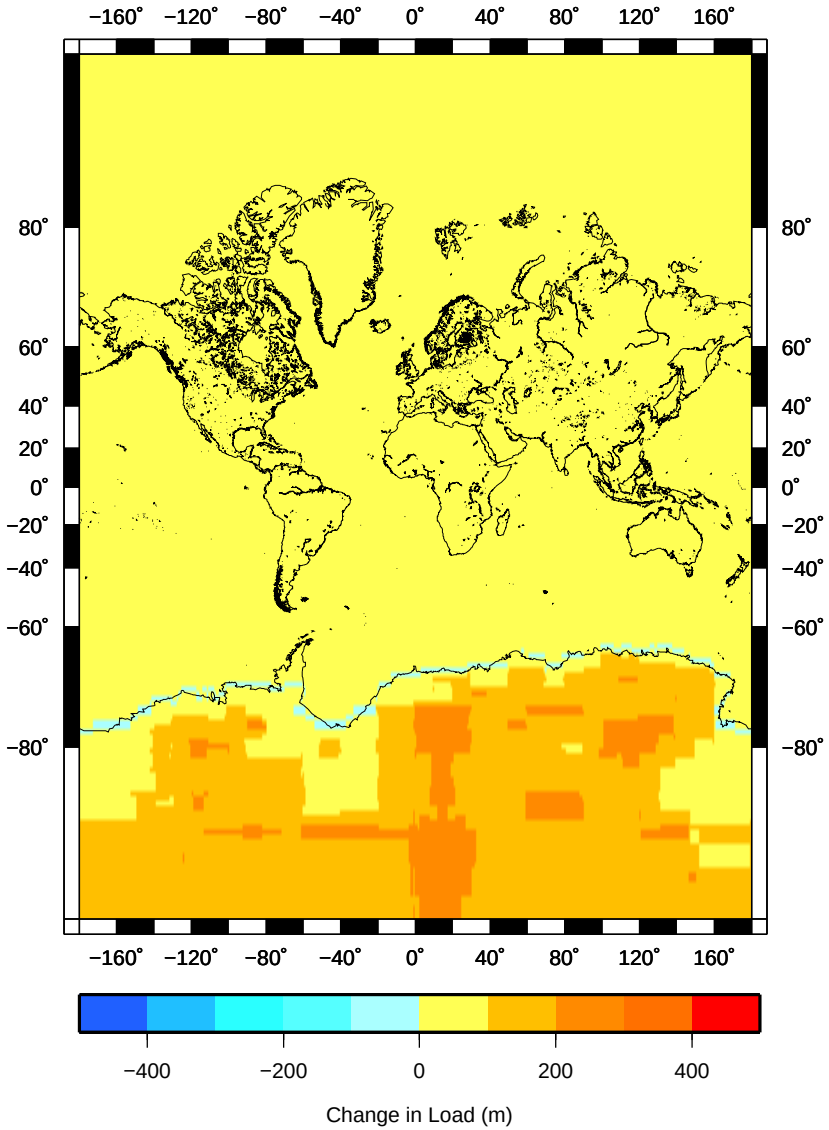

Ice load at 117 kyr BP for Antarctica experiment

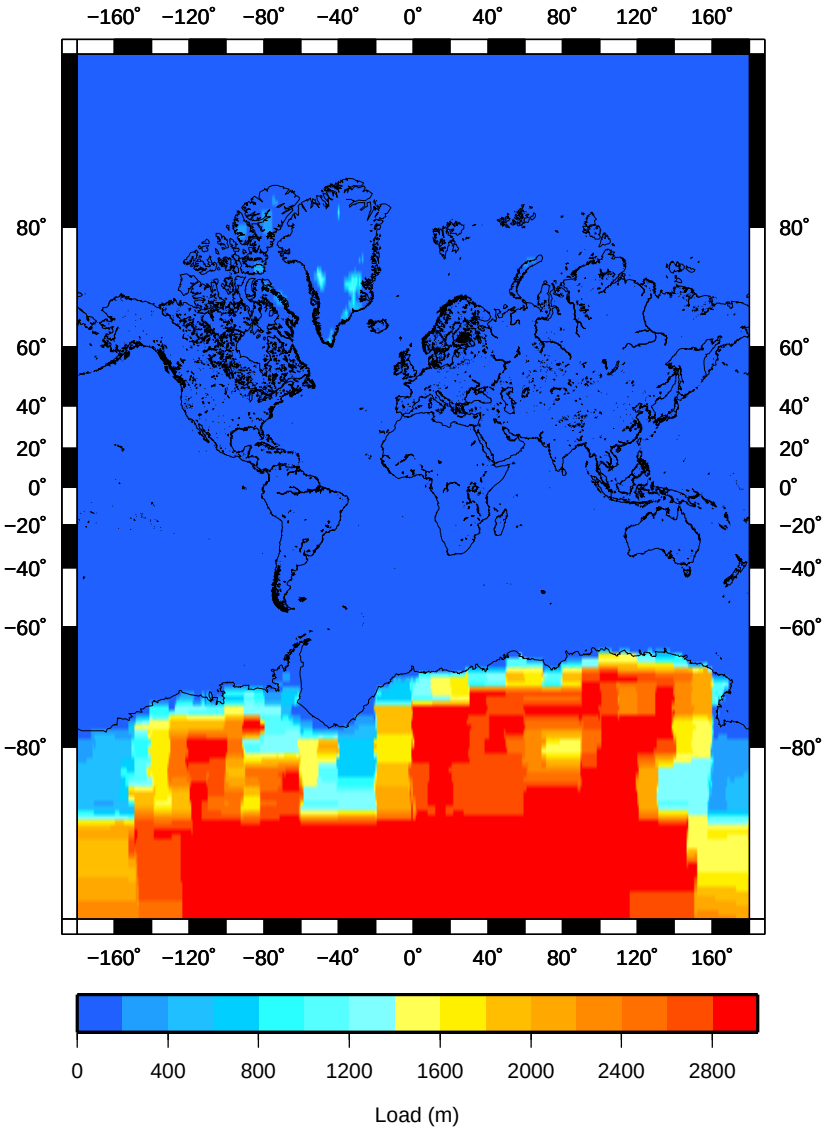

Change in ice load at 117 kyr BP for Antarctica experiment

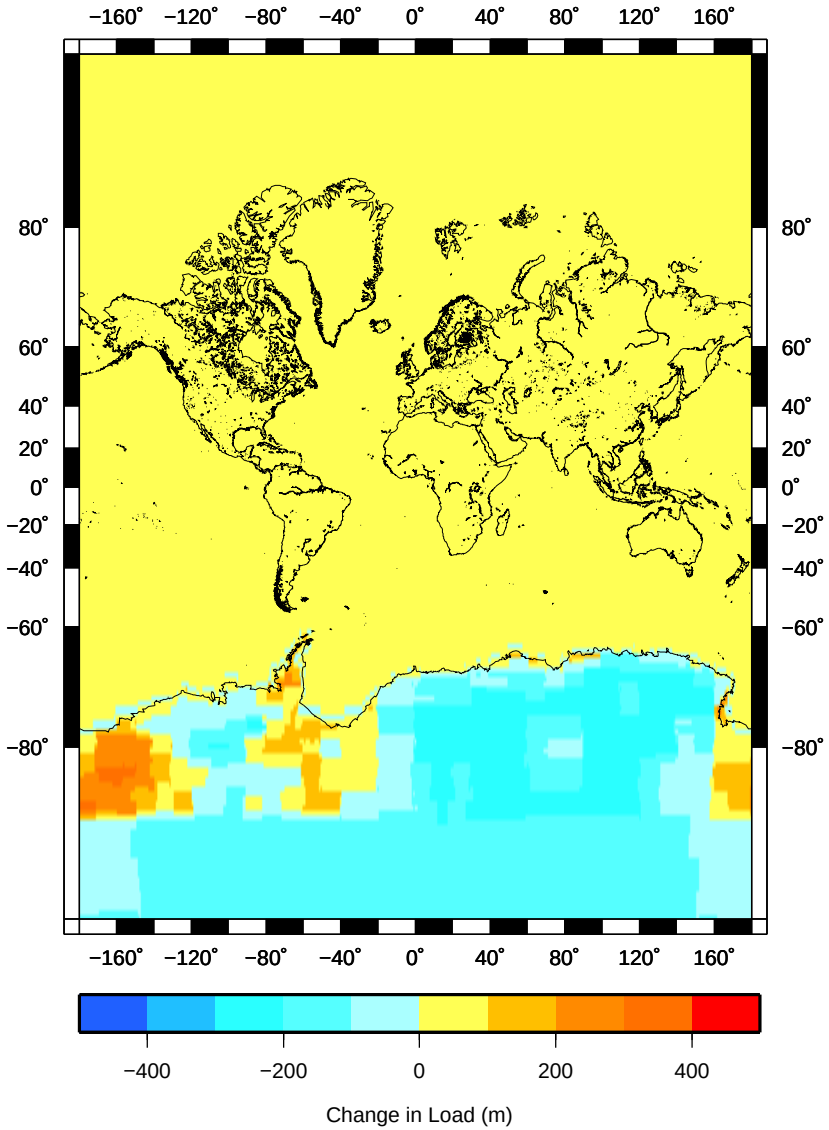

Ice load at 116 kyr BP for Antarctica experiment

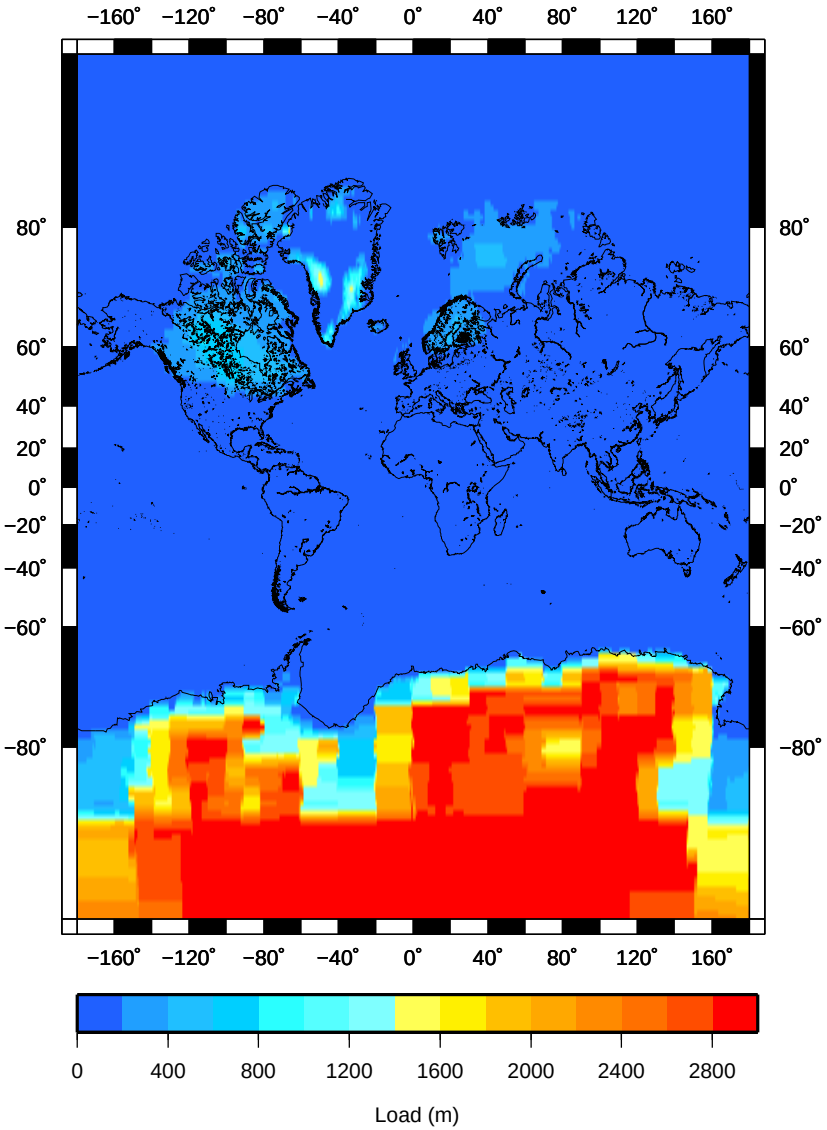

Change in ice load at 116 kyr BP for Antarctica experiment

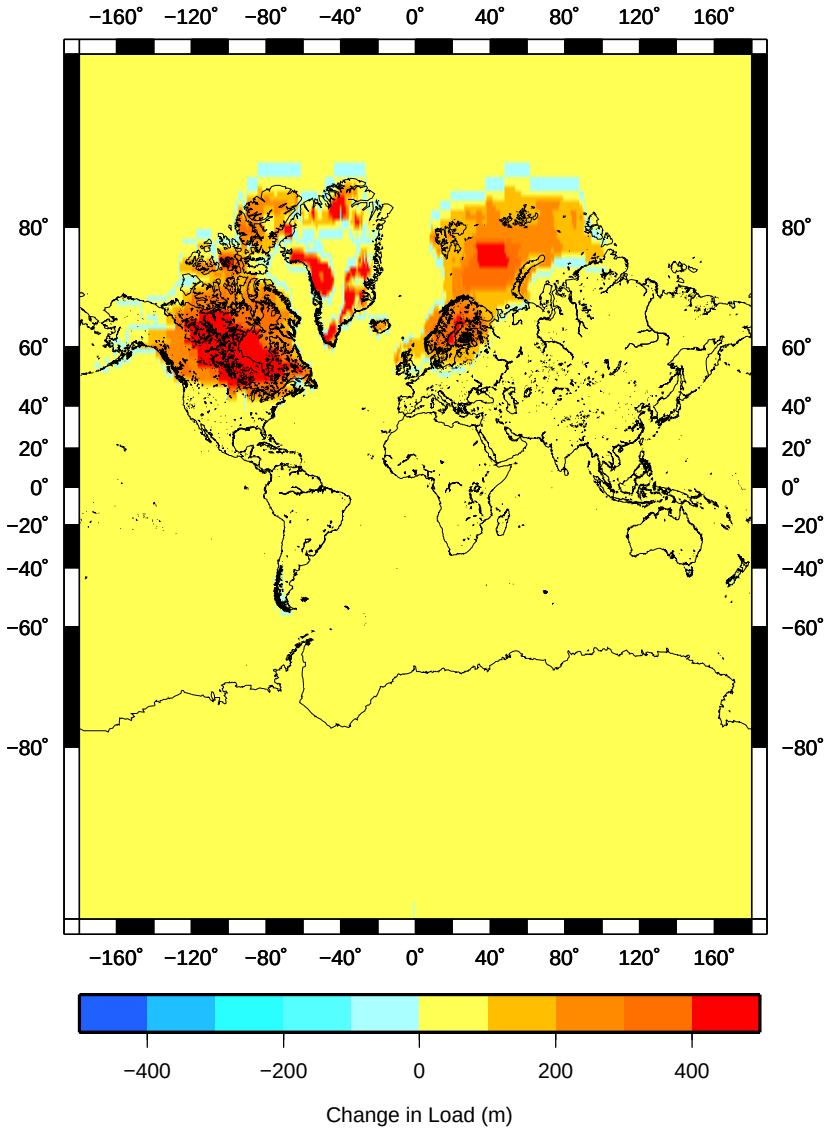

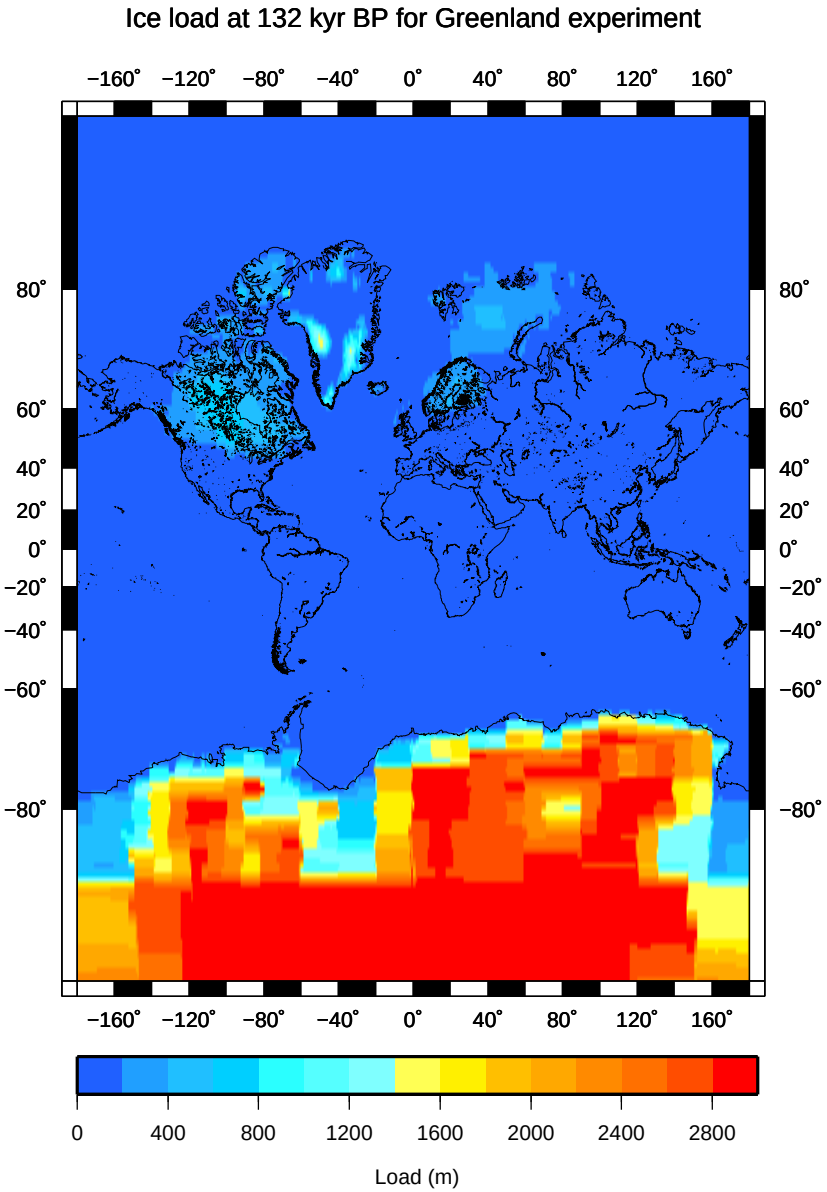
Ice load at 132 kyr BP for Greenland experiment
−160° −120° −80° −40° 0° 40° 80° 120° 160°
80°
60°
40°
20°
0°
−20°
−40°
−60°
−80°
0 400 800 1200 1600 2000 2400 2800
Load (m)

Ice load at 127 kyr BP for Greenland experiment

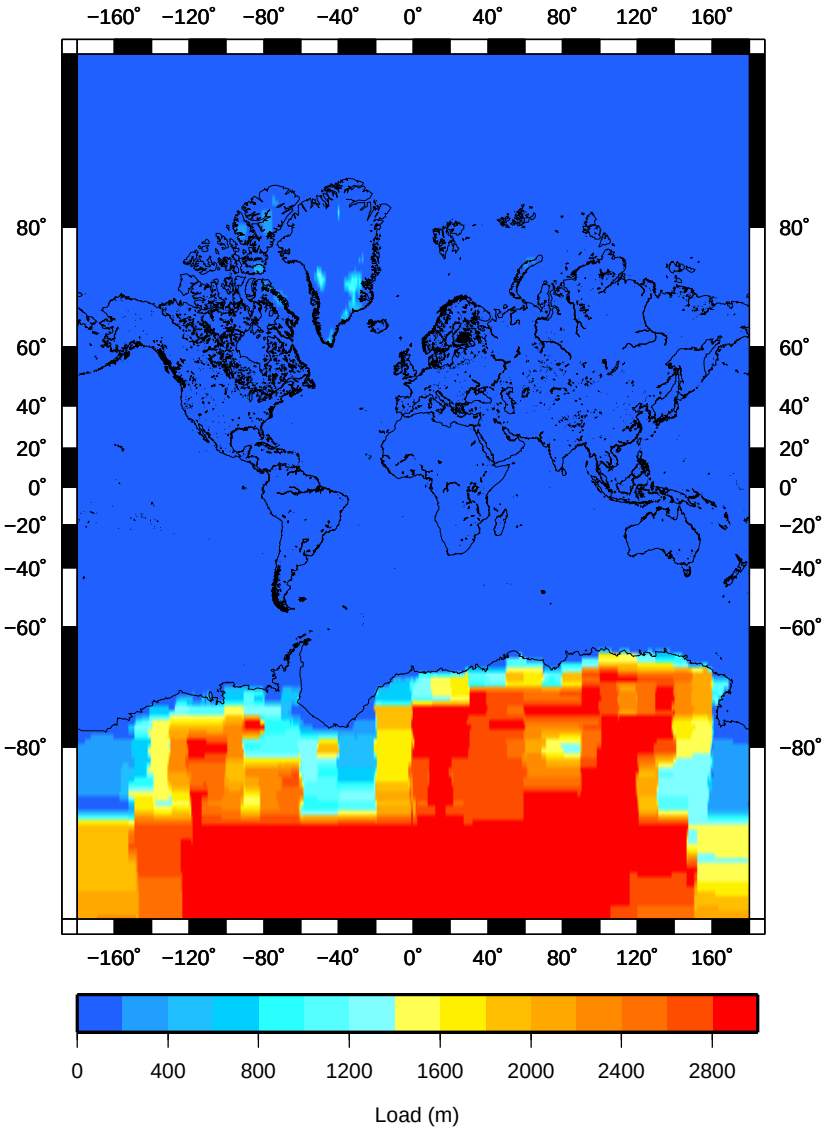

Change in ice load at 127 kyr BP for Greenland experiment

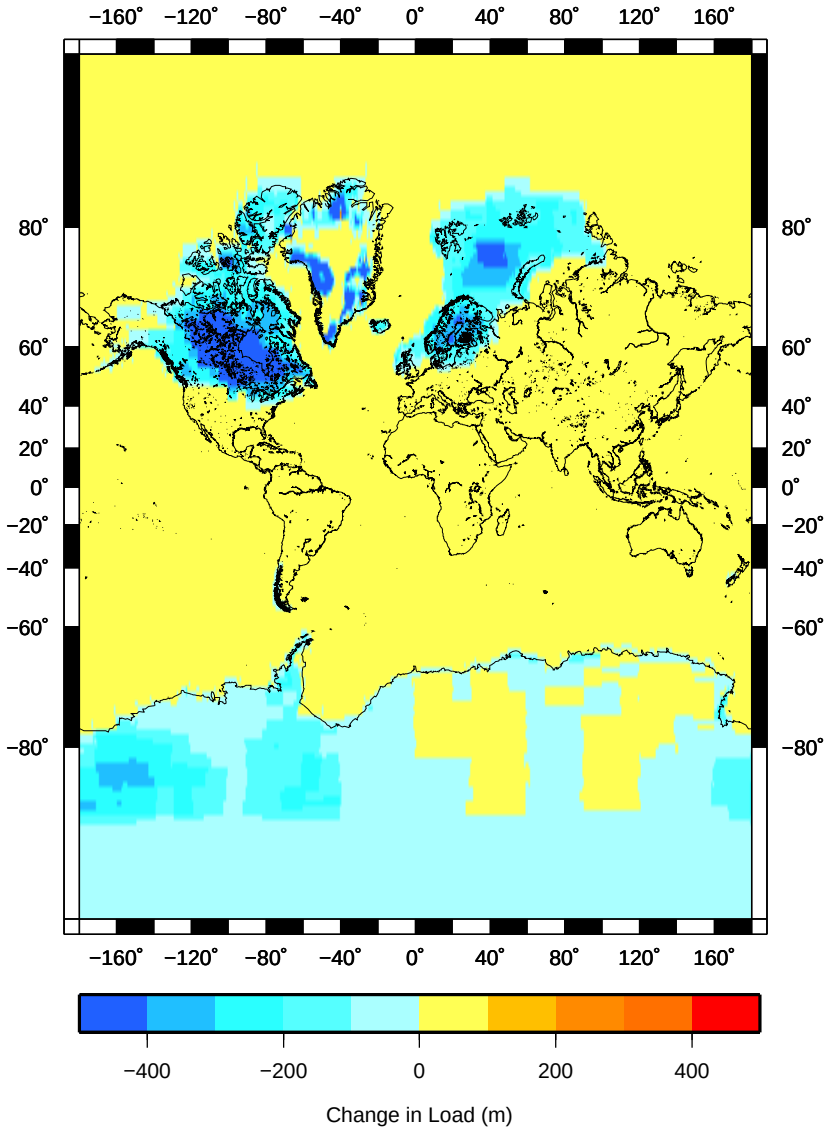

Ice load at 126 kyr BP for Greenland experiment

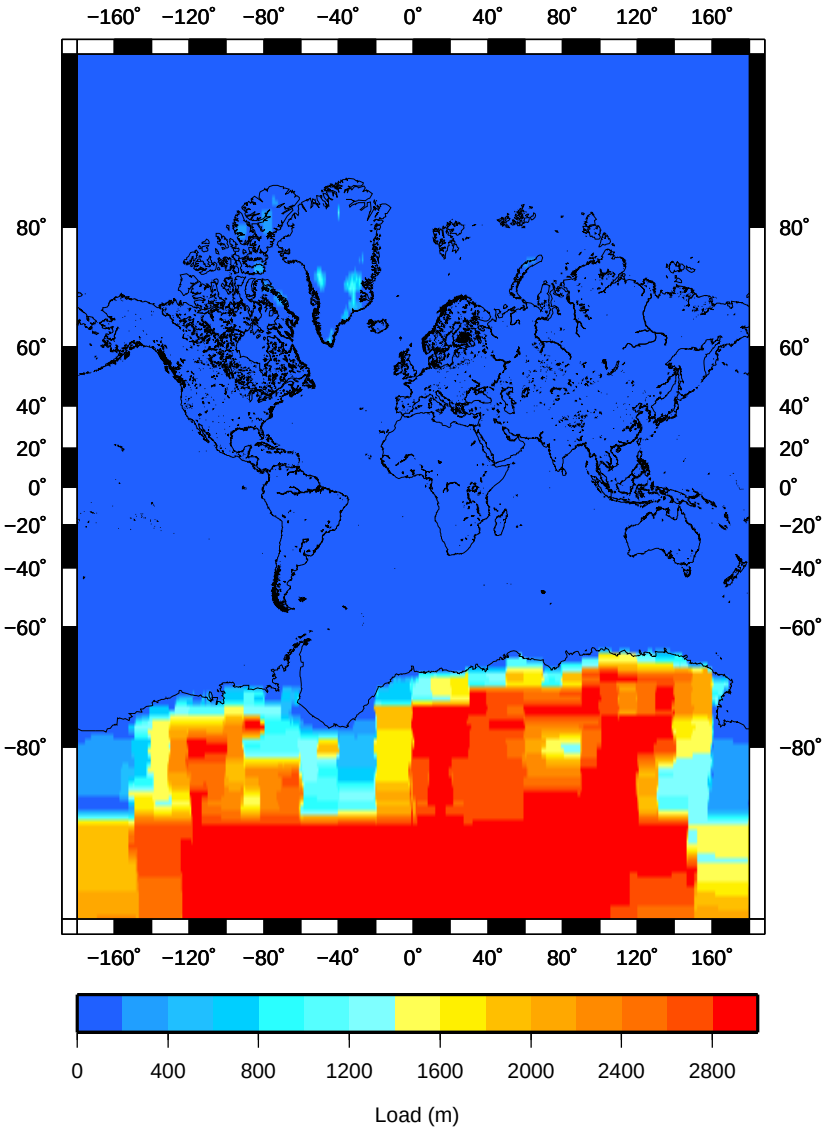

Change in ice load at 126 kyr BP for Greenland experiment

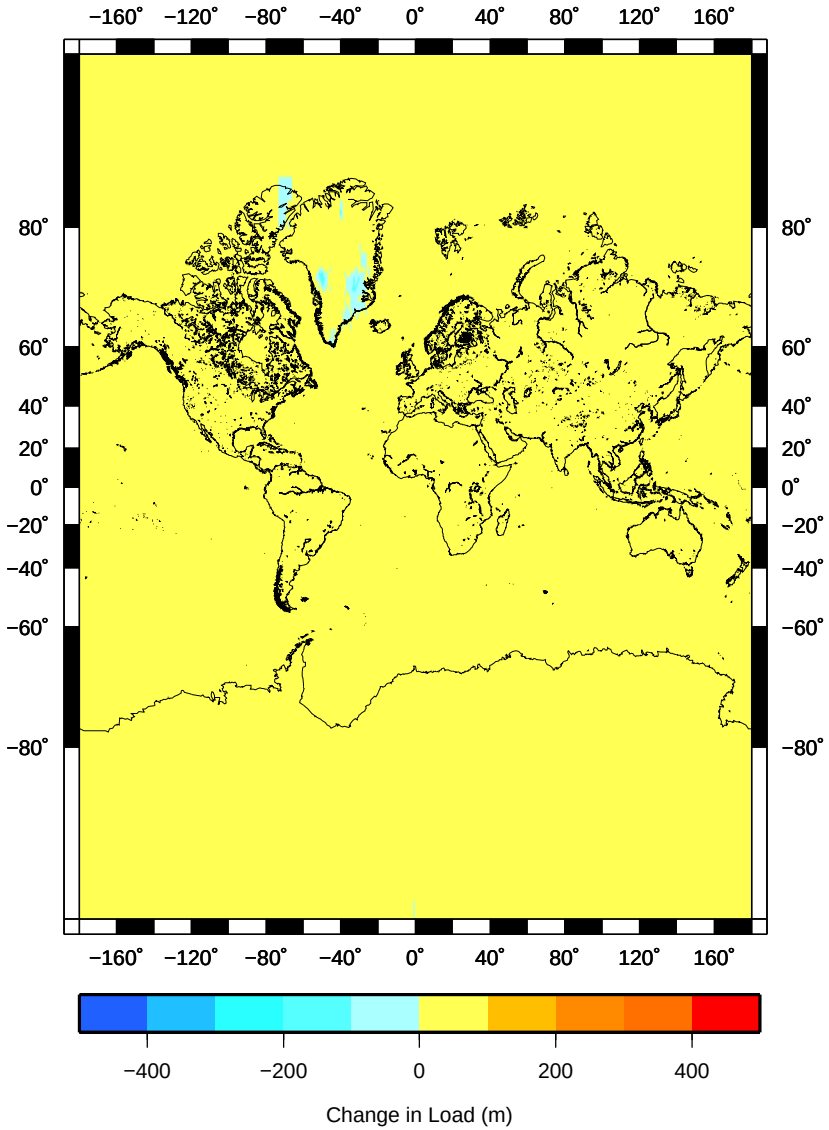

Ice load at 125 kyr BP for Greenland experiment

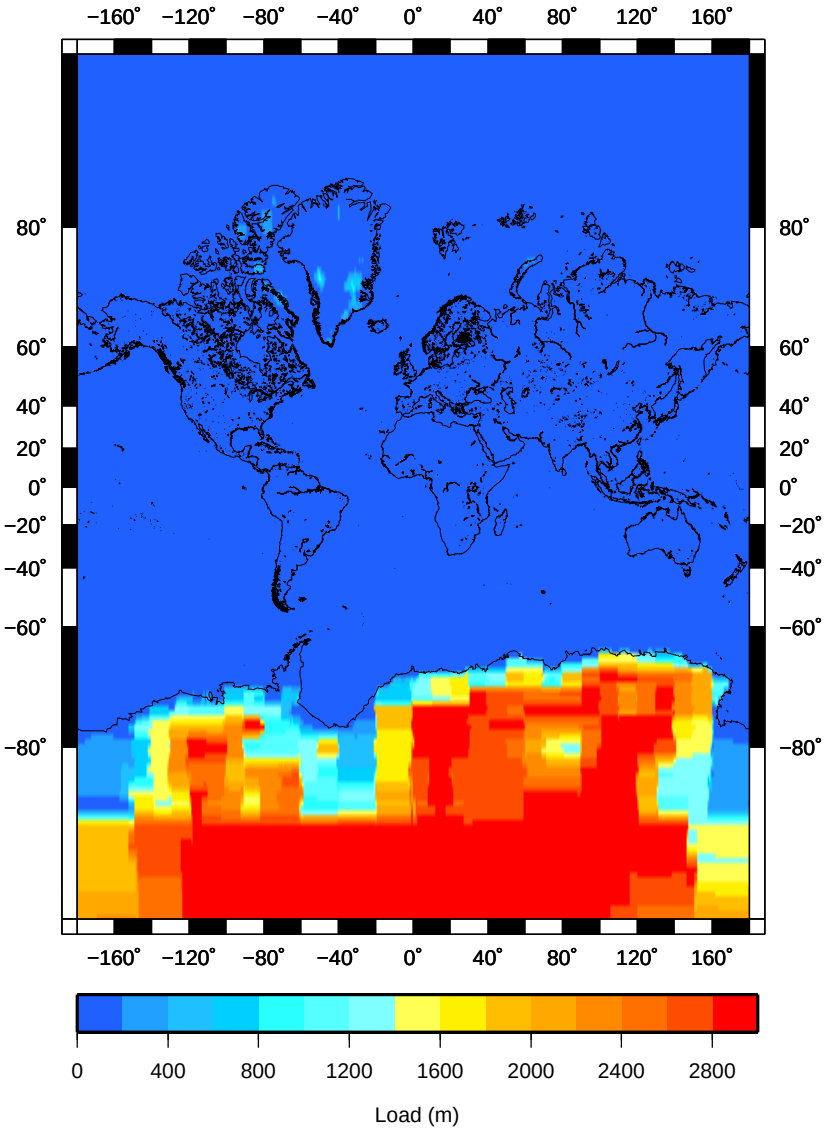

Change in ice load at 125 kyr BP for Greenland experiment

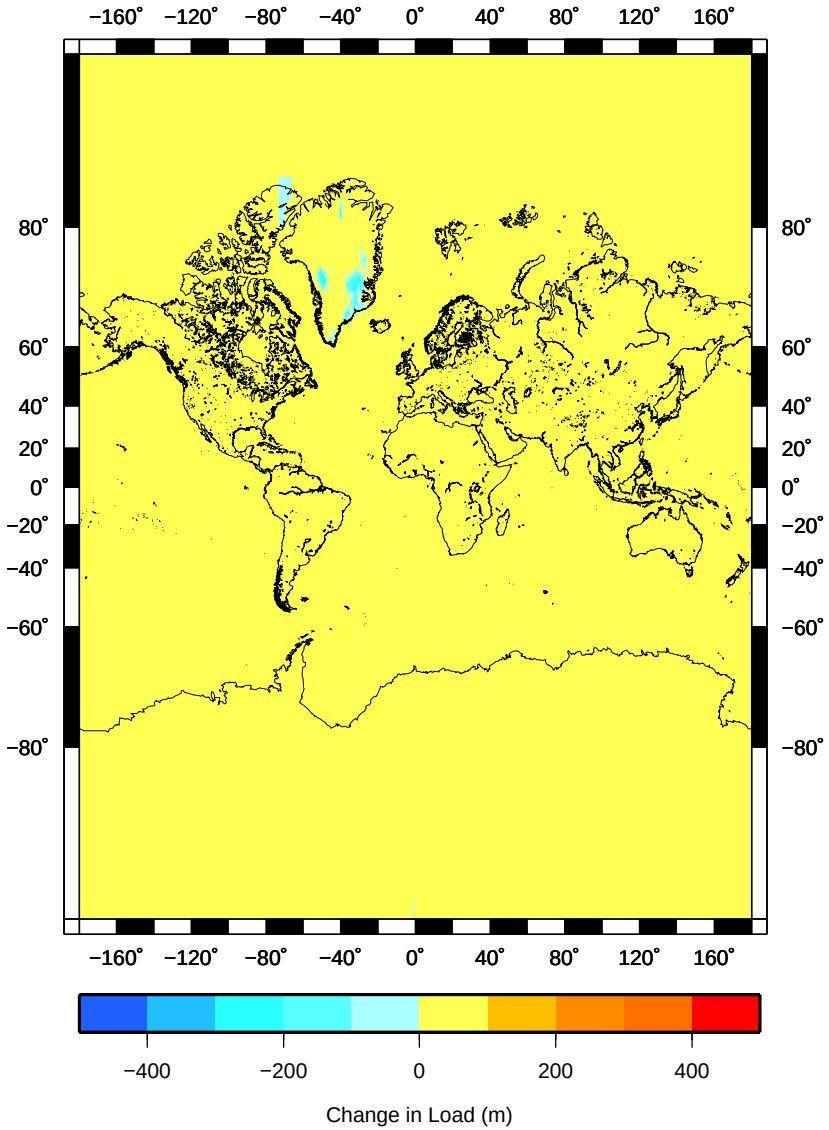

Ice load at 124 kyr BP for Greenland experiment

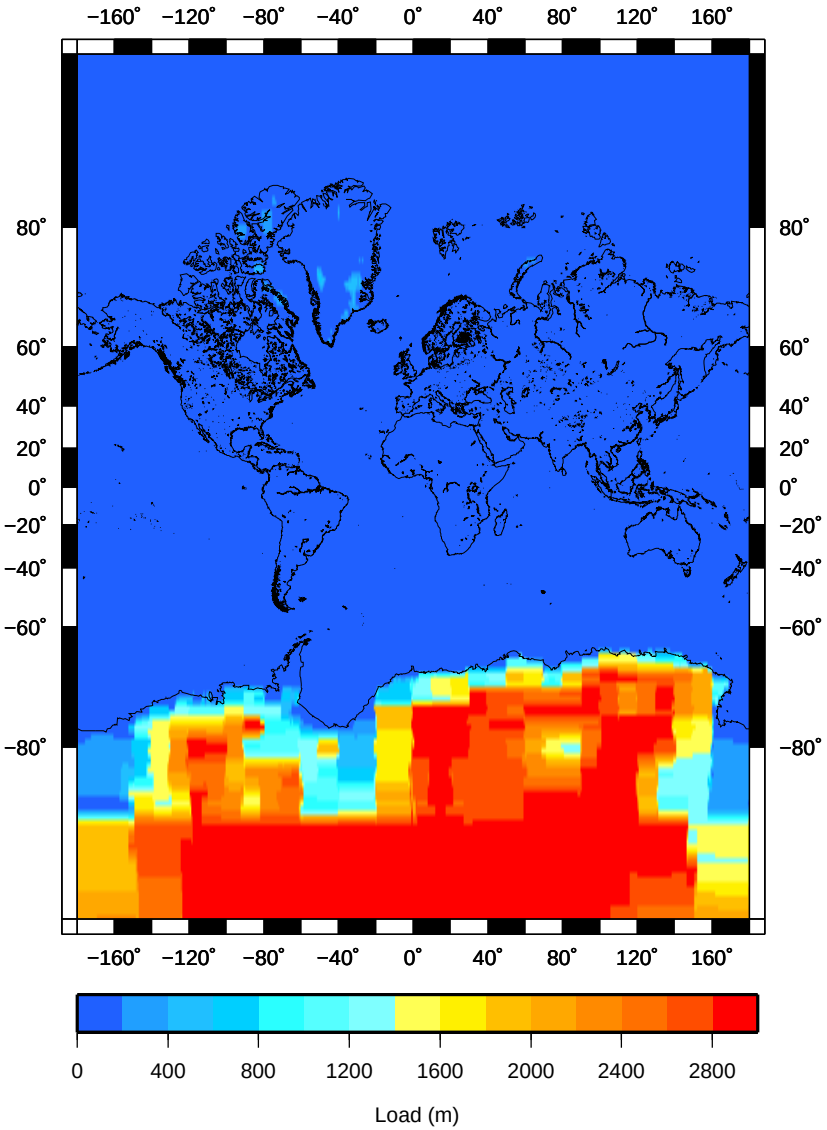

Change in ice load at 124 kyr BP for Greenland experiment

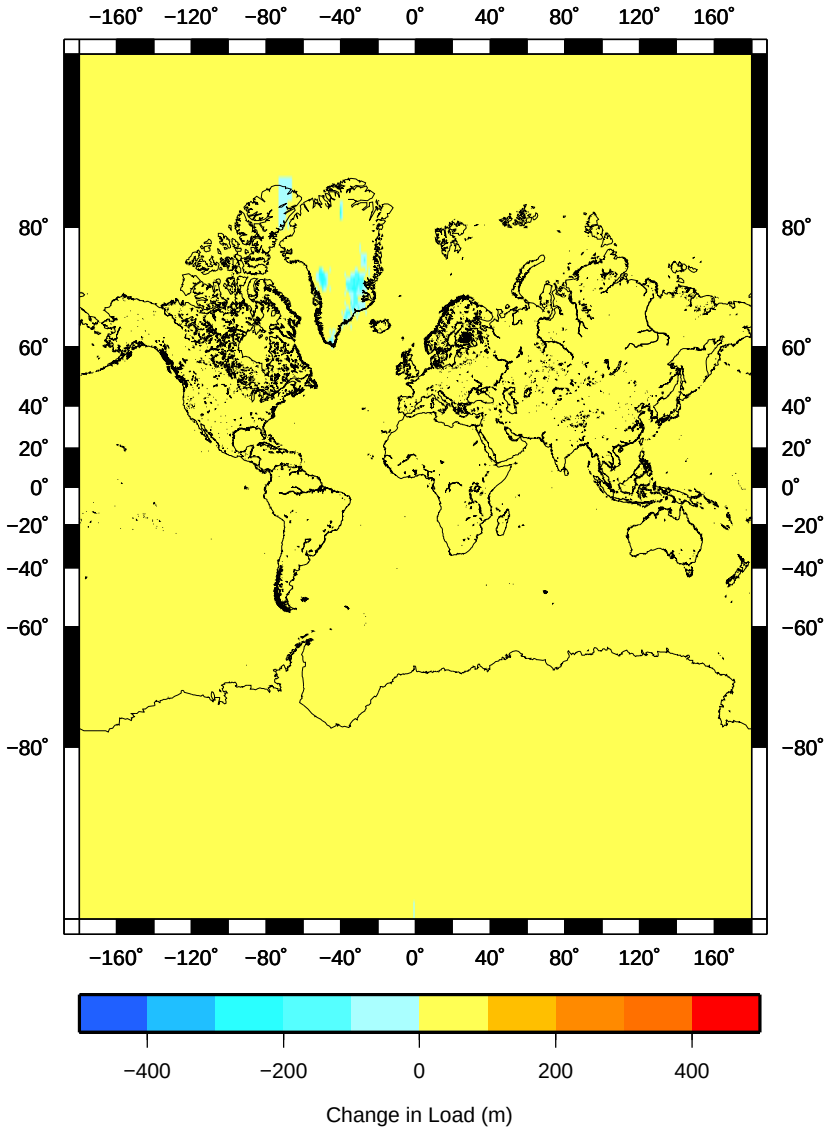

Ice load at 123 kyr BP for Greenland experiment

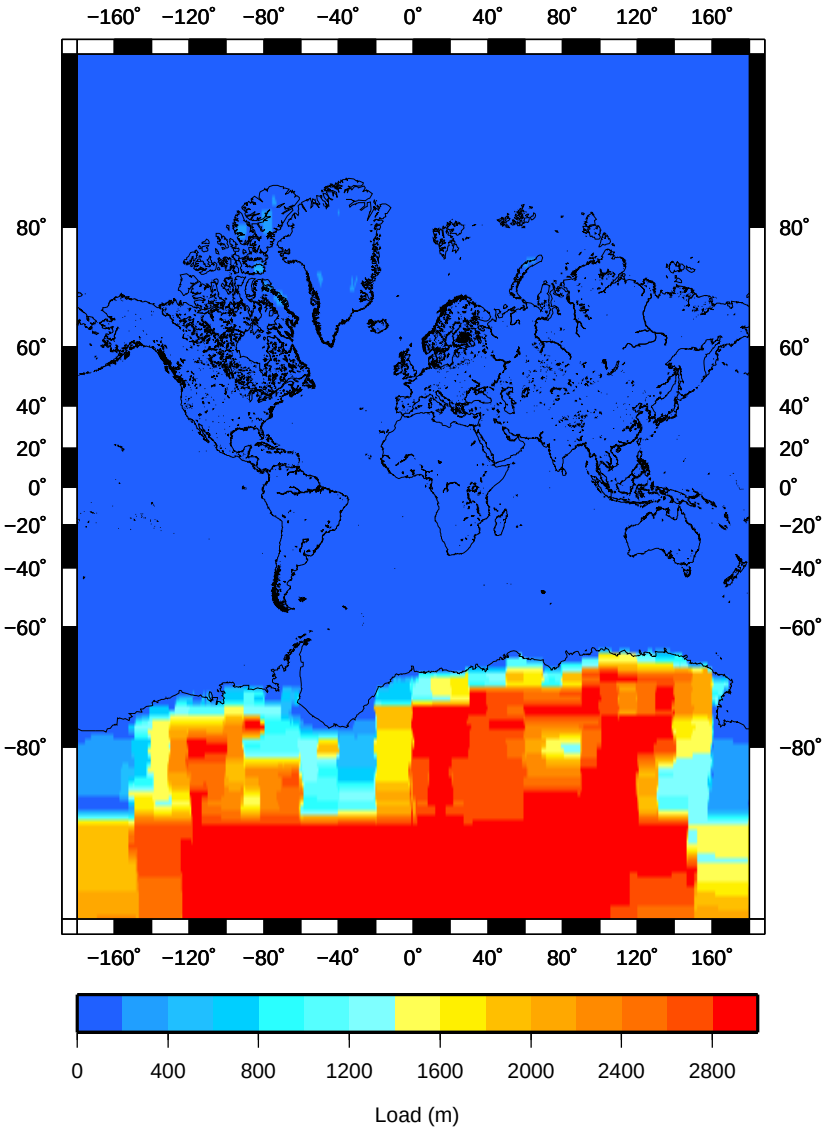

Change in ice load at 123 kyr BP for Greenland experiment

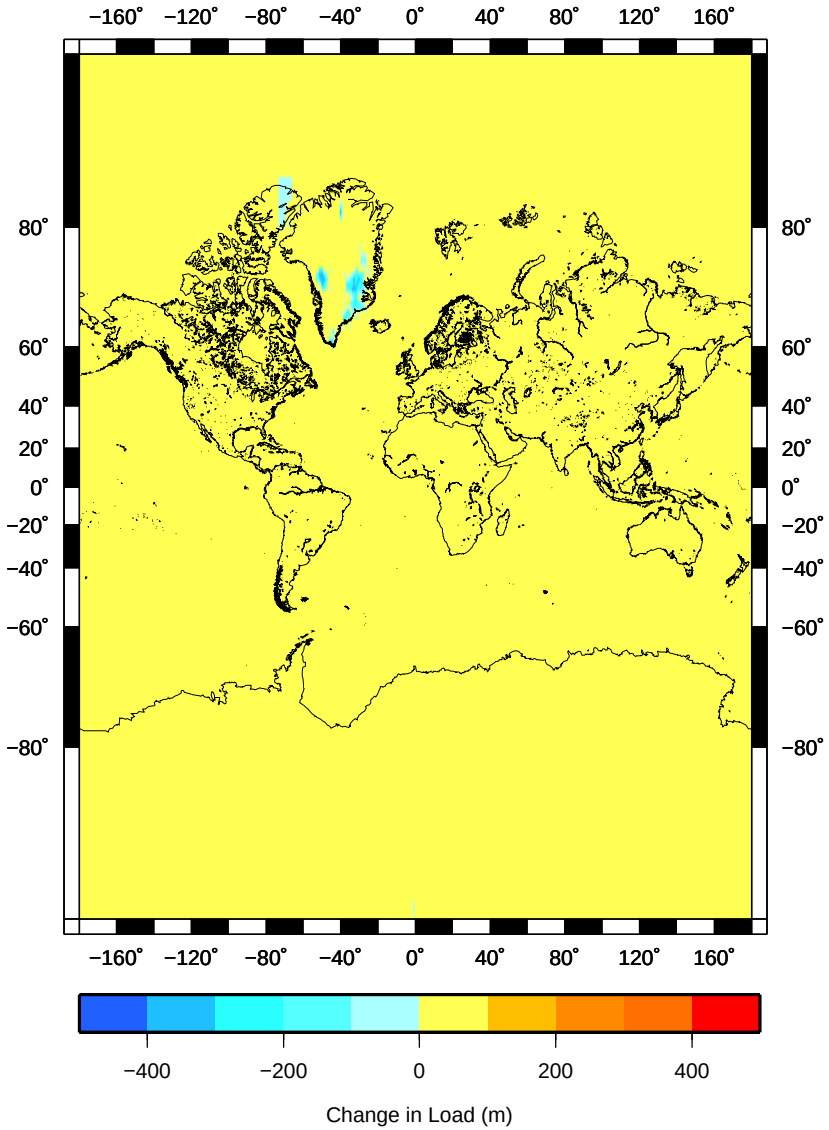

Ice load at 122 kyr BP for Greenland experiment

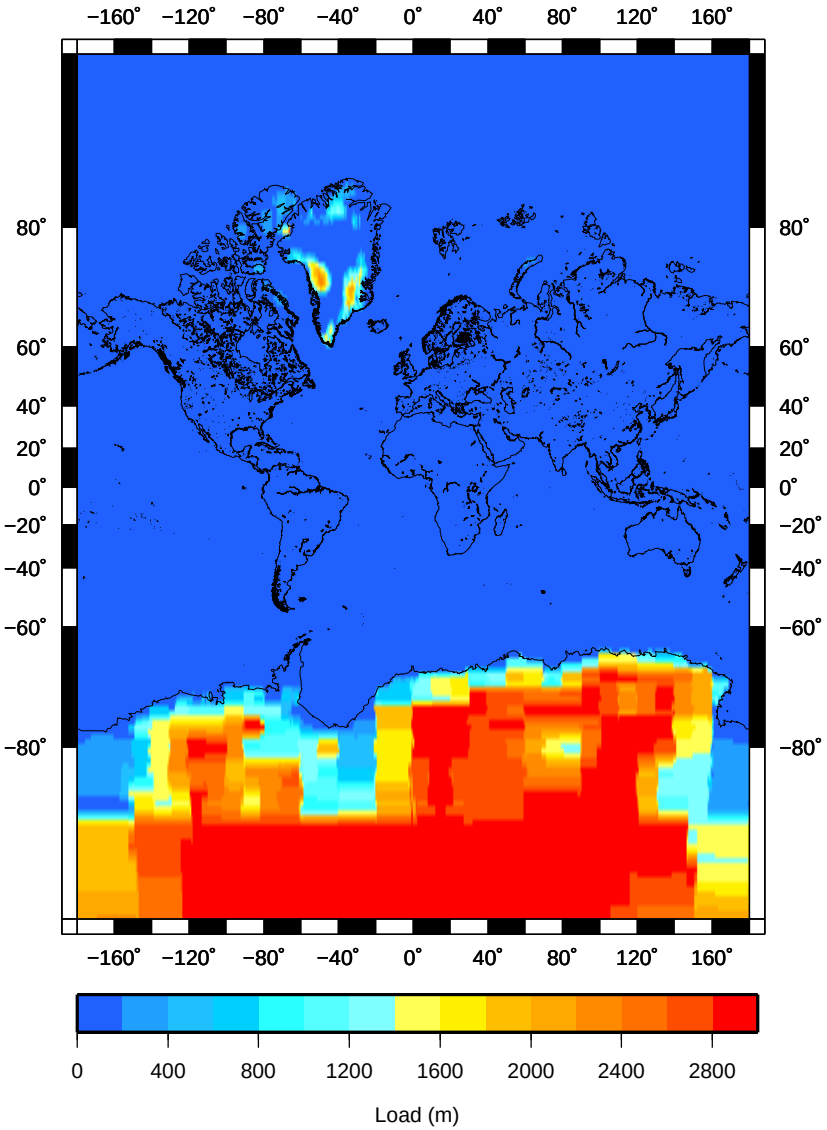

Change in ice load at 122 kyr BP for Greenland experiment

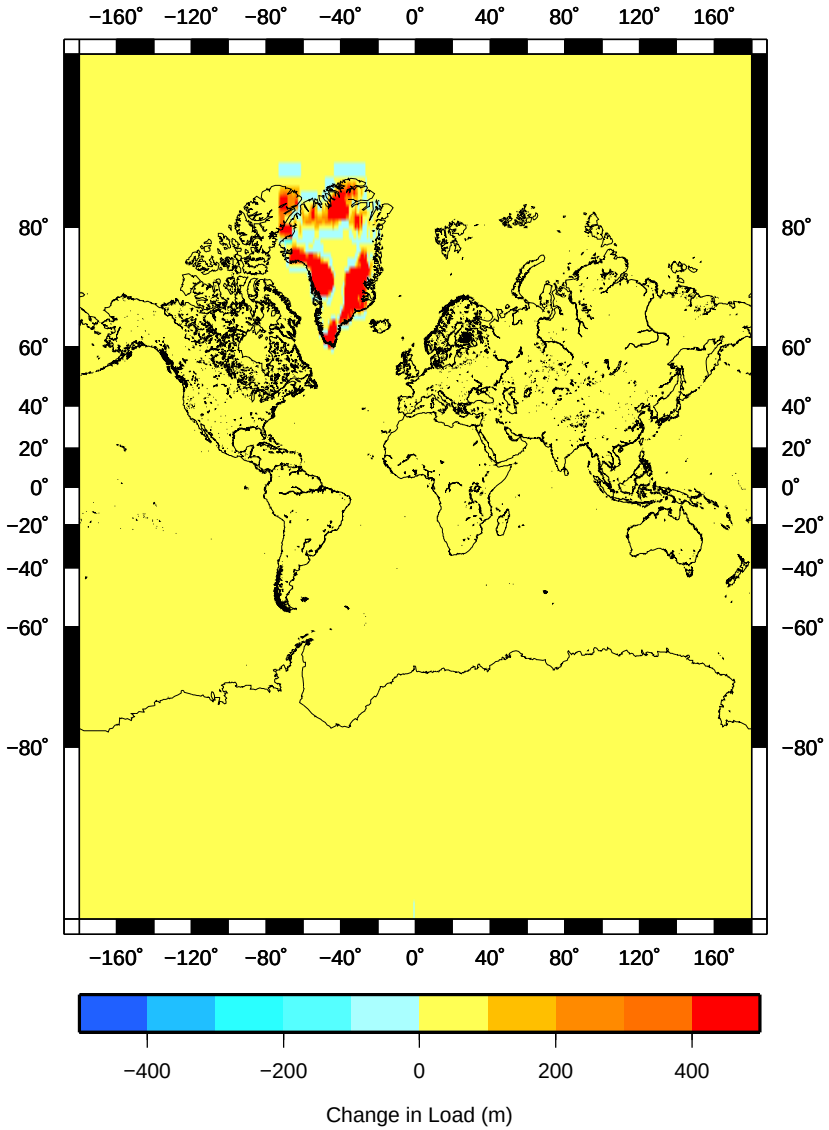

Ice load at 121 kyr BP for Greenland experiment

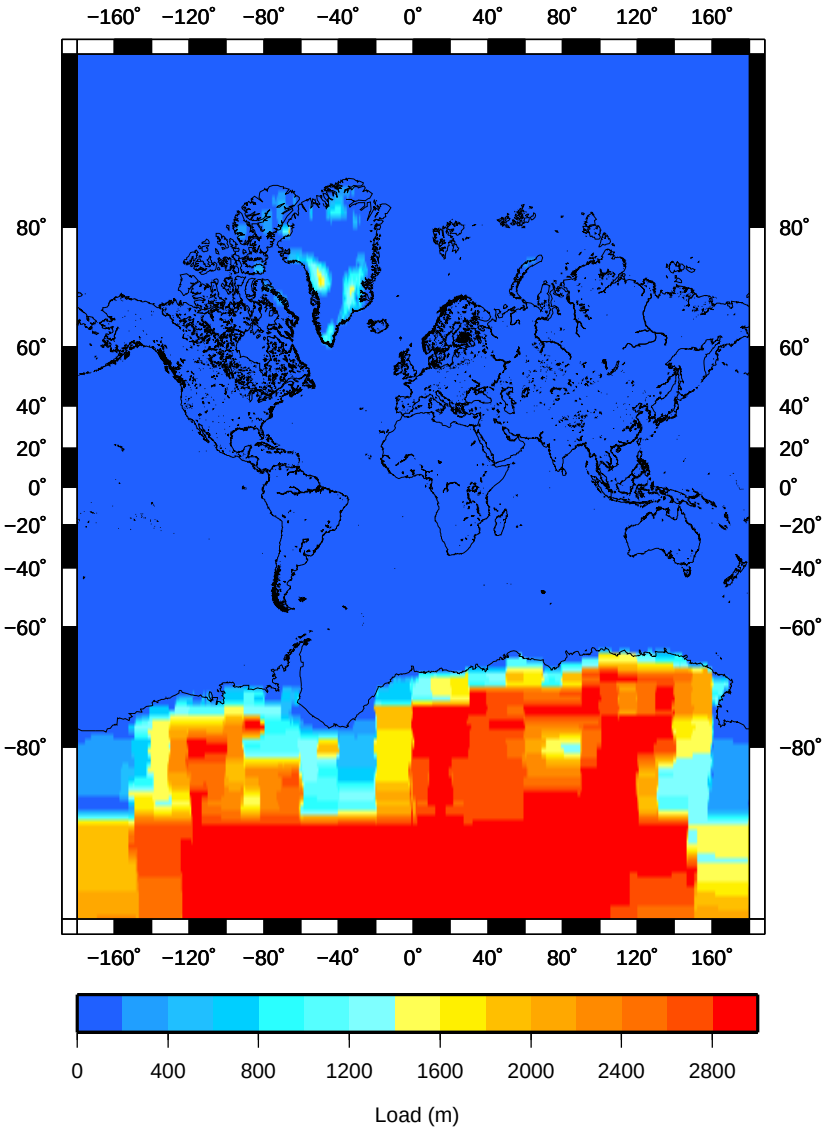

Change in ice load at 121 kyr BP for Greenland experiment

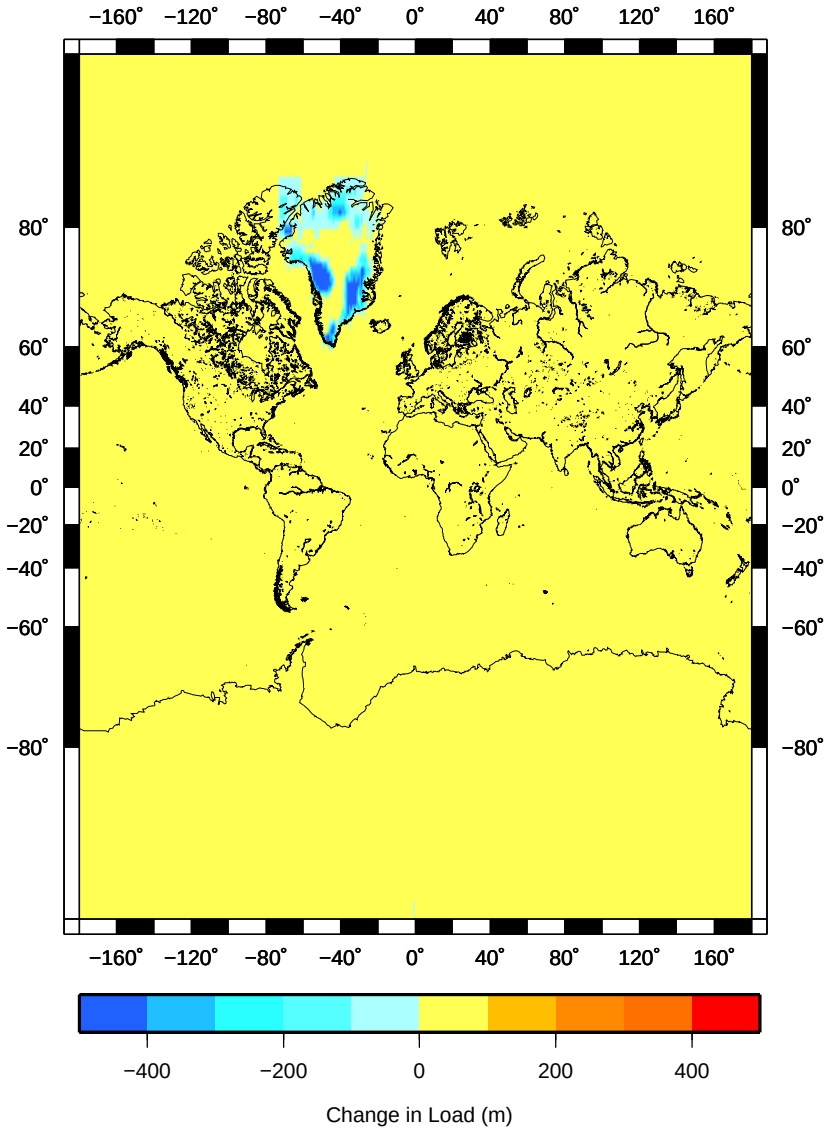

Ice load at 120 kyr BP for Greenland experiment

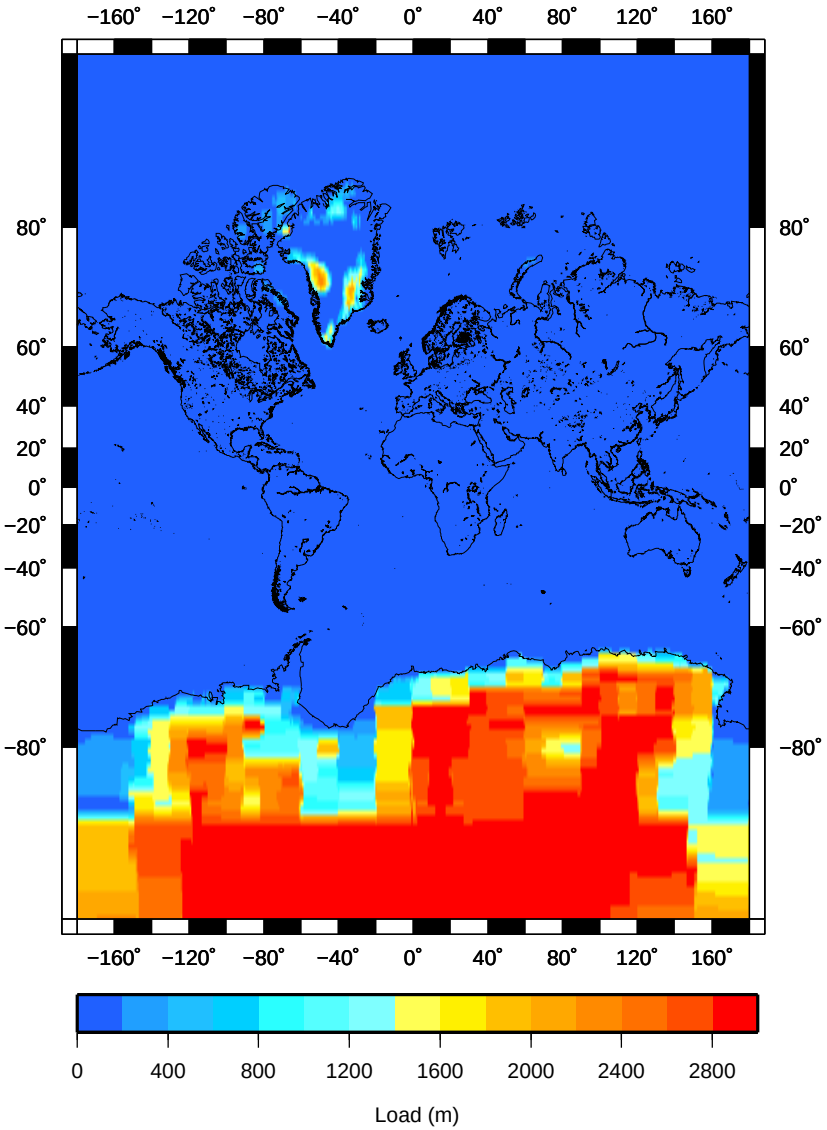

Change in ice load at 120 kyr BP for Greenland experiment

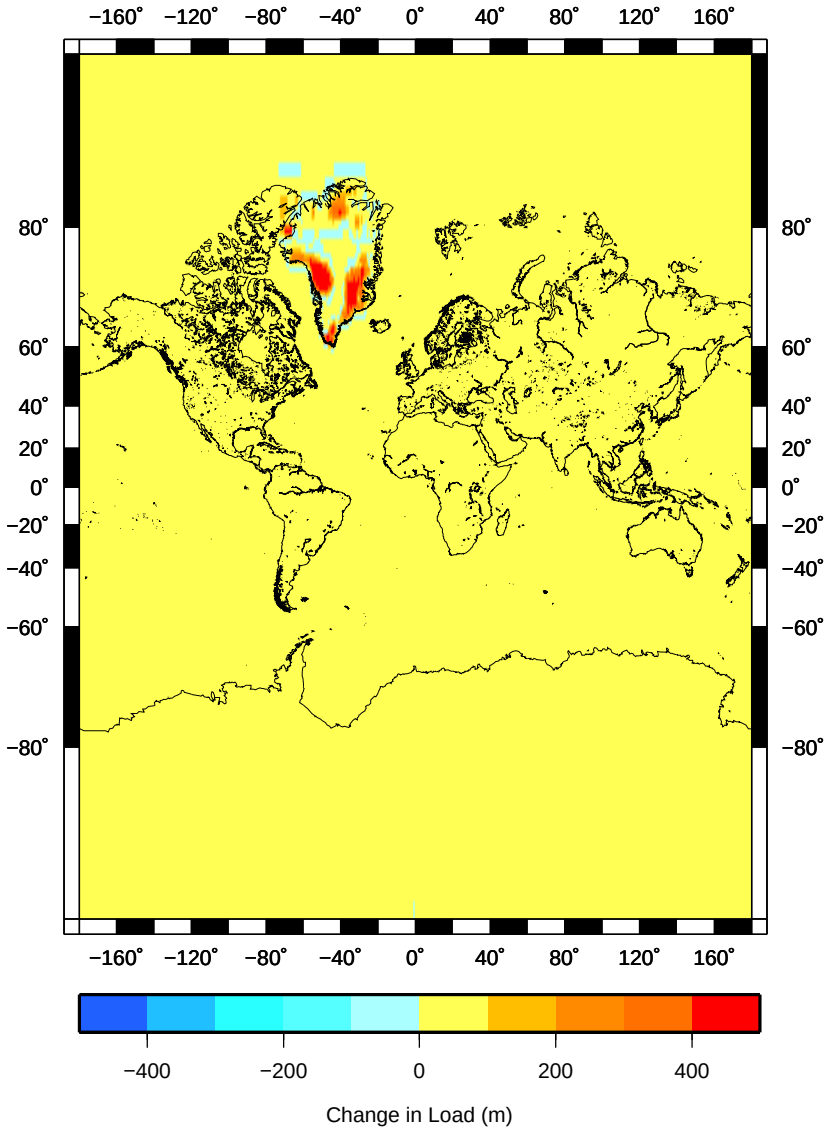

Ice load at 119 kyr BP for Greenland experiment

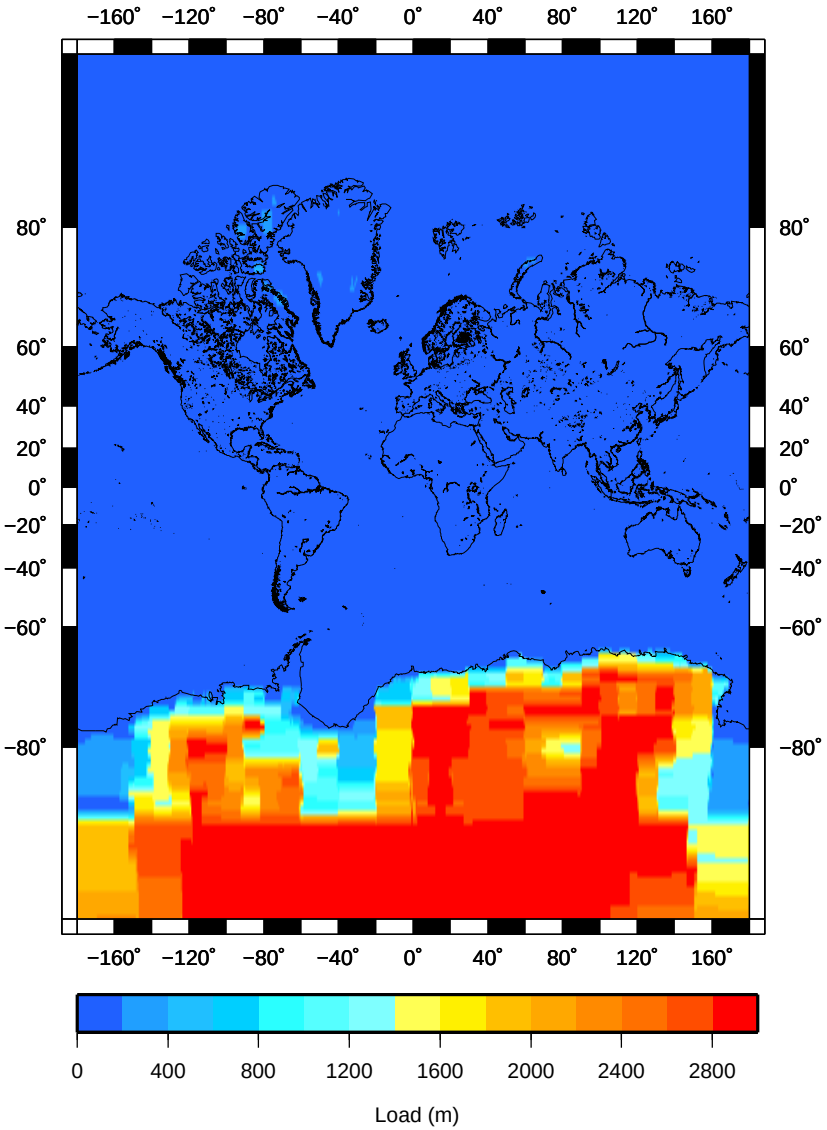

Change in ice load at 119 kyr BP for Greenland experiment

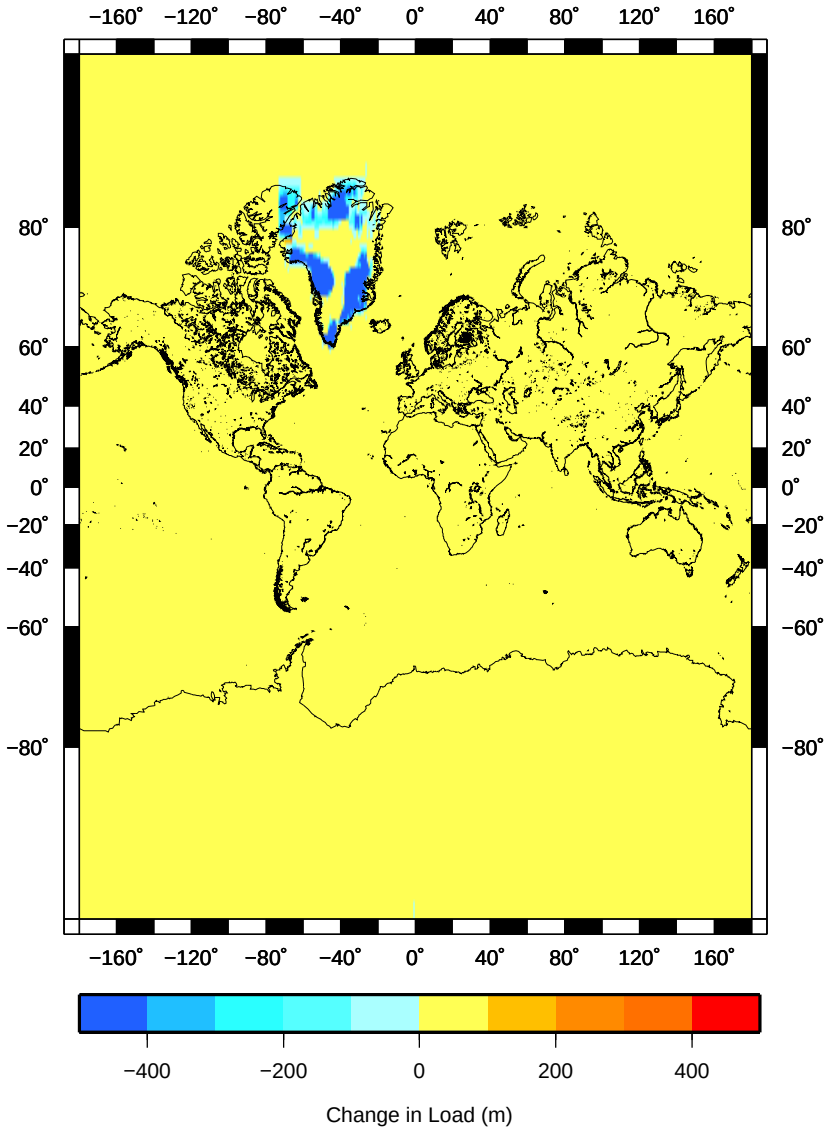

Ice load at 118 kyr BP for Greenland experiment

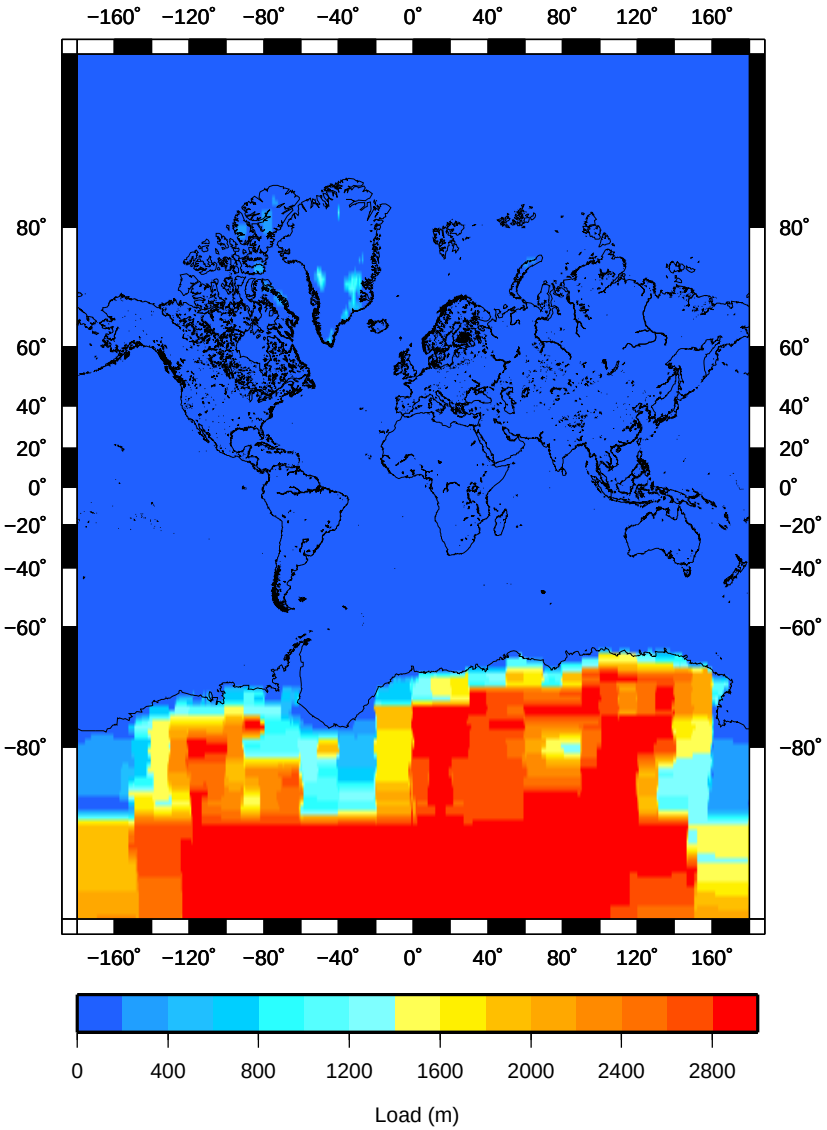

Change in ice load at 118 kyr BP for Greenland experiment

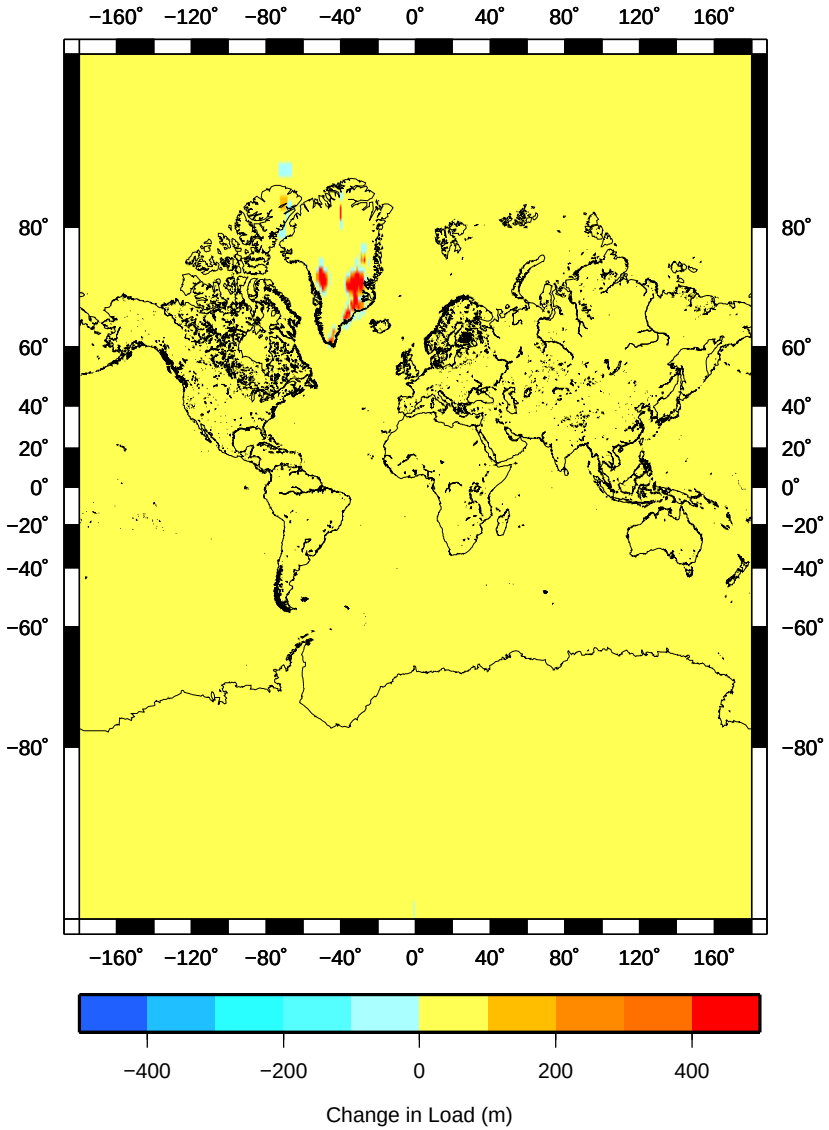

Ice load at 117 kyr BP for Greenland experiment

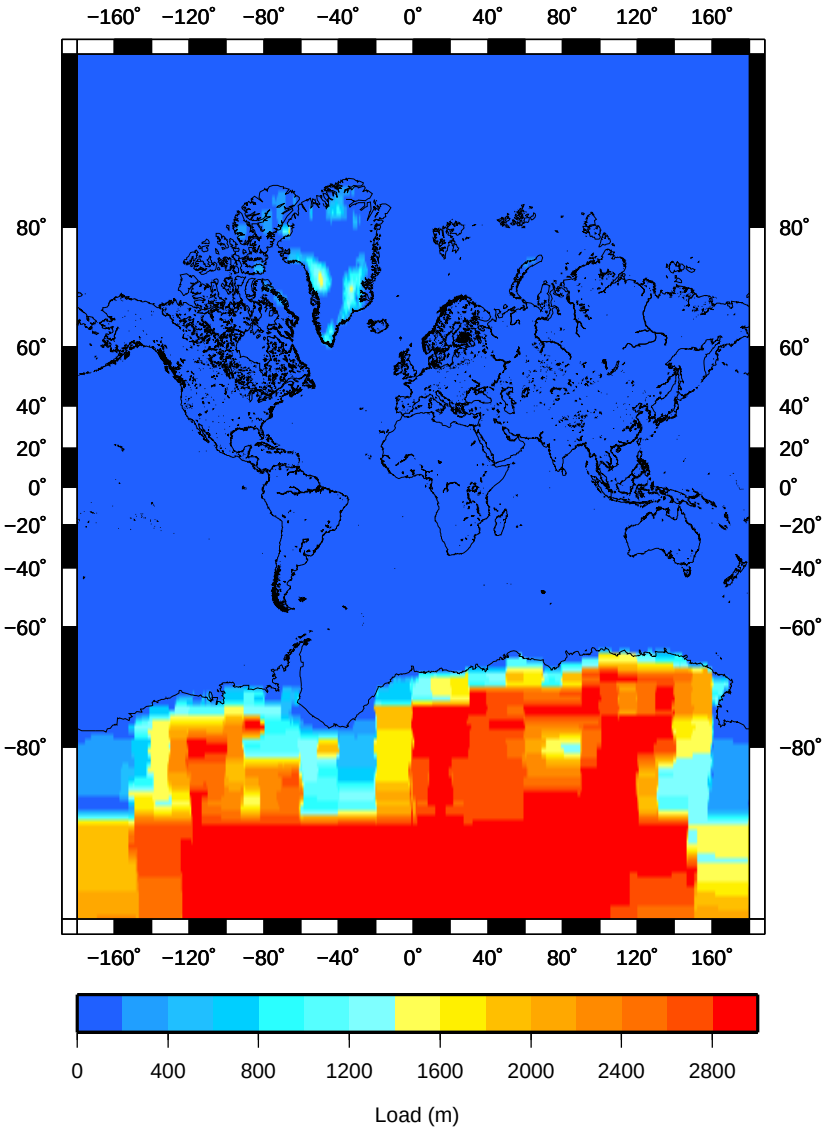

Change in ice load at 117 kyr BP for Greenland experiment

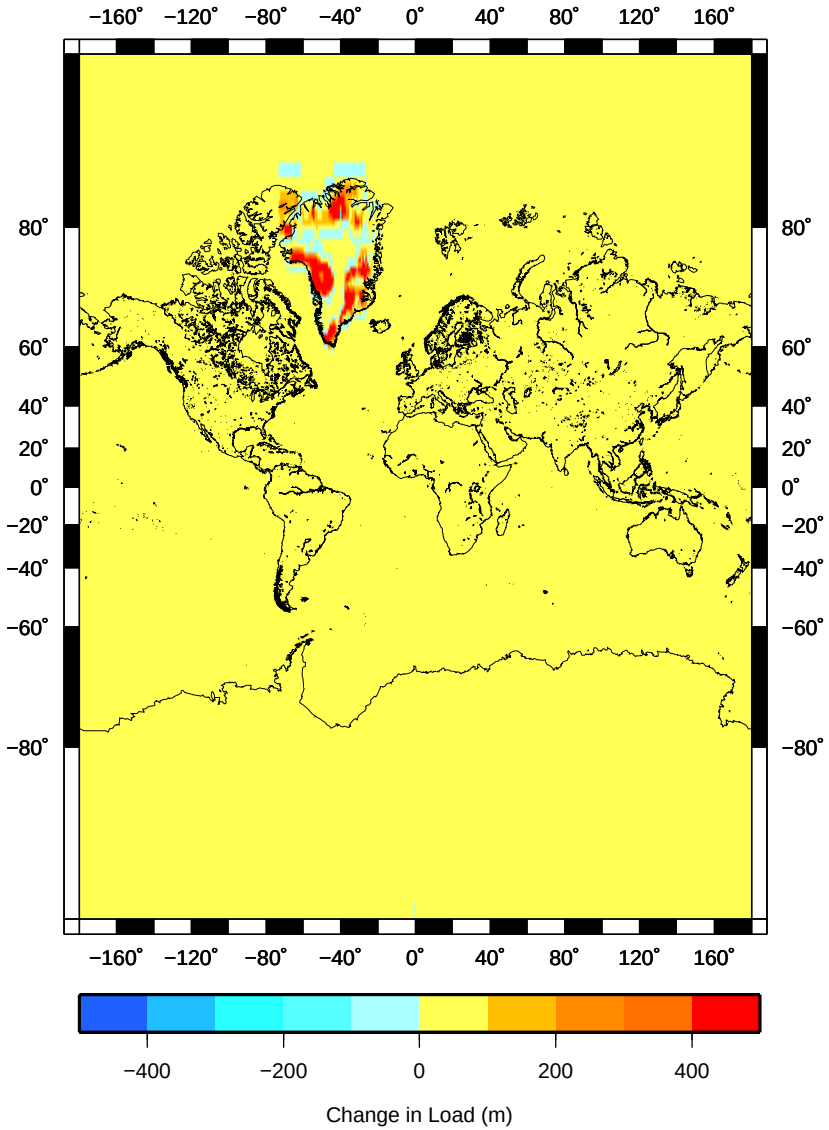

Ice load at 116 kyr BP for Greenland experiment

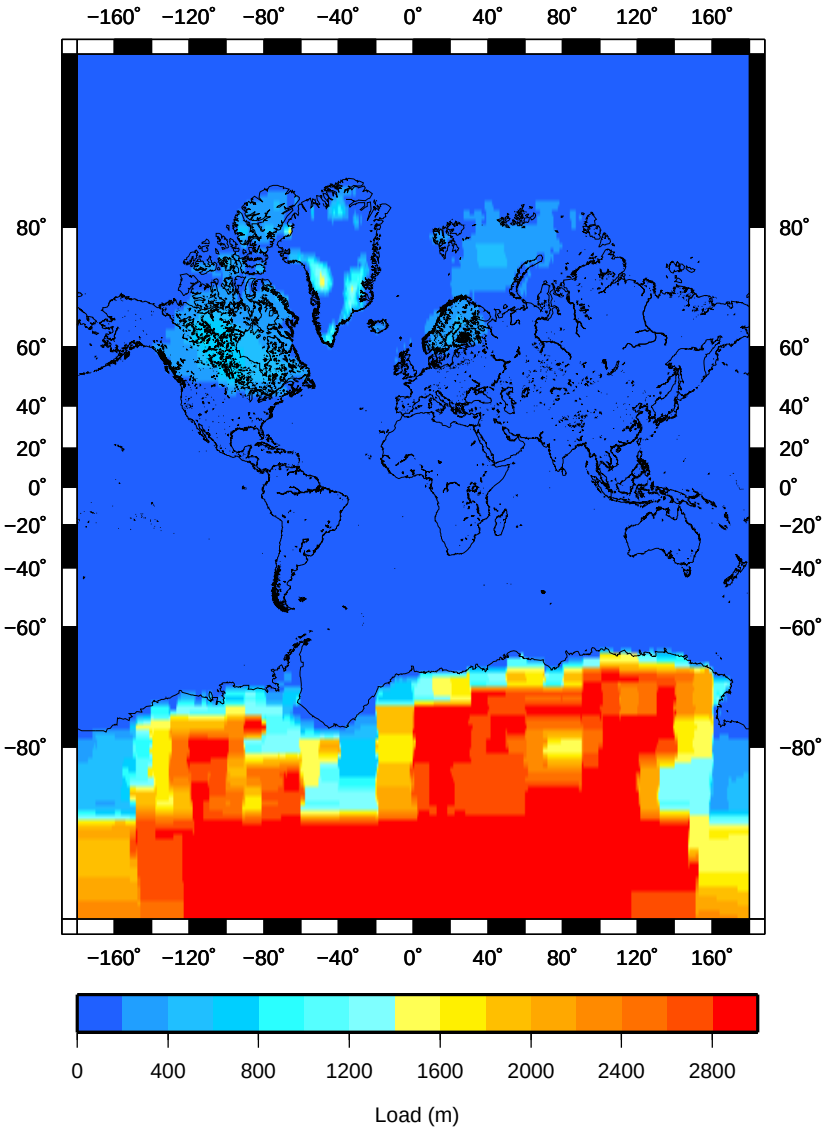

Change in ice load at 116 kyr BP for Greenland experiment